Part IV.

Hurricane Surge Hazard Analysis for Polders

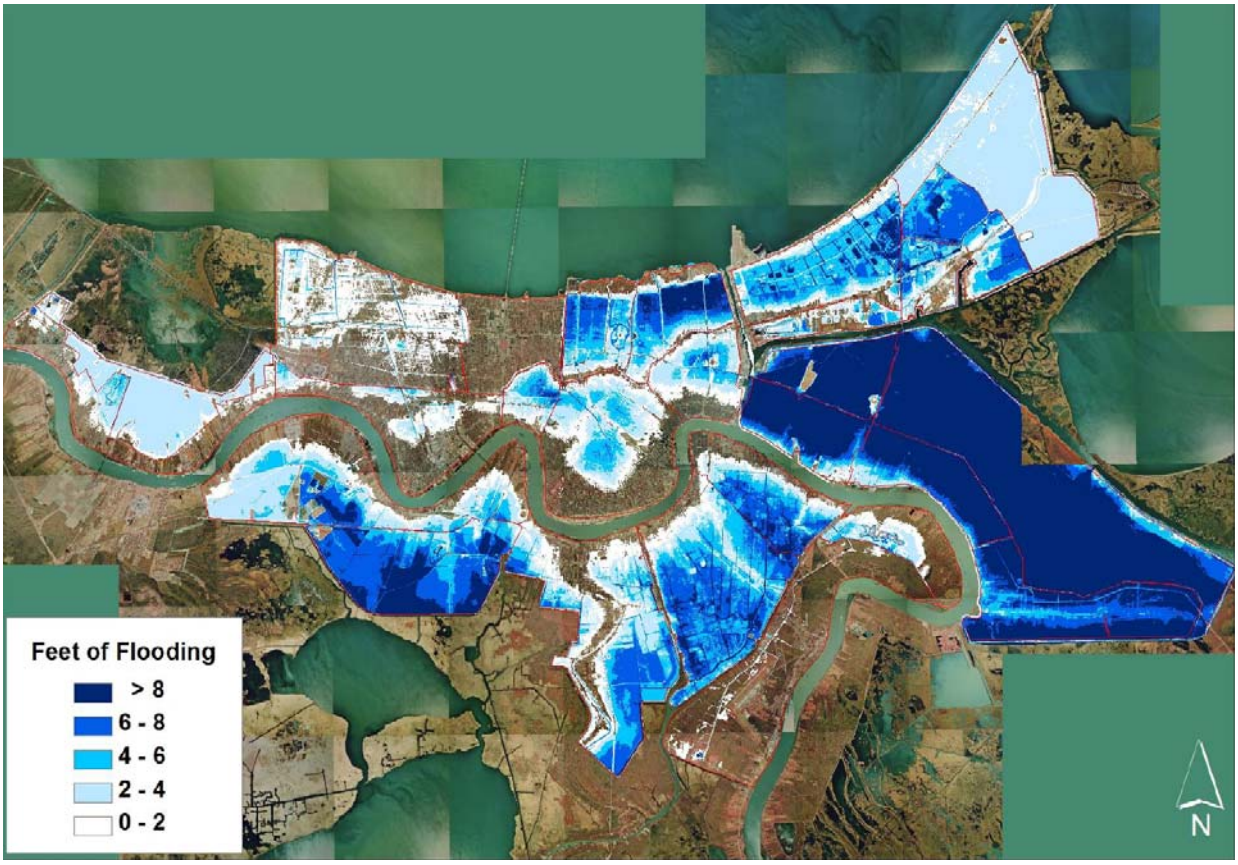

IPET 2009a

Critical urban portions of the New Orleans Metropolitan Area in southeast Louisiana are surrounded by federally or locally sponsored hurricane surge protection systems (see Figure 15.1). Such perimeter systems can have lengths approaching one hundred miles, enclosing large polders[1] encompassing many tens of thousands of acres. Inundation hazards for these polders are exacerbated by interior drainage and reduced water tables, which lead to oxidation and consolidation/compression of the organic deltaic soils, causing the internal topography to subside well below LMSL.

Each perimeter system is comprised of numerous reaches, with various structures—e.g., earthen levees, floodwalls, and gates. The individual reaches within polder systems can be exposed to markedly different storm surge hazards. Eastern portions of the New Orleans regional system are oriented towards Breton Sound, Lake Borgne, and the "funnel" described in Section 7. Northern parts of the system face the massive Lake Pontchartrain, with Jefferson and Orleans Parish reaches located along the open lake but St. Charles Parish segments fronted by miles of degrading cypress swamps. Southern reaches on the west-bank are sheltered by the expansive but eroding coastal marshes of Barataria Bay. Furthermore, the entire system is bifurcated by Mississippi River levees.

As discussed in Part II, Subpart A, the surge dynamics of individual hurricane can produce highly variable SWL and wave conditions around polder perimeters. Importantly, the particular surge hazard level posed by an individual storm can vary dramatically along the system. For example, for east-bank New Orleans Hurricane Katrina produced an extreme surge hazard near the "funnel"—possibly exceeding a 500-yr event, a 100-yr surge along the central Lake Pontchartrain south shore, but well under a 100-yr surge event at the western end of the Lake Pontchartrain south shore. Part III discussed the technical approaches to evaluating the variable surge hazard outside of polders.

The assessment of polder interior surge inundation hazards—i.e. the return frequency of particular surge-induced flood levels at any location inside the perimeter system—is further complicated by additional hydrologic/hydraulic processes associated with storm-specific perimeter inflows, rainfall, forced drainage performance, internal flood routing, and interior wind setup and wave . Critical polder inundation processes—especially breach inflow but also rainfall and pumping—are also conditioned on probabilities, requiring a sophisticated expanded JPA to determine interior inundation hazards.

This Part IV reviews the current state of the practice in hurricane surge polder inundation hazard analysis, including the following subjects:

> Section 15., deterministic and probabilistic methods for examining polder hydrologic/hydraulic processes;
>
> Section 16., expanding the JPA to combine the exterior hurricane surge hazard with the additional polder inundation processes and probabilities; and
>
> Section 17., recent applications of the hurricane surge polder inundation hazard analysis, including IPET's 2009 post-Katrina risk and reliability study, the USACE's 2009 CPR Study, and the USACE's HSDRRS 100-yr and resiliency design and residual risk assessment.

In addition to examining the approaches established in the current literature, these sections expand on methodology requirements, assumptions, and limitations based on sound scientific and engineering practice. Afterwards, a list of conclusions is presented, together with recommendations for improving hurricane surge polder inundation analyses. Part V addresses technical approaches to evaluating hurricane surge hazard for future conditions and surge estimates for selected storm-scenarios.

---

[1] *Polder* is a Dutch word for low-lying area protected from coastal flooding by an encircling barrier.

Section 15. Additional Hydrologic and Hydraulic Analysis

Figure 15.1 depicts the four main New Orleans area federally sponsored HSDRRS polders—Metro New Orleans, New Orleans East, Lower 9th Ward/St. Bernard Polder, and West Bank. Flooding of polders during a hurricane surge event occurs through eight hydrologic/hydraulic processes:

1. The storm surge dynamics producing the exterior surge SWL and wave conditions;
2. Seepage perimeter inflows;
3. Overtopping perimeter inflows;
4. Breach perimeter inflows;
5. Rainfall accumulation;
6. Drainage pumping outflows;
7. Internal routing of the time-varying and location-specific perimeter inflows, rainfall, and pumping outflows; and
8. Local wind-induced interior setup and waves.

The following sections describe additional analyses for quantifying these eight processes, including limitations and uncertainties associated with each analysis.

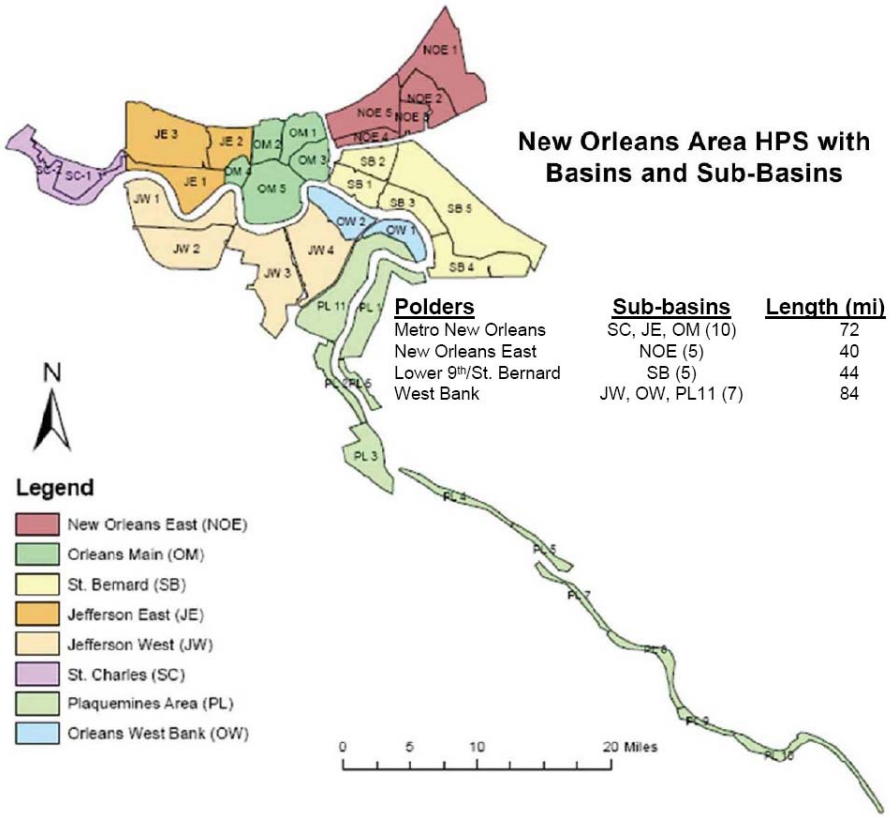

Figure 15.1. New Orleans Area Polders and Sub-Basins

IPET 2009a

15.1 Perimeter Surge SWL and Wave Conditions

The three polder perimeter inflows—seepage, overtopping, and breaching—are dependent on the exterior surge SWL. The physics of surge SWL are described Part II, Subpart A. Time-varying physics for hindcast and synthetic storms (e.g., for a surge JPA) are evaluated with a high resolution 2D hydrodynamic model as described in Subpart B. The rise, peak, and fall in surge SWL (i.e., hydrograph) is often compared to the barrier crown elevation in terms of the *freeboard* (equal to the crown elevation minus SWL)—the value is positive when SWL is below the structure crown and negative when SWL is above the crown.

Detailed time-series results from the high resolution 2D surge model are expensive to output and retain. Thus, model output is often limited to peak SWL at all mesh nodes, with time-series at selected locations. To construct a hydrograph for additional perimeter locations a curve shape can be assumed and curve coefficients obtained from those model hydrographs retained. For example, a Normal Distribution type curve can be used, with separate σ_R and σ_F values for the rising and falling hydrograph limb (IPET 2009). If a Surge-Response relationship is being used to evaluate a range of hurricane conditions, the values of σ_R and σ_F can also be developed as functions of the perimeter location and storm parameters.

Overtopping and breaching inflows are also dependent on the local wave conditions (H_S, T_P, and direction). As discussed in Section 5.1, storm surge wave fields are irregular, with a Rayleigh Distribution typically used to describe the relative statistical frequency of different wave heights (e.g., $H_{50\%}$, H_s, $H_{1\%}$, and $H_{0.1\%}$). This distribution is appropriate for a long-term steady wave field, such as for slow-moving weak storms, which can sustain intensity while stalled over many hours. However, more intense storms tend to decay and only sustain local peak conditions for a few hours. In the latter case, the Rayleigh Distribution may not describe the relationship between various wave heights—i.e., the ratio of $H_{1\%}$:H_S may be somewhat lower. The assumption of a Rayleigh Distribution for extreme storms would likely therefore be conservative. To date there have been no studies suggesting alternative distributions for hurricane surge wave fields.

Wave characteristics undergo successive transformations as they pass through different zones, illustrated in Figure 15.2:

A. Open water—including the GoM and large, open coastal sounds, bays, and lakes. The high resolution 2D surge model, coupled with a linear wave model, provides a reasonable analysis of transformations in H_S, T_P, and θ in Zone A (see Section 10.2).

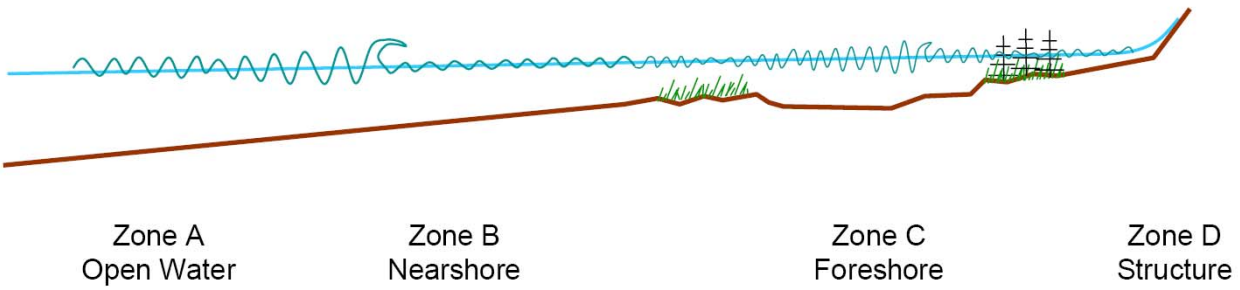

Figure 15.2. Transformation of Waves Approaching a Perimeter Barrier
(Not to scale)

B. Nearshore—this zone includes bathymetry-driven shoaling, breaking, refraction, and diffraction of the open water waves, modifying H_S, T_P, θ, and associated radiation stress. The wave models coupled with the high resolution surge model are intended to capture most of these processes. However, as noted in Section-6.2, little surge wave data exists for evaluating these models.

C. Inundated foreshore zone between the water body and the barrier. This zone can extend just a few hundred feet, (e.g., along the Lake Pontchartrain south shore) or many miles (e.g., east-bank St. Charles Parish and West Bank). Foreshore regions can include a wide variety of landscapes at a range of distances: open interior water; marsh at various states of integrity and inundation; forested wetlands/swamps, some with modestly elevated ridges; coastal communities; etc. The landscape friction applies varying amounts of energy dampening to the wave fields. The greatest perimeter wave heights generally occur at those barriers that are within a short distance of deeper open water, and where the foreshore provides for little or no shoaling/breaking at the peak SWL. However, as surge SWL rises higher waves can pass into the foreshore region. Given sufficient local winds, inundation, and open fetch, the foreshore wave field can regenerate to H_S of several feet. Importantly, as waves move through Zones B and C they become increasingly asymmetric—with disproportionate crests/troughs (amplitude above SWL > amplitude below SWL) and profiles.

D. The Structure, from the outside toe to the structure crest. The zone usually includes a compound sloping embankment, with 100 ft or more of gentle sloping outer embankment (e.g., 10:1 to 20:1) followed by a steeper main embankment (e.g., 4:1 for the actually levee or floodwall support). The outer embankment may include shoreline armoring which can aid in wave breaking, berms, and other features. During inundation of this zone wave heights are typically reduced at the transition from the foreshore to the outer slope, and again at the transition from the outer to the main embankment, by the rapid changes in surge depth.

The wave conditions across and along perimeter Zones C/D are not covered by the high resolution surge SWL-wave coupled model for either hindcast or synthetic storms. While values for Zones C/D wave T_P and θ[1] are generally regarded as consistent from Zone A/B, wave heights can change significantly. Therefore, reach-specific, storm-specific wave height analysis is required for Zones C/D. Four approaches are:

1. Employ a ceiling criteria—termed breaker parameter (or index)—limiting the ratio of H_S to the surge depth. Values ranging from 40 to 70% may be considered. As noted in Section 6.2, Kennedy found a ratio of 50% for observed nearshore waves along the Texas coast during Hurricane Ike. However, there is very little published data on appropriate limiting ratios for the highly asymmetric wave conditions in Zones C/D. Importantly, a ceiling ratio may over- or under-estimate H_S. depending on actual local storm wind conditions.
2. Use WHAFIS where simple 1D, steady-state analysis of wave transformations is adequate.

[1] Wave periods can also be assumed based on literature values. For a worst case analysis a perpendicular wave direction (to the perimeter structure) is usually assumed, although this may not be consistent with the orientation of the nearby water body fetch.

3. Model foreshore waves with STWAVE or SWAN for more complex cases requiring analysis of unsteady 2D processes, but still assuming linear (symmetric) wave processes.
4. For non-linear wave processes utilize higher-order Boussinesq model.

There is currently no technical literature providing a thorough validation of WHAFIS, STWAVE, SWAN, or Boussinesq models for Zones C/D during hurricane surge events.

Use of WHAFIS, STWAVE, SWAN, or Boussinesq models for Zones C/D wave analysis can be facilitated by programming one-way loose coupling of foreshore models with the high resolution Zone A/B surge-wave model (to automate input of SWLs, currents, and wave boundary conditions at suitable time steps). If the local Zones C/D wave conditions imply significant modification of local radiation stress gradients, and influence on local SWL setdowns and setups, further two-way loose coupling with the high resolution 2D surge model may be required. To date there have been no publications addressing such two-way coupling Zones A/B modeling with Zones C/D wave analysis and it is considered beyond the current state-of the-practice.

15.2 Seepage

Perimeter seepage can occur along reaches which are penetrated by highly permeable subterranean flow paths. The most significant type of flow path is a broad, naturally occurring sand layer beneath the local area. The shallow subsurface geology of southeastern Louisiana is known to include such sand layers. A major example is the Pine Island buried beach complex in the New Orleans area near Lake Pontchartrain, shown in Figure 15.3.

Water pressure in the subsurface sand layer will naturally build as the SWL rises on the exterior-side of the barrier. The pressure difference between the flood and interior sides within the sand layer will then induce sand layer groundwater to flow underneath the barrier toward the interior. The high porosity, and hence permeability, of the sand layer will cause the subsurface pressure to rapidly rise at the protected side. Such a rapid transmission of the external subsurface pore-water pressure to the internal side does not occur in areas where the barrier is underlain by low permeability soils (e.g., clay).

The high interior-side pressure in the sand layer will induce the groundwater to seek flow paths to the surface. Natural variations in the overlying interior strata can lead to a “piping” type flow to the surface. Rising flow rates along a higher permeability conduit to the surface can “flush the pipe,” widening it, and accelerating seepage flow to the surface. At points where the sand is only a few feet below the surface, the pressure may be sufficient to push the sand through the overlying soil. This phenomenon, often described as a “sand boil,” is common along the Mississippi River levee during high river stages[2]. “Piping” and “sand boil” flows to the surface can initiate in locations where the interior ground surface is very low and can be enhanced by man-made penetrations—such as sand-filled (or poorly-filled) excavations (e.g., building foundations and infrastructure trenches).

[2] Over the course of many decades of experience with high Mississippi River stages, the USACE and local officials have identified most “sand boil” locations and therefore closely monitor them during river floods. They also employ precautionary measures to relieve the interior-side sand layer pressure, which prevents the sand boils from expanding and possibly leading to a river levee failure.

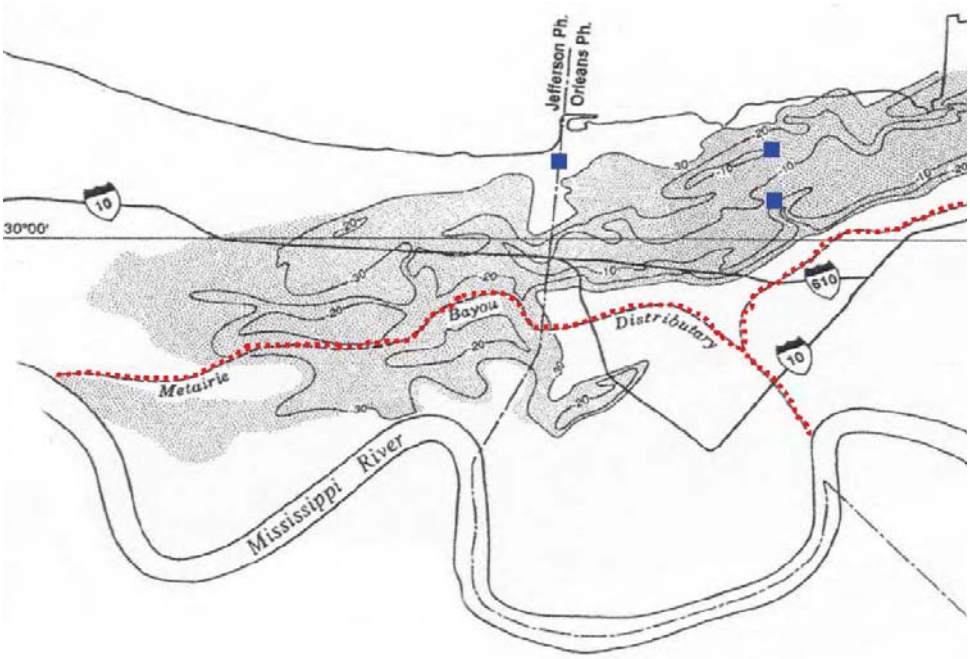

Figure 15.3. Pine Island Buried Beach Complex in the New Orleans Area

Contours are Depth Below Surface, ft; points show Hurricane Katrina Breaches
IPET 2006

In addition to seepage facilitated by natural sand layers, inflow can also occur along man-made preferential pathways underneath and within the barrier itself. Examples include:

- Legacy excavations underlying the barrier that pre-date barrier construction;
- The annular space around subsurface pipelines crossing underneath the barrier;
- Interconnected exterior and interior excavations in close proximity to the barrier—e.g., by natural subsurface "piping" pathways; and
- Material used in older levee embankments which over time allows for the formation of significant voids; such as non-cohesive soils which settle differentially within the embankment; degradable organic matter; and debris.[3]

During Hurricane Katrina a major "sand boil" occurred at the north and south ends of the London Avenue Canal. High surge entered the outfall canal from Lake Pontchartrain and induced flow in the Pine Island sand layer underneath the canal floodwall. The locations are noted on Figure 15.3, and Figure 15.4 presents a schematic of the northern sand boil. During Hurricane Katrina seepage was also suspected along the IHNC (ILIT 2006)

Researchers are investigating the use of remote geophysical sensing techniques to identify potentially significant natural and man-made seepage pathways, as well as the integrity of sheet pile "cut-off" walls used to reduce seepage. Important techniques include the use of ground

[3] Current design and construction practices attempt to greatly minimize the presence of potential void-forming materials (USACE 2008b).

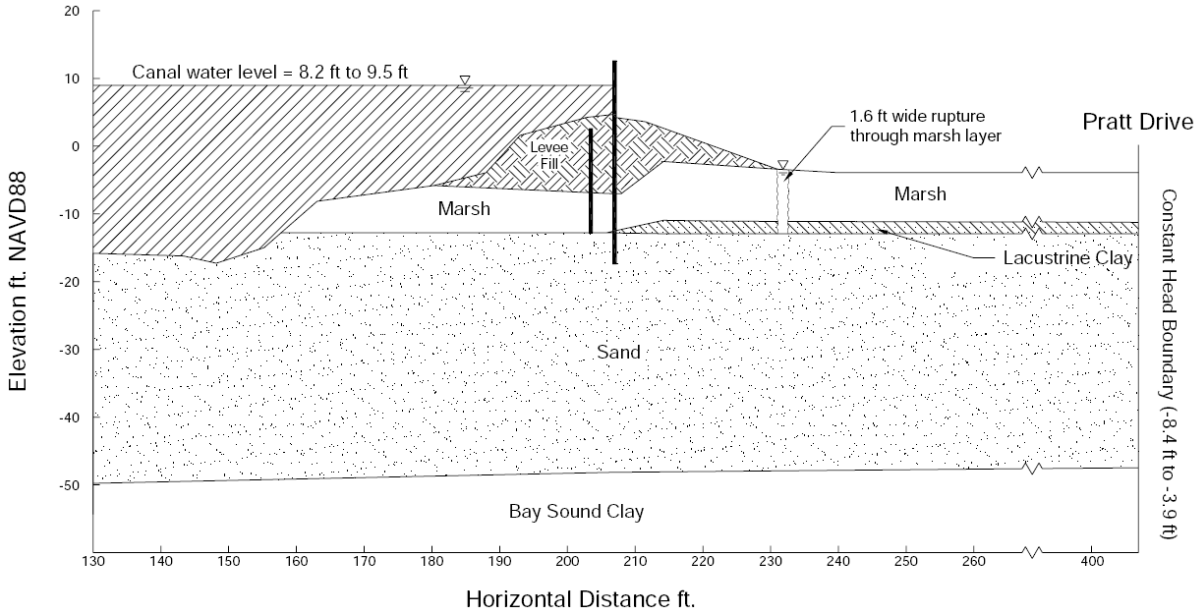

Figure 15.4. Cross Section at London Avenue North Floodwall Seepage Location
IPET 2006

penetrating radar,[4] soil electro-magnetic conductivity surveys, and shallow seismic profiling.[5] To date, techniques for identifying seepage paths have not been standardized, and a comprehensive data base of significant paths has not been compiled for southeastern Louisiana polder perimeter systems.

Techniques are available for estimating seepage discharge—which is proportional to the head loss and porosity along the flow path—given geologic and other data or assumptions. The techniques include analysis with flow nets and computer groundwater flow models. The interior discharge associated with a major seepage inflow can potentially exceed 0.1 acre-ft/hr (1.2 cfs) for several hours.[6]

While seepage inflow can contribute to localized interior inundation the cumulative volumes are much less than those associated with overtopping or breaching and generally do not pose a polder-wide inundation hazard. The more significant hazard from seepage is the potential contribution to a barrier breach, which is discussed below. Investigations have yet to be undertaken of potential seepage rates associated with hurricane surge for southeastern Louisiana polders and a detailed review of the techniques for quantifying seepage inflows alone is beyond the scope of this report.

---

[4] See the website for the Center for Nondestructive Evaluation, http://www.cnde.iastate.edu/research-areas/ground-penetrating-radar

[5] See the website for the LSU-UNO Levee Monitoring Group, http://lmg.uno.edu/

[6] Time-varying perimeter inflow rates (or discharges)—for seepage, overtopping, and breaching—are typically evaluated as volumetric rates per unit length along a particular reach (in units such as cubic feet per second, cfs, per linear foot, cfs/ft). An inflow rate of 1 cfs/ft over a length of 1 mile (or 5,280 cfs), over a period of 1 hour, accumulates to 436.4 acre-ft of water (1 foot of inundation over an area of 436 acres). At any point during a particular storm the inflow rate—and the cumulative inflow--will vary greatly by reach.

15.3 Overtopping

Figure 15.5, illustrates five phases of overtopping, with dramatically increasing overflow rates in succeeding phases:

1. The SWL and all Zone D wave crests are below the barrier crown (positive freeboard) but the elevation of wave runup for the more extreme waves (e.g., runup associated with Zone D wave heights ≥ H_S) on the barrier's exterior-side slope exceeds the barrier crown. Since waves arrive intermittently, runup overtopping may occur only a couple of times per minute. As the SWL rises and/or wave heights increase, the overtopping frequency and overflow increases.
2. The SWL is still below the barrier crown (positive freeboard) but some Zone D wave crests now exceed the crown. This second phase includes runup overtopping from a large percentage of waves plus direct overtopping from the higher Zone D waves. Figure 15.6 illustrates intermittent overtopping against the vertical floodwalls of the Inner Harbor Navigation Canal during Hurricane Gustav that appears to be in Phase 2. As the SWL rises and/or Zone D wave heights increase, more waves will directly overtop the barrier.
3. The surge SWL reaches the crown (zero freeboard) and all Zone D waves directly overtop the barrier. However, the overflow is still associated with the wave volume and overtopping briefly ceases when wave troughs reach the crown. As the SWL rises more wave troughs are above the crown and the overflow eventually becomes continuous.
4. The surge SWL is sufficiently above the crown (negative freeboard) for all Zone D wave troughs to exceed the crown. The overflow is now continuous but still has significant "pulsing."

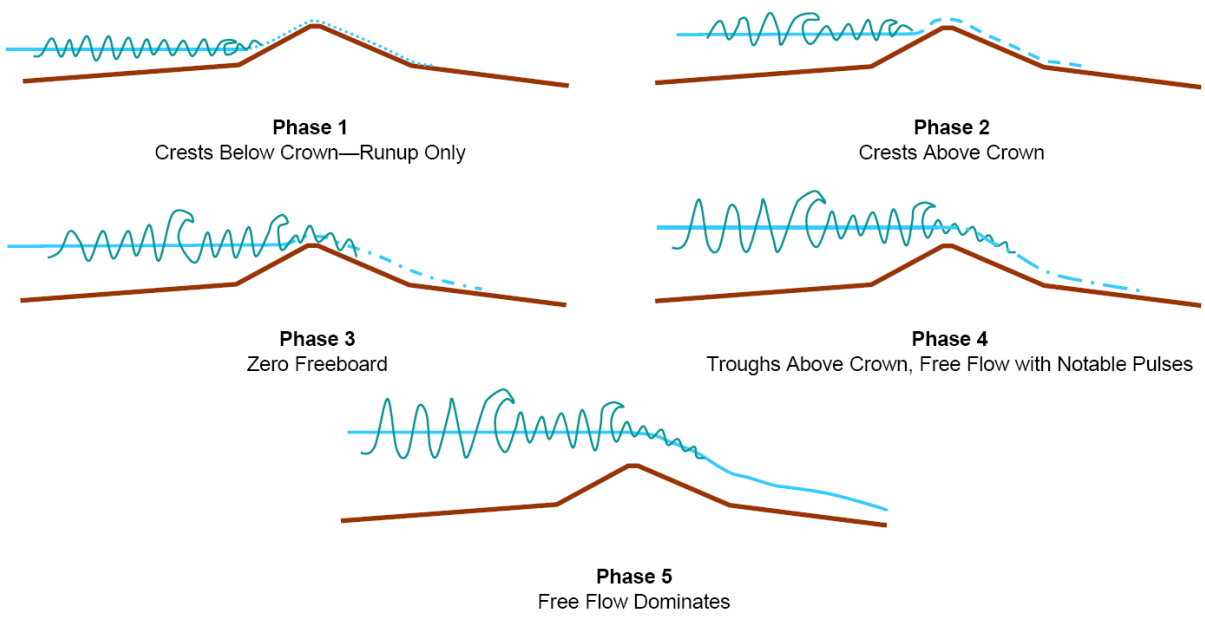

Figure 15.5. Five Phases of Barrier Overtopping
(Not to scale)

Figure 15.6. Phase 2 Overtopping of the IHNC Floodwall During Hurricane Gustav

Eliot Kamenitzd Times Picayune

5. As SWL continues to rise (as the freeboard becomes more negative) the overflow becomes more and more dominated by near-steady "weir flow," which dwarfs the variation from the Zone D waves.

When the surge peak passes, the overtopping phases are reversed.

Zone D waves at a highly sheltered barrier may exhibit very small amplitude (e.g., H_S<1 ft). In this case the SWL may need to rise very close to the barrier crown before any overflow occurs. A reach experiencing small waves and rapidly rising SWL, may see very limited Phases 1 through 4 overtopping, with overtopping transitioning quickly from zero to a near-steady discharge. Conversely, a reach experiencing larger waves with a slow decline in freeboard can experience more prolonged pulsing overflow associated with Phases 1 through 4.

The technical literature provides empirical expressions for quantifying an average overflow for the various phases—ignoring pulsing. To assess wave-only overtopping—Phase 1 through 3—researchers have conducted controlled wave runup and overtopping experiments with irregular wave fields. The USACE Coastal Engineering Manual (CEM) Part VI (USACE 2005), Chapter 5, Table VI-5-7 summarizes overtopping research for various barrier structures, including simple trapezoidal shaped levees with smooth impermeable surfaces, permeable rock structures, and floodwalls. An expression proposed by Van der Meer, described in the CEM Table VI-5-11, is typically used for wave-only overtopping of levees. CEM Tables VI-5-7 and VI-5-11 are reproduced as Tables 15.1 and 15.2.

Table 15.1. Empirical Overtopping Equations for Various Barriers

USACE 2005

Table VI-5-7
Models for Average Overtopping Discharge Formulae

Authors	Structures	Overtopping model	Dimensionless discharge Q	Dimensionless freeboard R
Owen (1980,1982)	Impermeable smooth, rough, straight and bermed slopes	$Q = a\ exp(-b\,R)$	$\frac{q}{g\,H_s\,T_{om}}$	$\frac{R_c}{H_s}\left(\frac{s_{om}}{2\,\pi}\right)^{0.5}\frac{1}{\gamma}$
Bradbury and Allsop (1988)	Rock armored impermeable slopes with crown walls	$Q = a\,R^{-b}$	$\frac{q}{g\,H_s\,T_{om}}$	$\left(\frac{R_c}{H_s}\right)^2\left(\frac{s_{om}}{2\,\pi}\right)^{0.5}$
Aminti and Franco (1988)	Rock, cube, and Tetrapod double layer armor on rather impermeable slopes with crown walls, (single sea state)	$Q = a\,R^{-b}$	$\frac{q}{g\,H_s\,T_{om}}$	$\left(\frac{R_c}{H_s}\right)^2\left(\frac{s_{om}}{2\,\pi}\right)^{0.5}$
Ahrens and Heimbaugh (1988b)	7 different seawall/revetment designs	$Q = a\,exp(-b\,R)$	$\frac{q}{\sqrt{g\,H_s^3}}$	$\frac{R_c}{(H_s^2\,L_{op})^{1/3}}$
Pedersen and Burcharth (1992)	Rock armored rather impermeable slopes with crown walls	$Q = a\,R$	$\frac{q\,T_{om}}{L_{om}^2}$	$\frac{H_s}{R_c}$
van der Meer and Janssen (1995)	Impermeable smooth, rough straight and bermed slopes	$Q = a\,exp(-b\,R)$	$\frac{q}{\sqrt{g\,H_s^3}}\sqrt{\frac{s_{op}}{\tan\alpha}}$ for $\xi_{op} < 2$ $\frac{q}{\sqrt{g\,H_s^3}}$ for $\xi_{op} > 2$	$\frac{R_c}{H_s}\frac{\sqrt{s_{op}}}{\tan\alpha}\frac{1}{\gamma}$ for $\xi_{op} < 2$ $\frac{R_c}{H_s}\frac{1}{\gamma}$ for $\xi_{op} > 2$
Franco et al. (1994)	Vertical wall breakwater with and without perforated front	$Q = a\,exp(-b\,R)$	$\frac{q}{\sqrt{g\,H_s^3}}$	$\frac{R_c}{H_s}\frac{1}{\gamma}$
Pedersen (1996)	Rock armored permeable slopes with crown walls	$Q = R$	$\frac{q\,T_{om}}{L_{om}^2}$	$3.2\cdot 10^{-5}\frac{H_s^5\,\tan\alpha}{R_c^3\,A_c\cdot B}$

Table 15.2. Van der Meer Empirical Overtopping Equation for Levees

USACE 2005

Table VI-5-11
Overtopping Formula by van der Meer and Janssen (1995)

Straight and bermed impermeable slopes including influence of surface roughness, shallow foreshore, oblique, and short-crested waves, Figures VI-5-14a and VI-5-14b.

$\xi_{op} < 2$

$$\frac{q}{\sqrt{g\,H_s^3}}\sqrt{\frac{s_{op}}{\tan\alpha}} = 0.06\,exp\left(-5.2\,\frac{R_c}{H_s}\,\frac{\sqrt{s_{op}}}{\tan\alpha}\,\frac{1}{\gamma_r\,\gamma_b\,\gamma_h\,\gamma_\beta}\right) \qquad \text{(VI−5−24)}$$

application range: $0.3 < \dfrac{R_c}{H_s}\,\dfrac{\sqrt{s_{op}}}{\tan\alpha}\,\dfrac{1}{\gamma_r\,\gamma_b\,\gamma_h\,\gamma_\beta} < 2$

Uncertainty: Standard deviation of factor 5.2 is $\sigma = 0.55$ (See Figure VI-5-15).

$\xi_{op} > 2$

$$\frac{q}{\sqrt{g\,H_s^3}} = 0.2\,exp\left(-2.6\,\frac{R_c}{H_s}\,\frac{1}{\gamma_r\,\gamma_b\,\gamma_h\,\gamma_\beta}\right) \qquad \text{(VI−5−25)}$$

Uncertainty: Standard deviation of factor 2.6 is $\sigma = 0.35$ (See Figure VI-5-15).

The reduction factors references are

γ_r Table VI-5-3

γ_b Eq VI-5-8

γ_h Eq VI-5-10

Short-crested waves

$\gamma_\beta = 1 - 0.0033\,\beta$

Long-crested waves (swell)

$$\gamma_\beta = \begin{cases} 1.0 & \text{for } 0° \le \beta \le 10° \\ \cos^2(\beta - 10°) & \text{for } 10° < \beta \le 50° \\ 0.6 & \text{for } \beta > 50° \end{cases} \qquad \text{(VI−5−26)}$$

The minimum value of any combination of the γ-factors is 0.5.

In the Van der Meer equation the average discharge per unit barrier length, q, is a function of

- The Zone D wave height, H_S ;
- Freeboard, R_c (R_c/H_S is termed the relative freeboard);
- Slope of the levee floodside bank, tan α;
- Peak open water (deepwater, pre-shoaling) wave steepness, S_{op} (equal H_S divided by wave length L_o); the ratio of the levee slope to wave steepness, tan α/S_{op}, is termed the surf similarity parameter, ξ_{op}; slightly different equations are used for $\xi_{op}<2$ and $\xi_{op}>2$; and
- Reduction factors (or transmission coefficients) to account for slope roughness, fronting berm, shallow Zone D, and wave incident angle, γ_r, γ_b, γ_h, γ_β . (The combined factor is typically not less than 0.5).

As R_c declines toward 0, the exp term in Table 15.2 converges to 1 and

$$q = C_{wave}\sqrt{H_s^{\,3}}$$

C_{wave} is a lumped transmission coefficient for wave overtopping. For large ξ_{op} (steeper levee slope relative to wave face) C_{wave} approaches 1.1. For smaller ξ_{op} C_{wave} is much less than 1.

The technical literature suggests that these empirical equations for average wave overtopping while useful have significant uncertainty. Figure 15.7 illustrates the uncertainty for the Van Der Meer equation. Note that the overflow on the y-axis is presented on a logarithmic scale. Importantly, there are no data, and thus no empirical studies, for wave-only overtopping during brief, intense hurricane surge events. This implies considerable uncertainties *in addition to* the kind illustrated in Figure 15.7. For example, overtopping estimates are highly sensitive to the assumed breaker parameter. In the Van der Meer equation a 20% increase in H_S. from 5 to 6 ft with R_c of 1 ft and ξ_{op} of 2, with all γ at 1, translates into a 46% increase in overtopping discharge. Another source of uncertainty is the assumption of a Rayleigh Distribution, which may tend to over-estimate extreme wave frequency and associated overtopping.

For negative freeboard and negligible waves the average barrier overflow, q, is typically given using a version of the standard equation for steady supercritical flow over a broad-crested weir:

$$q = C\sqrt{|R_c|^3}$$

where the absolute value of the negative freeboard is the height in ft of the SWL above the barrier crest. Typical values of the weir transmission coefficient, C, range from 1 to 3.1 ($ft^{½}/s$).[7] Thus, for Phase 3 at a large ξ_{op} the average wave overflow for a levee is equivalent a simple broad-crested weir overflow at a low transmission factor, using $|R_c|$ equal to H_S.

[7] Another version of the broad crested weir equation derived directly from basic hydraulics is $q = \frac{2}{3}C^*\sqrt{2g|Rc|^3}$,

thus $C = \frac{2}{3}C^*\sqrt{2g}$

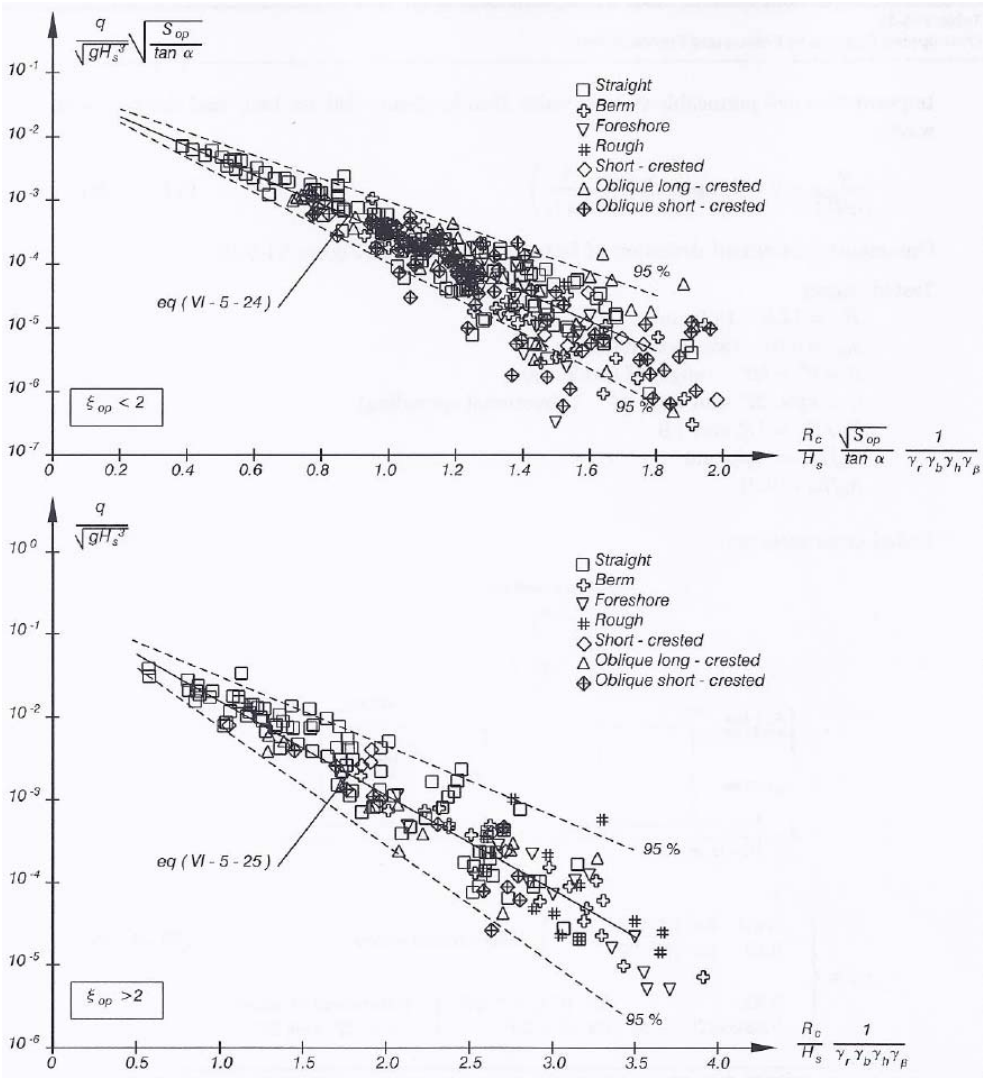

Figure 15.7. Van der Meer Empirical Wave Overtopping Equation for Levees with Confidence Bands

Van der Meer and Jannssen, 1995 in USACE 2005

For Phases 4 and 5, levee overflow can be estimated using the sum of two broad crested weir formulas, one with H_S and the other with $|R_c|$ for $R_c<0$, and each with their respective transmission factors:

$$q = C_w \sqrt{H_s^{\,3}} + C\sqrt{|R_c|^3}$$

Thus, as SWL rises and $|R_c|>H_S$, the second equation will dominate the estimate of overflow. The broad-crested weir equation is typically used throughout rising/falling SWL during Phase 5 by modifying $|R_c|$. The steady overtopping flow using the broad-crested weir equation is been widely applied, but defining appropriate values for C for a wide variety of overtopped surge barriers has not been studied. The uncertainties in steady Phase 5 overtopping are not as high as for Phase 1 and 2 wave-only overtopping. A range of ±25% in the value of C translates to a ±25% range in the discharge rate.

In 2010 Lynette et al employed Boussinesq modeling to aid in simulating the initial average wave overtopping along the MRGO during Hurricane Katrina. Noting that Hurricane Katrina wave heights along the MRGO generally correlated to freeboard, they provided a simple empirical equation for the average overflow as a function of R_c encompassing all five phases:

$$q \approx 0 \ for \ R_c > 0.75m$$
$$q = 0.17(R_c) + 0.13 \ for \ 0.75m > R_c \geq 0$$
$$q = 0.48\sqrt{g|R_c|^3} + 0.13 \ for \ R_c < 0$$

Figure 15.8 compares the above equation to the MRGO Boussinesq model output. Figure 15.9 presents the average overflow on a log-scale and more clearly illustrates the overflow by phase. Dashed lines have been included on Figure 15.9 to depict overflow associated with smaller waves.

As shown in Figure 15.9, overtopping can begin to contribute significantly to polder inundation when freeboard turn negative, with accumulations reaching 610 acre-ft/hour per mile (equivalent to 1.4 cfs/ft) at zero freeboard. During Hurricane Katrina the New Orleans East Polder was inundated largely due to overtopping inflow (IPET 2009). High overtopping rates have also been associated with the interior-side embankment scour and the additional hazard of barrier breaching, discussed further below.

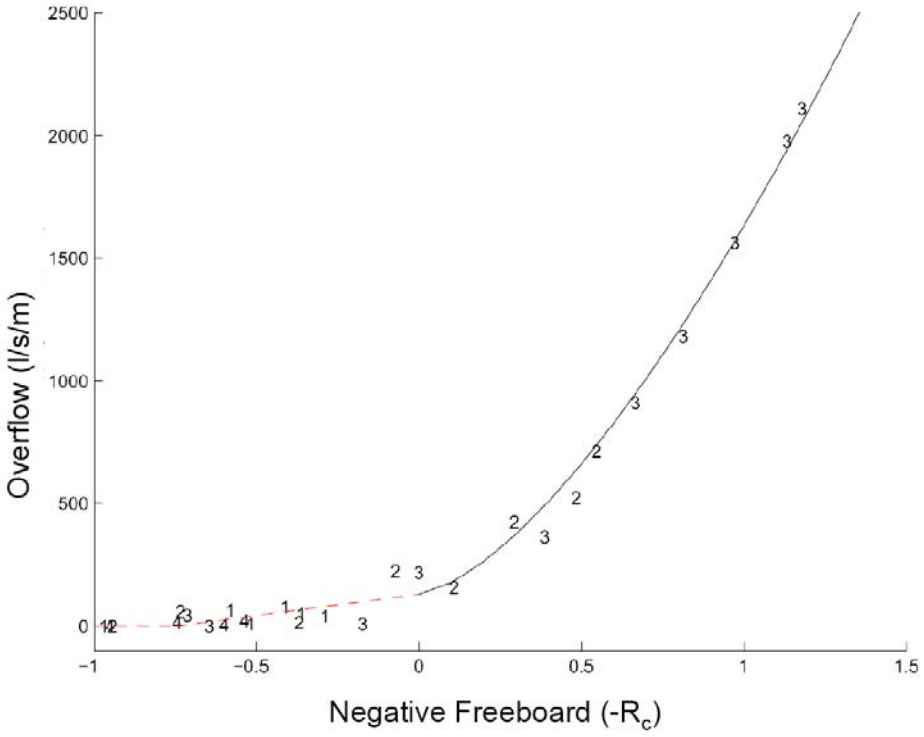

Figure 15.8. Modelled MRGO Levee Overtopping versus Simple Equation
Lynett et al 2010

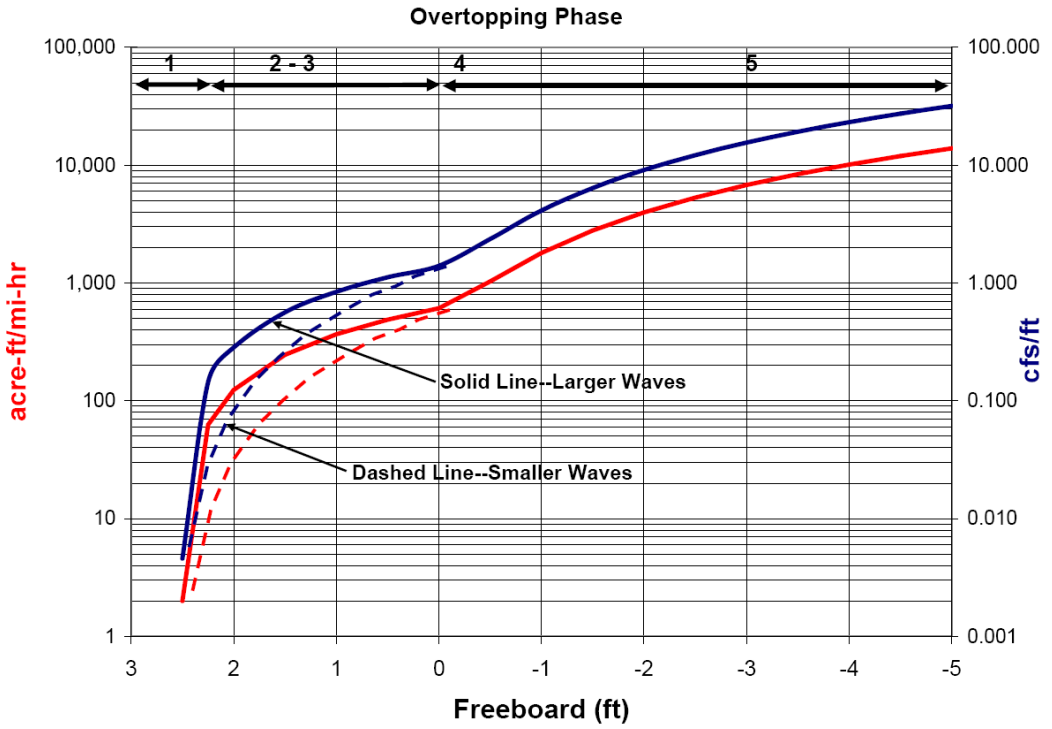

Figure 15.9. Simple Overtopping by Phase

based on Lynett et al 2010

As noted above, when wave contributions to overtopping are significant the overflow is not steady but pulsates. The variability in the instantaneous overflow discharge can be extreme, with peak rates more than 100 times the average (USACE CEM p., VI-5-19), exacerbating potential protected-side scour and breach hazards. In 2008 Hughes reviewed the empirical equations for wave-only overtopping and provided additional equations for determining overflow depth and velocity exceedance levels along the interior slope. In one example Hughes showed that an average overtopping discharge of 0.1 cfs/ft could include a 50% exceedance velocity (the velocity exceeded by an average of 5 out of every 10 waves) of over 17 ft/s at a distance of 20 ft down the inside levee slope.

15.4 Breaching

Breaching dynamics are often quite complex and experts often disagree on the exact sequence and relative importance of various contributing mechanisms.[8] While a detailed discussion of breach processes is beyond scope of this report, a brief overview is warranted.

Breaching is a failure to some degree in the integrity of a polder perimeter barrier which allows a significant increase in surge inflow that would not have otherwise occurred during seepage or overtopping. Two important broad categories of breaches are those *with erosion and those without erosion, i.e., a pure collapse*. A third category includes unsecured openings, such as gates left open and

[8] For a further detailed assessment of Hurricane Katrina breaches see IPET 2006, ILIT 2006, and Team Louisiana 2006.

temporary barriers insufficient to withstanding exterior conditions. A variety of breach processes that occurred in Hurricane Katrina along New Orleans area perimeter system are shown in Figure 15.10.

Exterior- and interior-side erosion of soil on barrier embankment surfaces can lead directly to barrier breaching. Exterior-side erosion can occur with extremely high currents or current eddies (with velocities of several ft/s) acting along the embankment—in a manner similar to river bank erosion. Waves breaking and running up the exterior-side of an embankment can also cause erosion—in a manner similar to shoreline beach erosion (Figure 15.10.a). On the protected side, free-falling water over steep walls or crowns and accelerating down-slope overflows can quickly erode soils (Figures 15.10.b, c, d, e, and f).

Both exterior- and interior-side erosion can be exacerbated by the presence of weak, non-cohesive soils; exposed soil surfaces (e.g., due to absence of well-rooted vegetated cover or armoring); and transitions. Transitions—such as embankment slope changes (e.g., at the toe of the interior slope) and interfaces between soil embankments and other structures (e.g., exposed concrete or steel walls, aprons, pads, footings, piers, pipes, etc.)—create localized horizontal and vertical turbulence zones containing much higher velocities easily capable of initiating erosion; (Figure 15.10.e; the presence of the pipe rack and vehicle traffic over the levee were also hypothesized as pre-storm subsidence and erosion of the local crown, making this point vulnerable to overtopping).

Wherever the velocities of exterior currents and waves or interior overflow exceed erosion thresholds soil scour can begin. Once surface scour starts, the underlying soils are exposed to rapid erosion (e.g., from high velocity in the scour scar) and the initial opening can be quickly expanded. At critical weak points, both exterior- and interior-side erosion breaches can easily proceed from initial scour to a major crown breach in less than an hour.

If local conditions focus intense wave energy at a location, exterior-side erosion can lead to crown sloughing, creating a breach to rising surge. This type of failure has been hypothesized for portions of the MRGO levee during Hurricane Katrina (see Figure 15.10.a), ILIT 2006). During levee overtopping, interior-side erosion (which often starts at the slope transition at the toe of the slope) can rapidly scour upslope—referred to as “head cutting”—until it reaches the crown, where the erosion can then widen and deepen a breach (Figure 15.10.b). The USACE hypothesized that interior-side erosion led to most of the MRGO levee breaches (IPET 2006).

During pulsing overflow the high velocities associated with peaks can induce erosion (Figure 15.10.c and d). Along with the pulsating overflow rate, the depth and velocities of the overtopping vary widely on the barrier protected-side slope. Rapid depth and velocity changes can also produce sudden pressure changes on the wetted surface—including cavitation effects that can initiate erosion in soils with weak cohesive strength.

Breaches can also occur in the absence of erosion due to component movement and collapse. The component may be a floodwall, a supporting foundation structure (e.g., footing, pile member, etc.), a soil embankment, or even the natural underlying or adjacent soil. A crucial cause of movement is the differential static water pressure acting on the exterior and interior sides of the component, which at some magnitude can exceed the strength of the component and its related support to resist movement. When beyond strength tolerances, the magnitude of the differential pressure and associated movement can proceed in accelerating, exacerbating, increments. In the case of a vertical floodwall with a vertical sheet-pile support (termed an “I-wall”) when exterior-side SWLs exceed tolerances the wall can start to deflect, causing a further increase in stress, and then a further deflection and so on rapidly leading to a critical point of sudden and catastrophic collapse (Figure 15.10.g and h). The USACE considered this the primary contributing factor in the 17th St. Canal floodwall failure.(IPET 2006).

a. MRGO South Levee Erosion from Waves (ILIT 2006)

b. Overtopping Scar and Breach Initiation at New Orleans East Lakefront (Suhayda and Jacobsen 2005)

Figure 15.10. Breach Processes Illustrated During Hurricane Katrina

c. Pulsing Overtopping Flow at GIWW North Levee (IPET 2006)

d. Same Location Showing Erosion, No Breach (IPET 2006)

Figure 15.10. Breach Processes Illustrated During Hurricane Katrina (Continued)

e. Scour of Mississippi River West Bank at BP Refinery Pipe Rack (Jacobsen 2006)

f. Interior-Side Scour from Overtopped I-Wall, with Deflection, IHNC East (IPET 2006)

Figure 15.10. Breach Processes Illustrated During Hurricane Katrina (Continued)

g. I-Wall Deflection on London Ave Canal, No Overtopping (IPET 2006)

h. Translation of 17th St. Canal East I-Wall (IPET 2006)

Figure 15.10. Breach Processes Illustrated During Hurricane Katrina (Continued)

Barrier soil components—the barrier's underlying foundation, the barrier itself (in the case of an embankment), and the earth at the barrier's interior toe—are important supports to motion resistance. Reductions in either soil density or internal cohesion can weaken resistance to uplift (or "heaving") and lateral sliding. The sand boils at the London Avenue Canal floodwall breaches are an example of this failure mode.

Levee interior-side scour can remove significant mass to the point that slopes or interior toe foundations fail before crown erosion occurs. Similarly, floodwall interior-side scour from free-fall overtopping can weaken the interior soil's support of the wall, precipitating or exacerbating deflection and collapse. The USACE suggested that interior erosion was a major factor in a floodwall collapse along the eastern IHNC floodwall just north of the Claiborne Avenue bridge.

Natural and man-made seepage pathways can allow the rapid transmission of exterior-side water pressures through the groundwater, creating higher pore-water pressures in protected-side foundation soils, and causing them to expand and weaken. A separate floodwall breach on the eastern IHNC near Florida Avenue, which occurred during Hurricane Katrina hours before SWL reached overtopping levels, was found to be associated with seepage induced interior soil movement (IPET 2006).

Engineers employ "failure rules" for basic breaching mechanisms that can be applied to individual reaches/transitions. These failure rules describe the conditions—i.e., breach invert and length (I-L)—that would result at reach due to the various location-specific factors in combination with the time-varying exterior SWL. The location-specific factors can be summarized as:

a. Type—levee, I-wall, T-wall, gate, levee-floodwall transition, etc.;

b. Critical Design Features—elevation, embankment soil type (e.g., clay versus hydraulic fill), slopes, pile depths, etc.; and

c. Reach Geology—depth and permeability of seepage zones; depth, density, and cohesive strength of overlying soils; presence of seepage pathways; etc.

A failure rule for seepage induced breaching could specify I-L as a function of estimated soil pore water pressures at the interior barrier toe. These pressures would be estimated using the reach-specific geology information and the exterior and interior SWLs. A failure rule for erosion or collapse breaching at reach with given location-specific factors might specify breach I-L as a "step function" of R_c—with a lower I resulting from increasingly negative freeboard to some limit. A very simple breach failure rule would be to specify only a single step—e.g., a single I-L for each reach based on the peak exterior SWL.

Rather than specifying an absolute I-L step or steps, the failure rules can be written to account for uncertainty in each step. For example, the probability of a particular I-L step can start at 0 and become 1.0 as the negative freeboard worsens beyond the step threshold R_c. (For each exterior SWL the sum of all failure condition probabilities, including the no failure condition, must equal 1.0). The relationship between the probability of failure and the negative freeboard can be depicted in a "fragility curve" (or set of tabulated values). Figure 15.11 illustrates the concept of a fragility curve. Failure conditions and fragility curves can also be expanded to incorporate wave conditions and interior SWL.

At this time there is very limited empirical research for quantifying failure rules and probabilities (fragility expressions). As a result, polder inundation hazard analyses relying on these techniques primarily qualify as planning (or "what if") exercises.

For a polder-wide inundation analysis breach discharge can be estimated with stepped changes in the broad-crested weir equation. Most significant breach flow can be regarded as Phase 5 overflow (negative $\boldsymbol{R_c}$) and evaluated using the steady supercritical flow equation. The value of $|\boldsymbol{R_c}|$ will be

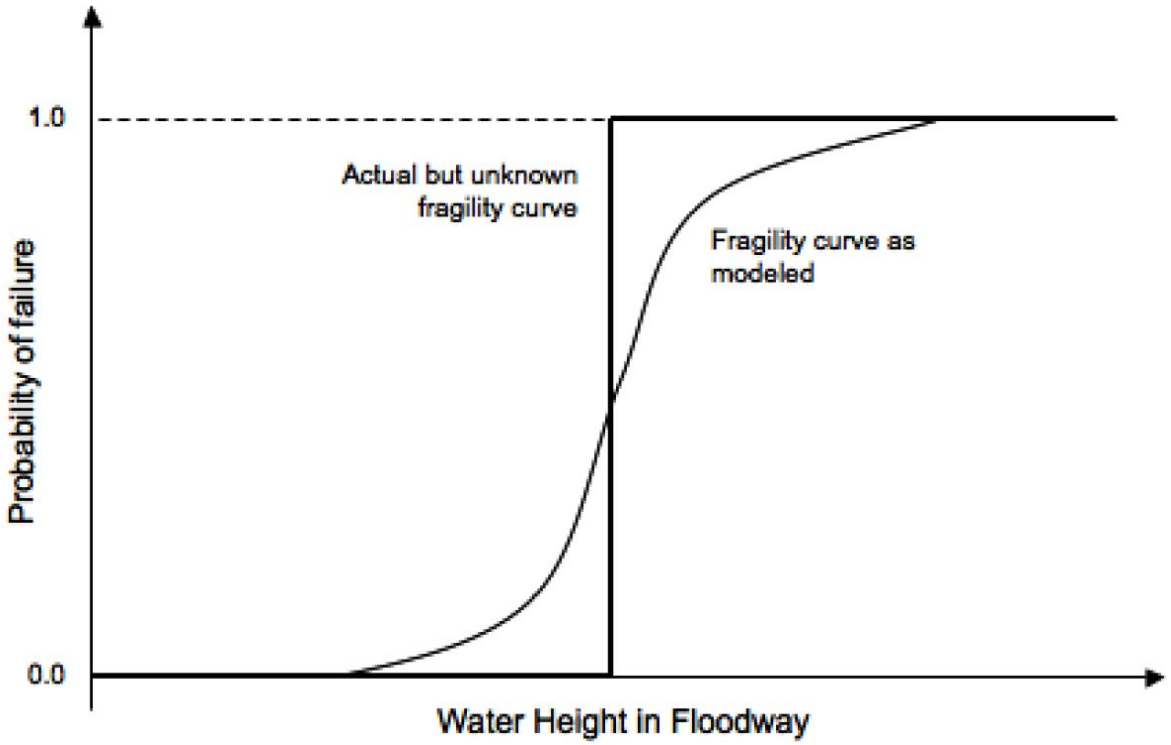

Figure 15.11. Concept of Fragility Curve For Breach Failure
IPET 2009

determined by the SWL and average breach invert. If the breach invert deepens over time (or as the exterior SWL changes), the value of $|R_c|$ can be adjusted accordingly.

As the interior SWL rises at some point the breach invert may be submerged (or "drowned"), in which case the inflow discharge will be affected by the interior tailwater elevation. A steady submerged flow equation for a broad-crested weir can be applied that takes into account both the exterior and interior SWL height above the breach invert—i.e., $|R_{c\text{-Exterior}}|$ and $|R_{c\text{-Interior}}|$ at the breach. The Villemonte equation for submerged flow equation multiplies the supercritical equation by a second transmission factor, C':

$$C' = \left[1 - \left(\frac{R_{c-Interio\ r}}{R_{c-Exterior}}\right)^{1.5}\right]^{0.385}$$

Another version of the submerged weir flow equation is

$$q = C_{sub}\,|R_{c\text{-Interior}}|\sqrt{2g\left(\left|R_{c-Exterior}\right| - \left|R_{c-Interior}\right|\right)}$$

which is used for $|R_{c\text{-Interior}}| > 0.667|R_{c\text{-Exterior}}|$.(ADCIRC Development Group, http://www.adcirc.org). This equation uses a separate submerged transmission coefficient, C_{sub}:

Submerged and supercritical broad-crested weir equations can also be used to analyze breach outflows, which occurs when the exterior surge SWL falls below the internal SWL (i.e., $|R_{c\text{-Interior}}| > |R_{c\text{-Exterior}}|$).

The equations for supercritical and submerged breach discharge are highly sensitive to the choice of transmission coefficients. Appropriate values for levee or floodwall breach discharges have not been studied. Laboratory and field scale experimental data are needed to assess the fit of the broad-crested weir equations. In practice, lower transmission coefficients are applicable for breaches than for overtopping of a pre-breach barrier due to much rougher openings.

The above methods for analyzing polder-wide inundation are not applicable to interior conditions in the vicinity of the breach, especially in the moments following a sudden collapse. Detailed hydraulic studies of these conditions—including shock waves—require specialized "dam break" type analysis.

A very simple failure rule is specifying an invert that remains continuously submerged, i.e., below the final exterior SWL. In this case the polder interior SWL eventually equalizes with the exterior SWL. This occurred in Orleans Parish portion of the Metro New Orleans Polder the day after Hurricane Katrina landfall due to the low breach inverts along the 17th Street and London Avenue canals. The interior sub-basins connected to these breaches equalized with Lake Pontchartrain at between 2.5 and 3.0 ft NAVD88. For a polder hazard analysis this simplification makes level-pool routing easy—i.e., it is not necessary to calculate inflow rates. However, this simplified rule cannot account for massive breaches with interior levels peaking at higher, earlier SWLs, such as with the Lower 9th Ward/St. Bernard polder which reached interior SWLs above 10 ft NAVD88 in many areas during Hurricane Katrina.

15.5 Rainfall Accumulation

Throughout the CN-GoM, major rainfall events have often been associated with tropical cyclones. Under weak meteorological steering conditions, the forward motion of lower intensity tropical cyclones may become very slow and erratic, leading to prolonged rainfall, as exemplified by Category 1 Hurricane Juan (1985), Tropical Storm Allison (2001), and Hurricane Isaac (2012) compared to Category 3 Hurricane Katrina (2005), shown in Figure 15.12. Tropical cyclone precipitation can vary widely over short distances, as illustrated by the rainfall totals in Figure 15.12. A major reason is the "training" of intense rainfall cells within bands circulating the storm core. In slow moving storms a band may continue to pass over a location for many hours, subjecting it to repeated downpours from passing cells, while sites less than 10 miles receive a fraction of the heaviest rainfall.

Precipitation amounts for actual storms are estimated by the National Weather Service using meteorological rainfall gauge stations and radar reflectivity data. Due to rainfall spatial variation and the scarcity of gauge stations, radar reflectivity often provides a better estimate of precipitation on a sub-basin scale.

Low-lying, poorly-drained coastal areas can experience large rainfall amounts in addition to surge. For areas outside of polders, rainfall accumulations need to be added to the surge routing model to determine the total SWL. High resolution 2D models—such as the ADCIRC model—are expected to include rainfall in the near future (see Section 10.1) [9]

[9] Rainfall from tropical cyclones further inland can produce major river flooding. In the floodplains surrounding a coastal river outlet the inundation levels may be influenced by three hydraulic processes: a) residual surge that has yet to fully recede; b) direct rainfall in the locale; and c) river discharge. This type of combined flooding recently occurred in lower Livingston, Ascension, and St. James parishes at the mouth of the Amite and Blind Rivers in Lake Maurepas following Hurricane Isaac (2102). High resolution 2D surge modeling capabilities for these complicated flood events are also being developed.

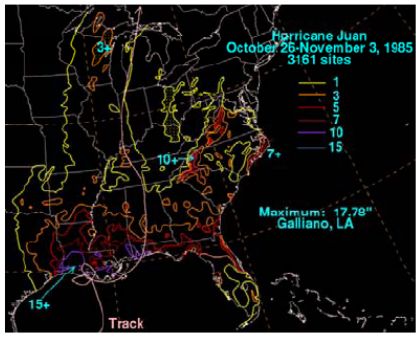

Hurricane Juan (1985)

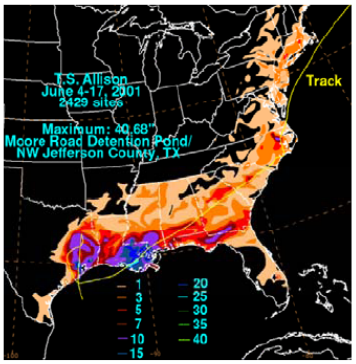

Tropical Storm Allison (2001)

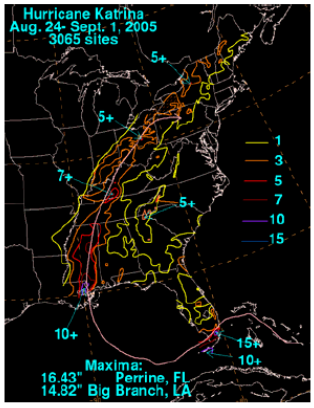

Hurricane Katrina (2005)

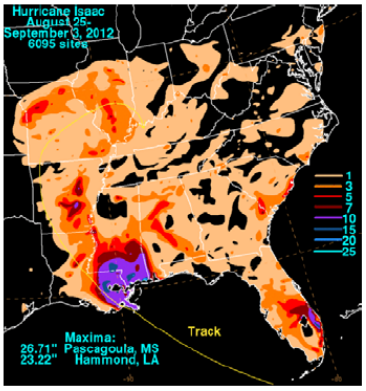

Hurricane Isaac (2012)

Figure 15.12. Example CN-GoM Tropical Rainfall Totals

http://www.hpc.ncep.noaa.gov/tropical/rain/

For surge events that threaten to flood a polder, the interior rainfall must be added to the perimeter inflows. The polder rainfall accumulations are usually considered according to internal "sub-basins," such as those depicted in Figure 15.1, which are delineated according to respective forced-drainage systems (i.e., conveyance network and pumping).

A small portion of precipitation which would otherwise contribute to inundation can be lost to:

- Interception of moisture above the ground (e.g., by tree leaves, rooftops, etc.);
- Evaporation near the ground surface; and
- Infiltration into the shallow soil, which is restricted by antecedent soil moisture and soil permeability.

In low-lying areas of southeast Louisiana such losses during tropical cyclone rainfalls probably equate to less than 0.1 ft of precipitation.

Meteorologists have evaluated generalized correlations of large scale rainfall precipitation with hurricane parameters, including intensity, size, and forward speed and some accounting for asymmetries (see, Lonfat et al 2004, Lonfat et al 2007, and Langousis and Veneziano 2008). However, generalized models have not been produced which describe highly localized rainfall variations.

15.6 Drainage Pumping

Polders require forced drainage systems to accommodate residual rainfall flood hazards and to operate during surge events (subject to limitations) to remove inundation water. The forced drainage systems typically have four components:

1. Local gravity collection systems, comprised of subsurface pipelines ranging up to several feet in diameter;
2. The major gravity channel network, which encompasses large open as well as covered canals (often concrete lined);
3. Local lift stations, which aid in transferring storm water from particularly low areas within the polder to the major gravity channel network; and
4. Perimeter pump stations which remove water at terminal points in the major gravity channel network and discharge into exterior water bodies.

The various components of the interior forced drainage systems typically have limited design capacities.[10]

The overall discharge rate at each perimeter pump station is controlled by the pump mechanical capacity, which is subject to the difference between exterior and interior SWL conditions. As the exterior to interior differential rises, the pump has to do more work and the discharge rate declines. Similarly, as the differential falls, discharge rates increase. The changing pump discharge with SWL differential is not linear and is specified by the manufacturer with an associated uncertainty. A pump station usually include many pumps—with varying capacities designed to come online in stages to accommodate the gravity channel inflow. Overall pump tables relating discharge to the SWL differential, with uncertainty, can be prepared for each station as a whole.

During polder inundation, pump stations may be subject to outages due to:

- Loss of power, including back-up power (e.g., flooding of generators, exhaustion of back-up generator fuel);
- Submergence of electrical or mechanical components;
- Shutdowns or start-up failures by automated control systems (e.g., due to loss of cooling liquid and trigger of temperature limits); and
- Absence of manual control (operators may have been removed or they may be unable to access controls).

Table 15.3 summarizes pump station operating capacity in the various New Orleans regional polders during Hurricane Katrina inundation. For the Metro New Orleans polder less than 10% of the rated capacity was operational. In general. for planning purposes IPET and the USACE have used overall pumping capacity alternatives of 0, 50, and 100% (IPET 2009). However, they have not assessed the probabilities of these alternatives.

---

[10] Many urban drainage conveyance/pumping systems are designed to only accommodate a 10-year return frequency rainfall event and accept that low polder areas will experience occasional "flash flooding." (see http://tg.jeffparish.net/index.cfm?DocID=1162)

Table 15.3. New Orleans Area Pump Station Hurricane Katrina Outages

IPET 2006 (Volume VI)

	Rated Capacity (cfs)	Pumped During Katrina?
I) Orleans Parish		
A) East Bank (E-3)		
1) OP 1 – PS 1	6825 cfs	No
2) OP 2 – PS 2	3150 cfs	No
3) OP 3 – PS 3	4260 cfs	No
4) OP 4 – PS 4	3720 cfs	No
5) OP 5 – PS 5	2260 cfs	No
6) OP 6 – PS 6	9480 cfs	No
7) OP 7 – PS 7	2690 cfs	No
8) OP 12 – PS 12	1000 cfs	No
9) OP 19 – PS 19	3650 cfs	Yes
10) OP I 10 – PS I 10	860 cfs	Yes
11) OP 17 – PS 17	625 cfs	No
12) Whitney-Barataria	3750 cfs	No
13) Pric – Prichard	253 cfs	No
14) Mont – Monticello	99 cfs	No
B) East Bank (E-4a)		
1) OP 10 – PS 10 Citrus	1000 cfs	No
2) OP 14 – PS 14 Jahncke	1200 cfs	No
3) OP 16 – PS 16 St Charles	1000 cfs	Yes
4) OP 18 – PS 18 Maxent	60 cfs	No
5) OP 20 – PS 20 Amid	500 cfs	No
6) DR – Dwyer Rd	120 cfs	No
7) GS – Grant	192 cfs	No
8) Elai – Elaine St	90 cfs	No
9) OP 15 – PS 15	750 cfs	No
C) West Bank (W-3b & W-4b)		
1) OP 13 – PS 13 (W-3b)	4650 cfs	No
2) OP 11 – PS 11 (W-4b)	1670 cfs	Yes
II) Jefferson Parish		
A) East Bank (E-2)		
1) PS 1 – Bonnabel	3750 cfs	Yes
2) PS 2 – Suburban	5440 cfs	No
3) PS 3 – Elmwood	5700 cfs	No
4) PS 4 – Duncan	4800 cfs	No
5) PS 5 – Parish Line	900 cfs	No
6) Canal Street	160 cfs	Yes
B) West Bank (W-1)		
1) LC1-PS – Lake Cataouatche 1	500 cfs	No
2) LC2-PS – Lake Cataouatche 2	600 cfs	No
3) BS-PS – Bayou Segnette	936 cfs	No
4) H90-PS – Highway 90	90 cfs	
C) West Bank (W-2)		
5) A-PS – Ames	1930 cfs	No
6) W-PS – Westminster	1200 cfs	No
7) C2-PS – Cousins 2	2300 cfs	No
8) E2-PS – Estelle 2	1140 cfs	No
9) C1-PS – Cousins 1	960 cfs	No
10) Harv-PS – Harvey	960 cfs	Yes
11) W2-PS – Westwego 2	936 cfs	No
12) EST1 – Estelle 1	550 cfs	No
13) WEG1 –Westwego 1	300 cfs	Unk
14) MTKN – Mt Kennedy	274 cfs	Unk
D) West Bank (W-3)		
15) Hero-PS – Hero	3902 cfs	No
16) P-PS – Planters	2360 cfs	No
III) St Bernard Parish		
A) East Bank (E-5a)		
1) F-1 – PS 1 Fortification	1245 cfs	No
2) M-4 – PS 4 Meraux	1245 cfs	No
3) JL-6 – PS 6 Jean Lafitte	1000 cfs	No
4) BD-7 – PS 7 Bayou Ducros	1017 cfs	No
5) SM-8 – PS 8 St Mary	834 cfs	No
6) BV-3 – PS 3 Bayou Villere	500 cfs	No
7) G-2 – PS 2 Guichard	350 cfs	No
8) EJG-5 – PS 5 E.J. Gore	660 cfs	No

15.7 Internal Routing

The spatial patterns of surge inundation and circulation over exposed coastal urban areas are controlled by the 2D depth-averaged physics described in Section 6.1. Open coast urban surge inundation can therefore be evaluated with the 2D depth-averaged hydrodynamic model codes employed in surge analysis (see Section 8)[11]—which has been done for many decades under coastal FISs. In recent years, high resolution FIS 2D ADCIRC surge models have addressed the inundation of low-lying coastal urban

[11] Hydrologists have applied 2D dynamic routing models (e.g., RMA2, MIKE21, SOBEK, TUFLOW, see Néelz and Pender 2009) to the inundation of urban areas in complex river floodplains for more than a decade. 1D dynamic river floodplain models—e.g., HEC-RAS, OTHER FEMA/DOT MODEL, MIKE 11—have been used since at least the mid-1990s (see USACE 1997). Use of steady-state flood models for river urban areas has an even longer history.

areas such as Gulfport/Biloxi in Mississippi (Hurricane Katrina) and Galveston/Houston/Port Arthur Texas (Hurricane Ike). No special modifications to the surge modeling applications described in Section 11 were required for these areas.

Polder inundation routing, however, must address the local, time-varying seepage, overtopping, breaching, rainfall, and pumping (SOBRP) processes occurring around and within the polder, as well as internal conditions:

- Detailed interior topography—including gradients toward low areas within the polder;
- Major internal gravity drainage features—such as canals which collect and convey stormwater to the major pump stations;
- Natural and man-made internal barriers—such as topographic ridges and elevated railroad and road embankments, which can modify internal circulation; and
- Major openings in the internal barriers—such as canal crossings (bridges and large culverts).

Figure 15.13 illustrates the internal features for the New Orleans East Polder in southeast Louisiana.

Internal topography is generally developed from high resolution DEMs (see GTN-2). In the case of southeast Louisiana, such models may include errors in excess of 1 ft due to vertical control issues, as well as inherent uncertainty on the order of 0.5 ft.

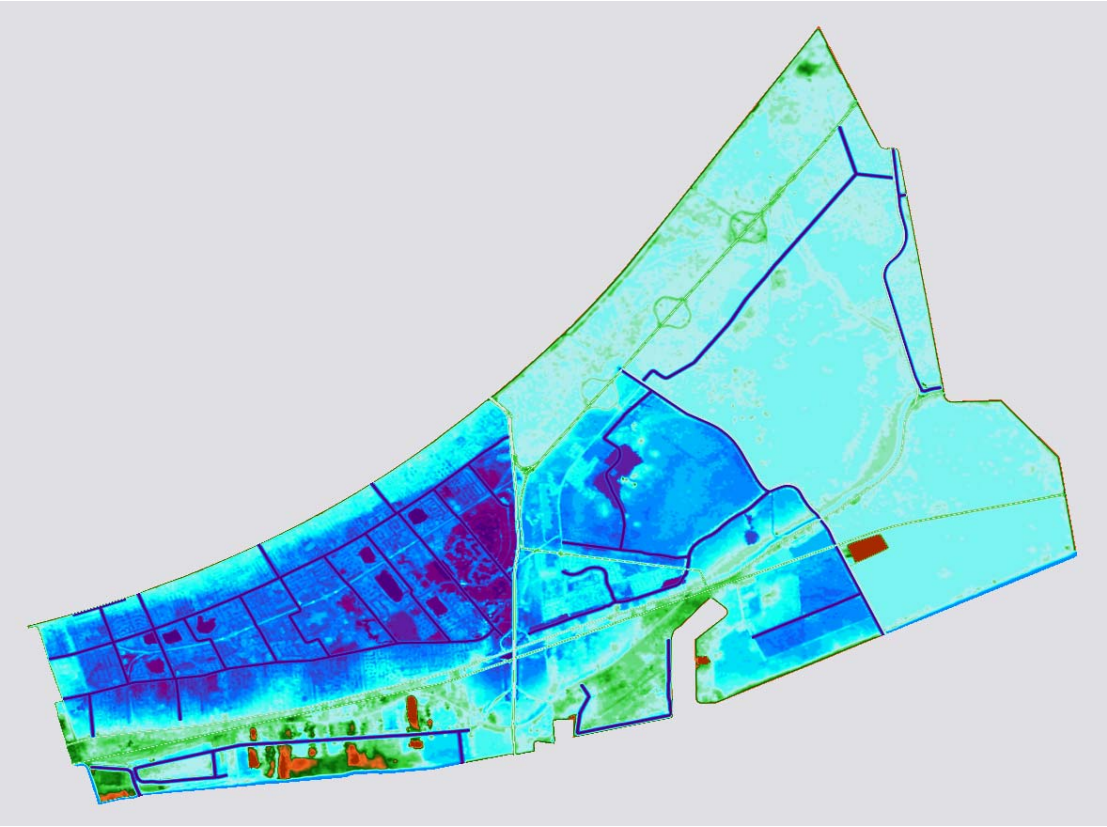

Figure 15.13. Features of New Orleans East Polder

Modified from LIDAR DEM to include channels

The unstructured meshes of high resolution 2D surge models, such as ADCIRC, can be refined to represent many of these conditions, subject to the general modeling limitations discussed in Sections 8 and 10 , including:

- Choice of numerical method (finite difference/element/volume, explicit/implicit, etc.) and associated settings and grid versus unstructured mesh;
- Model time-step requirements (e.g., for Courant stability condition);
- Treatment of acceleration terms; note that momentum terms for tide, Coriolis, and wave radiation stress gradients can typically be ignored for internal polder routing;
- Wetting and drying subroutines (e.g., control of gradients and oscillations);
- Resolution of the grid/mesh to depict topographic and bathymetric features and interior landscape conditions;
- Accuracy of the source topographic, bathymetric, and landscape data.
- Assignment of bottom friction coefficient values for land covers ranging from dense underbrush to open pavement to congested urban development; and
- Choice of eddy viscosity value.

Greater refinement of polder meshes allows a "high definition" depiction of spatial patterns of inundation associated with particular inputs and internal features.

The high resolution 2D surge models can have limitations when applied to polder routing, such as:

- Mesh refinement cannot capture sub-mesh scale interior drainage conveyances (e.g., storm sewers);
- The model may not address important interior mechanical structures—e.g., timed gates and lift stations;
- Some codes (e.g., ADCIRC) do not currently provide for sub-basin scale rainfall inputs;
- The code may not support assessment of interior near-breach inundation conditions. The initial inundation just inside the breach can experience supercritical (e.g., very steep) flow and shock waves. Simulating these conditions requires modeling of complex depth/velocity dynamics, as well as hydraulic jumps, similar to those associated with dam break scenarios. General 2D inundation models, such as ADCIRC, do not address these dynamics just inside the breach.

Code developers (e.g., ADCIRC Development Group) are currently researching ways to provide these capabilities.

The magnitude of high resolution 2D routing uncertainties—apart from uncertainties regarding inflows, outflows, and internal conditions—has not been thoroughly evaluated in the technical literature. Detailed sensitivity studies and hindcast validations for urban floodplain routing are not currently available.[12]

[12] The southeast Louisiana FIS Hurricane Katrina hindcast model provided some representation of the polders within the overall domain in order capture effects on regional exterior surge routing. However this model was not validated for the interior polder flooding.

Under some scenarios inundation can be nearly uniform polder-wide, with little spatial and temporal variation in interior SWL.[13] If these cases the hydrologist can employ a basic stage-storage relationship, which dictates the volume of water associated with a level pool at any given increment of SWL. In level-pool routing the net cumulative input volume at any time—cumulative rainfall and perimeter inflows minus cumulative pumping discharge—will equate to a specific polder-wide internal SWL. This simple level-pool routing method is often used for reservoirs and its accuracy and precision depend on the quality of inflow, outflow, and terrain information.

The level-pool routing method may be refined by dividing the inundation analysis according to several individual polder sub-basins, and providing for stage dependent exchange relationships between sub-basins—such as a broad-crested weir equation. As the number of sub-basins increases and interconnections become too complex for simple exchange relationships, 2D routing becomes a more effective tool for simulating spatially varying inundation. Sensitivity tests can be used to assess the degree of routing improvement with sub-basin refinements, as well as 2D routing.

To analyze inundation for any particular surge hindcast or scenario the interior routing model is coupled with a SOBRP model, which incorporates the methods described in Section 15.2 through 15.6:

- Seepage—simple SWL-dependent groundwater flow equations, parameterized to reflect local geology and infrastructure information, are used for those scenarios and reaches which may have non-negligible seepage inflow.
- Overtopping—reach-specific deterministic equations are employed to estimate inflows as a function of storm SWL (R_c) and waves. Reach-specific equations incorporate wave transmission coefficients (γ_r, γ_b, γ_h, γ_β) and weir coefficients (C_w, C, and C_{SUB}).
- Breaching—failure rules are used to describe potential breach dynamics—i.e., I-L at each reach/transition over time. Inflow rates are estimated using a broad-crested weir equation, which is a function of exterior and interior SWL, the breach I-L, and location-specific C or C'. (A simple failure rule for a deep I or long L could specify exterior-interior equalizing SWLs—e.g., at some time following peak exterior SWL—an eliminate the need for internal routing to assess peak interior inundation.)
- Rainfall—sub-basin accumulations are expressed as assumed quantities (e.g., a 24-hr/100-yr volume) or a hypothesized function of hurricane attributes, providing higher rainfall rates for slower moving storms.
- Pumping—withdrawal rates at each station are expressed as a tabulated function of local exterior and interior SWL.

The SOBRP model is *two-way* coupled with the interior routing model—the SOBRP output drives the routing model and the routing model output contributes to flow computations for pumping and submerged breaches. The SOBRP model in turn is *one-way* coupled with the exterior surge model and local wave model—the exterior surge and local wave model outputs drive the seepage, overtopping, and breaching inflow computations. Two way coupling of the exterior surge and SOBRP models would be required to consider the effect of perimeter inflows (primarily breaching) on drawing down exterior

[13] The Hurricane Katrina inundation in the New Orleans Metro Polder reached a peak of about 2.5 ft NAVD88 fairly uniformly as interior water levels gradually equalized with Lake Pontchartrain for over 24 hours after the storm. On the other hand, massive breaches in St. Bernard Parish and along the eastern IHNC floodwall caused peak inundation in the Lower 9th Ward/St. Bernard Polder to occurr near noon on the day of the storm.

SWL and the further impact on regional surge. The SOBRP and internal routing models require time stepping on the order of a few minutes. No commercial or research software programs are currently available to address SOBRP modeling and the associated coupling.[14] However, as the individual process calculations are relatively straightforward, FORTRAN, MS-EXCEL, or MATLAB etc. can be readily used for simulating SOBRP and to accommodate the necessary file actions.

The influence of variability/uncertainty in SOBRP process inputs and parameters on the flow rates and cumulative volumes for a selected storm can be studied with sensitivity tests. If the tests are focused only on the SOBRP process at individual locations, coupling with the exterior surge and wave model, as well as the routing model, can usually be ignored. Sensitivity tests of a SOBRP factor can be performed for specific scenarios (e.g., ± 50% of some base value), or a range of values to reflect normally or non-normally distributed probability. Sensitivity tests can address a single factor in a single SOBRP process at a location or can be expanded to cover multiple factors in combined SOBRP processes at a location. A Monte Carlo technique can be employed to examine the influence of multiple uncertainties (see GTN-1, Part J). An example is assessing the sensitivity of the overtopping rate at a particular segment of given crest elevation to combined uncertainties in exterior SWL, H_S, and T_P.

It is important to note that the limited observations of SOBRP and interior HWMs—such as for Hurricane Katrina—have not enabled validation of polder inundation modeling.

15.8 Interior Wind Setup and Waves

If an inundated polder includes areas oriented with a long, open fetch—such as canals (e.g., the GIWW and IHNC sub-basin) or submerged roads and greenways—the hydrologist can also examine the influence of interior wind setup (on SWL and routing) and waves. Most 2D hydrodynamic models—and surge models specifically—can address the effects of local wind stress, including changing wind fields, on polder inundation patterns. Level-pool routing does not address interior wind setup but can be supplemented with simple wind setup analyses.

The wind setup, h, across a confined body of water (e.g., an inundated polder) is a function of:

- The wind speed, U, typically estimated measured at 10 m above the surface;
- The fetch length, L;
- The water depth (SWL minus bathymetric elevation), d;
- An air-water drag coefficient, $C_{Dair\text{-}water}$; $C_{Dair\text{-}water}$ can be adjusted for local air-water interface factors (e.g., waves) and canopy conditions—such as the presence of dense trees and buildings. and
- The specific gravity of air and water, ρ_{air} and ρ_{water}.

Wind stress on the water, τ_W, is given by

$$\tau_W = C_{D\,air-water}\,\rho_{air}\,U^2$$

[14] Dynamic breaching has been recently included in ADCIRC surge modeling and, as noted in Section 15.7, ADCIRC can be used for internal routing. However, ADCIRC cannot provide complete SOBRP modeling as it does not currently address seepage, Zone C/D waves, wave-related overtopping, and rainfall. Thus, integrated modeling of surge and SOBRP processes within ADCIRC is beyond the current state-of-the practice.

A simple 1D approximation for a steady-state wind setup is given from a balance of the wind stress and hydrostatic forces (ignoring bottom friction and other forces):

$$h = C_{D\,air-water}\frac{\rho_{air}}{\rho_{water}}\frac{LU^2}{g\,d} \text{ with } C_{D\,air-water}\frac{\rho_{air}}{\rho_{water}} \approx 2.0\,x\,10^{-6}$$

Thus, a sustained 60 mph (88 ft/s) wind over an open 5 mile (26,400 ft) fetch with an inundation depth of 10 ft can contribute approximately 1.3 ft of setup. For a deeper water body—e.g., 30 ft—the setup would be 0.4 ft. To date there have been no empirical studies or hindcasts of localized wind setup acting within inundated polders to assist in addressing appropriate values for $\boldsymbol{C_{D\ air\text{-}water}}$ or canopy-induced wind stress reduction.[15]

Local winds acting on long open fetches also generate interior waves. Such waves can expose property that is above the SWL to flood damage. If interior wave heights reach several feet they can also influence polder SWL patterns through wave setup (see Section 6.2). However, for smaller wave heights interior wave setup can usually be ignored in a 2D routing analysis.

The wave field in a confined area at particular local wind speed is likely to be limited by depth, and breaker parameters can be used to provide a ceiling for interior, downwind H_S or $H_{1\%}$.[16] Wave heights can be further limited below the depth controlled ceiling, by:

- Insufficient fetch;
- The short duration of sustained peak winds along a particular fetch orientation;
- Bottom friction effects; and
- The fetch width, with narrower fetches introducing dampening;

For polders the actual applied winds at the water surface must also be reduced to account for canopy conditions. To estimate upper bounds on wave field $\boldsymbol{H_S}$ and T_p[17] in an open, confined water body, simple methods for wind wave generation normally consider only fetch and duration limitations and ignore possible limitations due to depth, bottom friction, and fetch width. Several simplified methods include:

- Sverdrup-Munk-Bretschneider (SMB, Bretschneider 1970),
- Wilson (1965),
- Donelan (1980),
- Joint North Sea Wave Project (JONSWAP, Hasselman et al 1973), and
- CEM (USACE 2006)

Figure 15.14.a and b illustrate estimated $\boldsymbol{H_S}$ and T_p for fetch-only limited conditions using the CEM method. A sustained 60 mph (27 m/s) wind over a 5 mile (8 km) fetch can induce $\boldsymbol{H_S}$ on the order of 4 ft.

[15] The Hurricane Katrina interior HWMs were of widely varying quality and—combined with wind and other data limitations—have made such a detailed hindcast of polder routing difficult.

[16] As noted in Section 10, the NFIP employs the 1% wave a breaker parameter of 0.78

[17] Wind wave $\boldsymbol{H_S}$ is often also assumed to reflect a JONSWAP distribution for the wave energy spectrum.

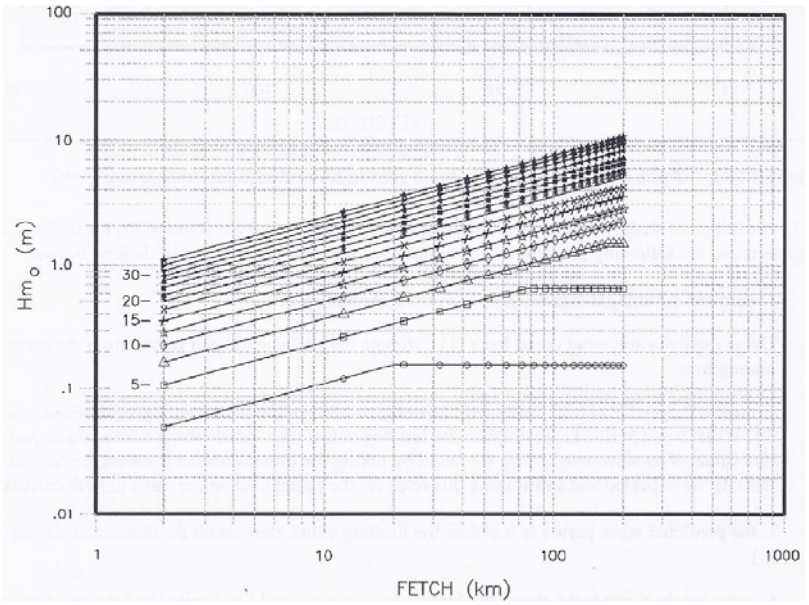

a. Wave Height

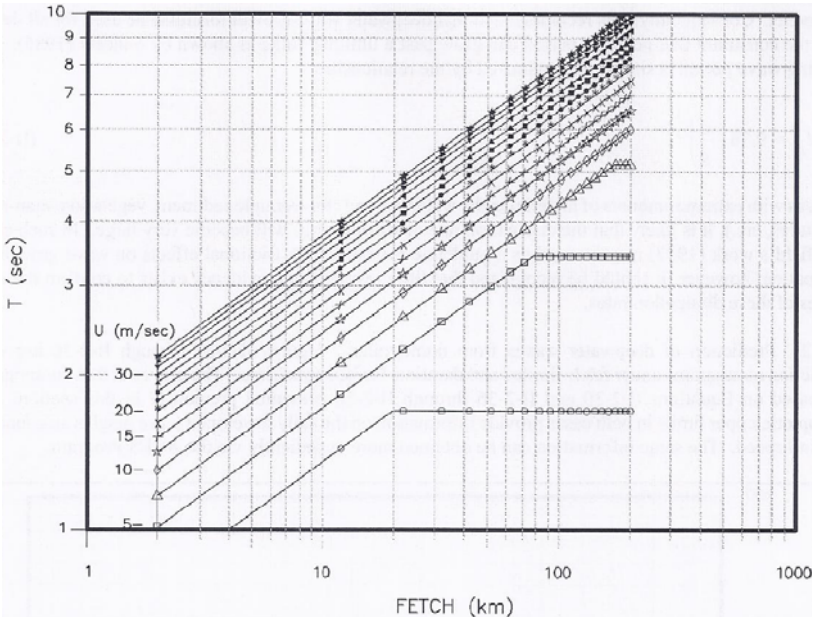

b. Wave Period

Figure 15.14. Fetch Limited Wave Heights and Periods (Winds in 2.5 m/s increments)
USACE 2006

In 2009 Etemad-Shahidi et al published a comparison of the SMB, Wilson, and CEM methods for predicting waves in fetch-only and fetch+duration limited conditions using wave data from Lake Ontario. Under fetch-only limiting conditions they found that all three methods exhibited slight height over-prediction bias, with the CEM method having the lowest bias. All three methods had similar scatter index values of about 25 to 28%. However, under fetch+duration limited conditions the methods

exhibited more notable under-prediction bias, as well as much higher SI values. The CEM method performed the worst in the fetch+duration limited condition.

FEMA FIS guidance (FEMA 2008) provides for use of these simplified methods in sheltered water bodies, and 1D wind-wave modeling codes (e.g., WHAFIS) and 2D codes (e.g., STWAVE or SWAN, see Section 9) for complex interior coastal regions.

While wind waves in shallow estuaries, bays, lakes, and harbors have been studied, no literature has been identified for channels or inundated polders.

Section 16. Polder Inundation JPA

16.1 Polder Inundation Hazards

Analysis of polder inundation hazards associated with hurricane surge events as described in Section 15 does **not** address three separate, independent and additional probabilities of polder flooding from:

a. Severe tropical rainfall only, i.e., without surge-driven inundation. Rainfall only accumulations with tropical cyclones can easily exceed the commonly referenced 25-year return period, 24 hour duration magnitudes—on the order of 9 to 11 in for southeast Louisiana (Faiers et al 1997). During Tropical Storm Allison (2001) over 15 in of rainfall fell in one 24-hr period, and nearly 30 in over the course of the storm, at Thibodaux Louisiana (NOAA NWS 2001).

b. Severe non-tropical rainfall events. On May 7-8, 1995 a non-tropical storm in southeast Louisiana produced up to 20 inches of rainfall, inundating some low areas inside the Metro New Orleans Polder by several feet (NOAA NWS 2005).

c. Non-surge perimeter failures. For example, portions of the New Orleans polder barriers fronting the Mississippi River protect the region from extreme river floods.

Within southeast Louisiana polders, some locations can experience significant flooding even during modest rainfall events. Internal topography—e.g., lower areas within the polder and the presence of sub-basin compartmentalization features—can cause localized ponding and higher hazard levels. Figure 16.1 illustrates the "bowl" characteristics of the Metro New Orleans polder. The performance of drainage pump stations and conveyance systems (which are typically designed only for 10-yr return rainfall events) can also influence localized inundation hazards. For large portions of the New Orleans regional polders, the rainfall-only 100-yr inundation depth is more than a foot.

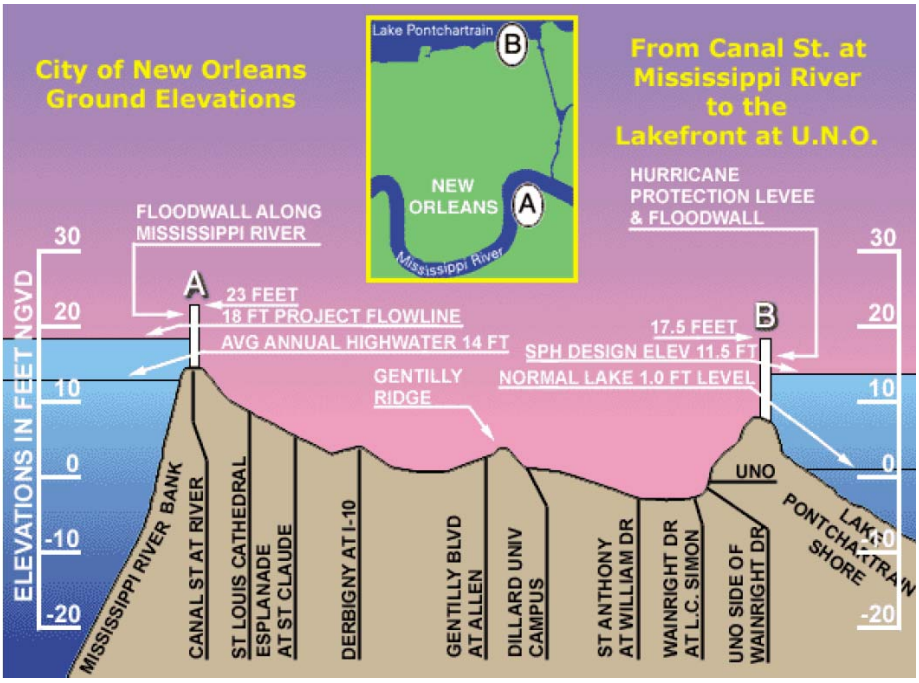

Figure 16.1. Metro New Orleans "Bowl"

(Note the Vertical Datum is outdated)

http://www.nola.com/weather/elevationsmap.html

A levee failure during an extreme Mississippi River flood (>800-yr return) has the potential to inundate the Metro New Orleans Polder to SWLs exceeding 15 ft—much higher than the equivalent >800-yr surge hazard. The technical approach to a combined assessment of all four inundation hazards—surge, tropical rainfall-only, non-tropical rainfall, and river flood—is beyond the scope of this report.

The sources of surge-related polder flooding described in Section 15 themselves pose different inundation hazards. Individual seepage locations alone (i.e., without breaching) pose the lowest hazard, with inflow discharges typically at much less than 0.1 cfs/ft (43.6 acre-ft/mi-hr). Minor-to-moderate overtopping at a reach can produce rates between 0.1 cfs/ft for positive freeboard with small waves to 4 cfs/ft (1,745 acre-ft/mi-hr) for a negative freeboard of 1 ft. The highest hazard is posed by major overtopping and breaching, with inflow rates capable of exceeding 20 cfs/ft (8,727 acre-ft/mi-hr) when SWL rises several feet above the barrier.

The equivalent volumes for five very simplified, steady inflow scenarios with six hour duration are:

Multiple Seepage/Small Wave Overtopping at 0.1 cfs/ft and 3 mi	785 acre-ft
Moderate Wave-Only Overtopping at 0.5 cfs/ft and 3 mi	3,924 acre-ft
Overtopping at 1 cfs/ft (<1 ft freeboard) and 3 mi	7,855 acre-ft
Major Breach at 20 cfs/ft and 2,000 ft	19,835 acre-ft[1]
Multiple Major Breaches at 20 cfs/ft and 10,000 ft	99,174 acre-ft

To put these inflow volumes in perspective Table 16.1 provides rainfall accumulation rates and volumes for the 6-hr/10-yr, 6-hr/100-yr, and 24-hr/100-yr hazards for the New Orleans area sub-basins (see Figure 15.1). The rainfall accumulation rate hazard is very localized, but for a point of reference volumes are summed using these rates across entire sub-basin areas. Inflow volumes for the first two scenarios are much less than the equivalent 6-hr/10-yr precipitation volumes for all five urban areas. The volume for the third scenario, <1 ft SWL overtopping, exceeds the 6-hr/10-yr precipitation volume for St. Charles parish urban area, but is well under the 6-hr/10-yr volumes for the other areas. The volume for the fourth scenario, a single breach, is less than the 24-hr/100-yr precipitation volume for three of the five parish urban areas. Only the volume for a multiple breach scenario far outstrips the 24-hr/100-yr precipitation hazard for all five areas.

For further context, Table 16.2 presents the observed inundation volumes for the New Orleans area urban sub-basins resulting from the extreme Hurricane Katrina exterior surge on the morning of August 29, 2005 (see Figure 5.5). The range of polder conditions demonstrates that for a single storm adjacent polders can experience drastically different SWL inundation hazards. (Importantly, variations in interior polder topography—major portions of each polder are well below 0 NAVD88—meant that the lower lying neighborhoods experienced more severe flood *depth* hazards.)

The particular exterior SWL exposure of each polder and the length and invert of breaches influenced the magnitude and timing of peak interior SWL. The Lower 9th Ward/St. Bernard Polder experienced massive erosion of levees along the MRGO and "the Funnel" in the face of 20+ ft exterior SWLs, together with the failure of floodwalls along the IHNC, which produced very high interior peak SWLs nearly within a short time following the peak exterior surge. The relatively shorter breaches (in length) for the Metro New Orleans system facing Lake Pontchartrain delayed peak SWLs (associated with equalization of the polder and lake) until over 24 hours after the peak exterior surge. An important reason for the lower inflows for the New Orleans East Polder was the relatively minor contribution of breaching.

[1] In these breach inflow scenarios the polder SWL does not equalize with the exterior SWL.

Table 16.1. Equivalent Volume for Precipitation

Acre-Ft of Accumulation Excluding Losses (Faiers et al 1997)

Polder	Sub-Basin	Area Acres	6-hr Duration		24-hr Duration
			10-yr 6.5 In	100-yr 10 In	100-yr 13 In
New Orleans East	NOE1 Maxent Lagoon	14,233	7,710	11,861	15,419
	NOE2 Maxent Wetland	5,683	3,078	4,736	6,157
	NOE3	2,866	1,552	2,388	3,105
	NOE4	2,338	1,266	1,948	2,533
	NOE5	9,588	5,194	7,990	10,387
	NOE3, 4, 5*	***14,792***	***8,012***	***12,327***	***16,025***
	Total Polder*	***34,708***	***18,800***	***28,923***	***37,600***
Lower 9th Ward/ St. Bernard	SB2 Central Wetland	5,066	2,744	4,222	5,488
	SB5 Central Wetland	24,340	13,184	20,283	26,368
	SB1	5,115	2,771	4,263	5,541
	SB3	5,485	2,971	4,571	5,942
	SB4	9,415	5,100	7,846	10,200
	SB1, 3, 4*	***20,015***	***10,841***	***16,679***	***21,683***
	Total Polder*	***49,421***	***26,770***	***41,184***	***53,539***
Metro New Orleans	SC1 (mostly swamp)	5,906	3,199	4,922	6,398
	SC2	7,364	3,989	6,137	7,978
	SC1 & 2*	***13,270***	***7,188***	***11,058***	***14,376***
	JE1	7,784	4,216	6,487	8,433
	JE2	5,510	2,985	4,592	5,969
	JE3	15,395	8,339	12,829	16,678
	JE1, 2, 3*	***28,689***	***15,540***	***23,908***	***31,080***
	OM1	5,041	2,731	4,201	5,461
	OM2	4,176	2,262	3,480	4,524
	OM3	4,720	2,557	3,933	5,113
	OM4	2,063	1,117	1,719	2,235
	OM5	11,268	6,104	9,390	12,207
	OM 1, 2, 3, 4, 5*	***27,268***	***14,770***	***22,723***	***29,540***
	Total Polder*	***69,227***	***37,498***	***57,689***	***74,996***

Table 16.2. Hurricane Katrina Inundation of New Orleans Regional Polders

IPET 2009, Volume VI Tables 7 and 8, and FEMA 2006[2]

Polder	Sub-Basins	Inundation Peak			Source of Inflow %		
		Time	SWL Ft NAVD88	Volume Acre-Ft	Breaching	Overtopping	Rainfall
Metro New Orleans	OM1, 2, 3, 4 &5	Late Afternoon 8/30	2.5 to 3	88,000 to 99,000	66	13	21
Lower 9th Ward/St. Bernard	SB1, 3, &4	Before Noon 8/29	10 to 12	153,000 to 192,000	63	29	8
New Orleans East	NOE3	High Water Marks Not Available					
	NOE4	Before Noon 8/29	2 to 2.5	4,000 to 5,000	17	70	13
	NOE5	Before Noon 8/29	-1.5 to -1	42,000 to 46,000			

16.2 Overview of Hurricane Surge Polder Inundation JPA

Quantifying polder inundation probabilities associated with hurricane surge events requires expanding the JPA for exterior surge approach described in Section 13. The equation for $\boldsymbol{F}(SWL_i)$—the cumulative probability of any surge SWL at an exterior LOI, (see Section 13.1)—is changed to $\boldsymbol{F^*}(SWL_i)$—for the cumulative probability of any surge related SWL at a polder interior LOI—as follows:

$$\boldsymbol{F^*}(SWL_i) = \int\int\int\int\int\int\int \boldsymbol{p^*}(CPD, R_{max}, V_f, \theta, X, I, L, R, t)\, \boldsymbol{H}[\boldsymbol{\psi_P}(\boldsymbol{\psi}, \boldsymbol{\psi_W}, \boldsymbol{\psi_{SOBRP}}) - SWL_i]\, d(CPD)\, d(R_{max})\, d(V_f)\, d(\theta)\, d(X)\, d(I)\, d(L)\, d(N_R,)$$

where

$\boldsymbol{p^*}$ is the joint probability expression modified to encompass additional probabilities (dimensions) for breach I and L (invert and length, see Section 15.4) at each individual reach/transition, N_R. Probability dimensions could be also be added for seepage, rainfall, and pumping.

$\boldsymbol{\psi_P}$ is the internal polder routing (level-pool or 2D as appropriate), which, in turn, is a function of

- $\boldsymbol{\psi}$, the high-resolution 2D surge SWL-wave model, which is a function of the hurricane variables CPD, R_{max}, V_f, θ, and X, as well as the mesh and other settings and parameters.
- $\boldsymbol{\psi_W}$,, the local Zone D wave conditions, which is in turn a function of $\boldsymbol{\psi}$, as well as local perimeter wind and bathymetric conditions.

[2] IPET stage-storage data for the sub-basins was not available and therefore volumes were computed using the regional LIDAR DEM (see GTN-2). Slight differences may occur due to sub-basin delineation

- $\boldsymbol{\psi_{SOBRP}}$, the inflow function for SOBRP. $\boldsymbol{\psi_{SOBRP}}$ is a function of both interior and exterior SWLs—i.e., $\boldsymbol{\psi}$ and $\boldsymbol{\psi_P}$—as well as perimeter crowns and other conditions.

$\boldsymbol{\psi_P}$ could also include the effect of interior wind setup.

Given the relative hazards of the inflows noted above, a JPA for more extreme surge-related polder inundation hazards may choose to ignore seepage-only inflow, and possibly wave-only overtopping inflow as well.

An expanded JPA approach is needed because the polder inundation hazard cannot be evaluated by simply routing the exterior surge hazard—e.g., routing the perimeter 500-yr SWLs to determine an internal 500-yr inundation hazard. While this analysis may be useful for some planning purpose (e.g., to roughly compare results for different polders, or results for different exterior surge hazards for the same polder), it does not provide an estimate of the polder 500-yr inundation hazard. In reality, a single storm is highly unlikely to produce a consistent 500-yr surge level along the entire perimeter system.

Furthermore, large perimeter systems have reaches with some independent exposure. *It follows that a surge overtopping event along a segment produces a volume that actually has a **MUCH LOWER** internal than reach-specific return period.*[3]

Given the range of independent factors contributing to the surge-related polder inundation hazard, an expanded JPM approach[4] is required to evaluate ***F****. This approach employs three steps:

1. Prepare a JPM set of exterior *whole-perimeter* surge events representative of the regional hurricane climatology joint probability, $\boldsymbol{p}$; each event encompasses i) the local surge SWL peaks and hydrographs—specified along the polder perimeter—which are a function, $\boldsymbol{\psi}$, of storm characteristics, and ii) the local exterior wave conditions associated with each SWL hydrograph, $\boldsymbol{\psi_W}$.
2. Define a range of scenarios to reflect SOBRP probabilities for each whole-perimeter surge event. For example, for breach probabilities include joint probabilities for combinations of N_R, I, and L (and rainfall and pumping if also considered probabilistically). For each scenario compute SOBRP flows as functions of $\boldsymbol{\psi}$, $\boldsymbol{\psi_W}$ and $\boldsymbol{\psi_P}$ and conduct the internal routing simulations, $\boldsymbol{\psi_P}$, (using level-pool or 2D, with or without wind setup, as appropriate).
3. Numerically integrate the resulting PDF to produce the CDF curve, with appropriate smoothing and treatment of potential bias and uncertainty.

In addition to employing the same 2D SWL routing model program described in Parts II and III (e.g., ADCIRC/STWAVE or SWAN+ADCIRC), the JPM approach to surge polder inundation requires three more hydraulic models: a local storm-specific wave model; polder SOBRP inflow modeling; and internal routing. The following five sections discuss the five JPM steps and associated models for evaluating ***F****. Afterwards, a sixth section describes the approach to analyzing potential interior wave hazards.

---

[3] Suppose a perimeter system has been designed with elevations that allows for a minor amount of wave-only overtopping when the exterior SWL at any reach is at the 100-yr level. If the 100-yr exterior surge hazard for this system actually reflects several totally independent exposures (e.g., storms passing along several widely different tracks), surge-related inflow into the polder at this minor overtopping rate (i.e., from ***anywhere*** along the overall perimeter) is in fact a much higher probability—e.g., close to a 33-yr hazard for three independent exposures. The South Lafourche Polder clearly illustrates an example of two independent exposures—east versus west side.

[4] For more background on JPA and the JPM approaches see GTN-1, Part J, as well as Section 4.1, and 14.1.

16.3 JPM Set of Perimeter Surge Events

A JPM approach to polder inundation hazard analysis requires a set of perimeter SWL events (SWL peaks and associated hydrographs) that reflects the regional hurricane climatology. Studies of extensive polder systems—with long and complex perimeters—examining a wide range of inundation probabilities—e.g., from 100-yr to >1,000-yr—necessitate a large set composed of a sufficient number of extreme exterior SWL events.

The set of SWL events is generated using a Full-JPM, Monte Carlo-JPM, or JPM-OS storm set (see GTN-1, Section J, and Sections 4.1 and 13.1)—with set size and composition appropriate for the range of polder inundation scenarios under consideration. Each storm is simulated with the high resolution 2D wind/surge/wave SWL routing model. Each storm event—composed of SWL peaks along the entire perimeter and hydrographs determined as described in Section 15.1—has the fractional joint probability associated with that storm. The set of perimeter results for all the storms then statistically represents the probability of perimeter surge SWL (peak and hydrograph) events.

For inundation studies of polders located near complex coastlines and sheltered water bodies it may be necessary to expand the set of storms to adequately portray the surge-response of these areas. For a JPM-OS storm set, the size and composition of the set can be tailored to better capture complex local surge-response through careful attention to the benchmark procedure described in Section 13.2.

The Surge Response-OS approach cannot be employed in analyzing polder inundation joint probabilities.[5] The Surge Response-OS approach is not developed to capture the combined probabilities of various exterior surge conditions at various reaches, i.e., to provide a set of *whole-perimeter surge events* effectively representing the full *whole-perimeter surge hazard*.

As seen in Section 15, seepage, overtopping, and breach inflows are highly sensitive to the estimates of exterior SWL. A polder inundation analysis requires that the high resolution 2D SWL model (described in Sections 8 through 11) be carefully reviewed for identifying/correcting residual bias and defining/minimizing uncertainty at perimeter system LOIs. To better capture the exterior surge response near perimeter LOIs it may be necessary to refine the surge model mesh and to improve nodal attributes (e.g., topography/bathymetry, Manning's n).

Results near LOIs for all JPM storm simulations can be examined for possible instabilities. The mesh near LOIs may require refinement and smoothing if numerical instabilities affect the results. The choice of model settings and other parameters (e.g., acceleration terms, eddy viscosity) may also need adjustment to improve the representation of local surge SWL conditions.

Polder hazard analysis—particularly consideration of wave-only overtopping—also requires information about the local exterior wave conditions for each perimeter surge event in the JPM. Zones C/D wave conditions must therefore be modeled at each reach for each JPM storm using one of the techniques described in Section 15.1. Assessment of overall SOBRP volume sensitivity to wave conditions, especially H_s, (see below) can support the selection of a wave modeling approach. For low sensitivities, use of simple breaker parameter limited H_s would be sufficient.

[5] As discussed in Section 14.3, a Surge Response-OS set is used in conjunction with a high resolution 2D routing model ONLY to define the SWL surge response, $\boldsymbol{\psi}$. The surge response, $\boldsymbol{\psi}$, is subsequently combined with the mathematical expression for $\boldsymbol{p}$, as a valid approach to defining *local, exterior surge hazards*. Under the assumption of smooth surge-response, the Surge Response-OS set can be much smaller than a JPM-OS set.

16.4 SOBRP Probability Scenarios

In an inundation JPA the time-varying inflows from seepage, overtopping, and breaching, together with rainfall accumulations and pumping withdrawals are estimated over the course of each JPM storm. As discussed in Section 15, these SOBRP flows are a function of changing exterior SWL and wave conditions, changing interior SWLs, and transmission coefficients. The inundation JPA must consider variability/ uncertainty for these conditions and coefficients when the magnitude of variability/uncertainty is significant to the interior inundation hazard. For example, in JPAs dominated by overtopping—or even more so by breaching—seepage, seepage uncertainty, and rainfall uncertainty are typically neglected. When breaching is not included in the inundation analysis rainfall uncertainty becomes more significant. Sensitivity tests can be used to assess the influence of input uncertainties.

Probabilistic variability/uncertainty in a SOBRP factor can be incorporated into the JPA in one of two ways, depending on whether the factor's influence on the interior volume is linear or nonlinear. Uncertainties in rainfall, pumping, general terrain DEMs, and overtopping and breach lengths and coefficients are examples of linear factors. For convenience, all linear factors can be considered to have a normal distribution. A combined overall σ_P can then be used directly during post-processing to assess the influence on peak inundation volume probability (see Section 16.5 below).

For SOBRP attributes with nonlinear influence—such as the effect of exterior SWL (i.e., R_C) on the likelihood of a breach failure condition, I-L, at any reach, as well as the effect of H_s/breaker parameter and R_C on the overtopping and breach volumes—examining this influence requires expanding the JPM methodology. The expanded JPM must include a *subset* of whole-polder SOBRP scenarios for each storm, and each storm's subset must represent the full range of perimeter inflow joint probabilities for that storm. For each JPM storm—with climatological joint-probability $\boldsymbol{p}$—the whole-polder SOBRP subset can be composed of either:

- Predefined whole-polder SOBRP scenarios to represent a broad combinations of attributes. The range of each attribute is discretized into a few alternative values. Each scenario is then assigned a fraction of $\boldsymbol{p}$ based on the scenario's $\boldsymbol{p^*}$). The total probability of all scenarios for any storm thus equals $\boldsymbol{p}$. This Full-JPM approach to constructing the subsets and is preferable when there are only one or two attributes.
- A sufficiently large number of randomly selected whole-polder SOBRP scenarios with their respective $\boldsymbol{p^*}$, This Monte Carlo-JPM approach to constructing the subsets with randomly selected scenarios is appropriate for multiple factors.

Depending on the complexity of model coupling and the resources required for additional SOBRP scenarios, the expanded JPM may be limited to only those factors which have a large impact on the inundation hazard. Given the large order of magnitude of the influence of breach fragility on inundation hazard, the above expression for $\boldsymbol{p^*}$ only incorporates probabilities for I-L at each reach (N_R). The numerical solution to $\boldsymbol{p^*}$ thus requires $\boldsymbol{\psi_{SOBRP}}$ solutions for a wide range of whole-polder scenarios—encompassing a number of combined breach I-L conditions encompassing every N_R—for each JPM storm. This expansion of the JPM can necessitate thousands of $\boldsymbol{\psi_{SOBRP}}$-$\boldsymbol{\psi_P}$ solutions per JPM storm, with more scenarios for the more extreme storms. The associated computational demands for thousands of scenarios can therefore dictate simplified internal level-pool routing—which allows the use of a combined $\boldsymbol{\psi_{SOBRP}}$-$\boldsymbol{\psi_P}$ model prepared in EXCEL, MATLAB, or FORTRAN (see Section 15.7).

For major overtopping and breaching hazard analyses the nonlinear influences of uncertainties in SWL, H_s, and pumping can also be meaningful, requiring more probability dimensions for $\boldsymbol{p^*}$. In the case of

SWL, the overall uncertainty factor σ_Σ discussed in Section 13.5 can be used to develop the SOBRP subsets.

During the simulation of some individual exterior-SOBRP scenarios it may be important to consider the effect of interior wind stress—e.g., where inundation is occurring simultaneously with presence of strong winds over long open fetches. Addressing the influence of time- and spatially-varying wind stress during inundation requires a 2D $\boldsymbol{\psi_P}$ model program (such as ADCIRC). If the peak inundation scenarios entail limited wind setup conditions, the level-pool routing results can be combined with a supplementary wind setup calculation. The results of the wind setup calculation can then be used to finalize sub-basin peak level-pool SWLs. As noted in Section 16.3, for polders with potential exposure to interior wind setup hazards it is crucial to include an appropriate number of storms in the JPM set reflecting attributes—such as tracks—that contribute to the wind setup hazard.

16.5 Preparation of Return Frequency Curves

Production runs for each JPM-storm/SOBRP-scenario combination—employing $\boldsymbol{\psi}$, $\boldsymbol{\psi_W}$, $\boldsymbol{\psi_{SOBRP}}$, and $\boldsymbol{\psi_P}$ models (and interior wind setup as needed)—must be reviewed and checked for completeness and quality. Quality control for surge modeling has been addressed in Section 13.6. Selected outputs from individual Zones C/D wave, SOBRP, and interior routing model runs are similarly prepared in graphical and map overlay formats to facilitate inspection. Output values can be screened to flag simulations that produce physically unrealistic results or results inconsistent with general trends. Nonconforming results may indicate that a model program has been inappropriately setup or the wrong input has been used. A final file of peak SWL results from the $\boldsymbol{\psi_P}$ model—for each of the thousands of scenarios at each polder sub-basin or mesh node—is then produced.

For each location (e.g., sub-basin or node), these thousands of peak interior SWL results are used to finalize surge-related flood return frequency curves, in four steps similar to those employed for exterior SWL (Section 13.6):

a. CDF integration;

b. CDF validation;

c. Adjustments to spatial variations in specific surge hazard levels; and

d. Construction of confidence limits.

The interior PDF can be numerically integrated to produce the cumulative probability at each incremental SWL. The integration step can include smoothing of the individual results using an overall σ_P. As discussed in the preceding sections the σ_P encompasses uncertainties which are regarded as normally distributed and related linearly to polder inundation volume. Example uncertainties include:

- The exterior SWL (computed with $\boldsymbol{\psi}$) as it affects seepage rates; if seepage flows are very small relative to the inundation hazards being assessed, this term can be ignored;
- The length of overtopping and breaching;
- Weir coefficients for overtopping and breaching;
- Rainfall rates;
- Pumping rates; and
- General terrain DEM.

These linear uncertainties, and thus $\sigma_{\boldsymbol{P}}$, are expressed in units of inundation volume. For smoothing the peak interior SWL results, $\sigma_{\boldsymbol{P}}$ would need to be converted to units of inundation elevation, either a single sub-basin wide $\sigma_{\boldsymbol{P}}$ for level-pool routing or spatially varying $\sigma_{\boldsymbol{P}}$ for 2D routing. The difficulty, however, with using $\sigma_{\boldsymbol{P}}$ is often a lack of data and empirical research for defining the component $\sigma_{\boldsymbol{P}}$ values, resulting in the use of educated guesses.

An alternative to numerical integration is to select an established PDF curve type (e.g., Gumbel, Weibull, etc., see GTN-1 Part H) and assign coefficients using the results. The CDF is then simply the standard integral of that PDF.

Unlike exterior surge CDFs, observations from a sufficient number of surge-driven polder inundation events are not available to validate interior CDFs. Sub-basin surge-related CDFs, however, can be evaluated for physical reasonableness by comparing them with

a. Each other—for example, assessing differences in the SWL at key hazard levels and whether such differences make physical sense. For a 1,000-yr return period, a sub-basin protected by compartmentalization features might be expected to have a lower inundation level relative to sub-basins in close proximity to potential breach locations.

b. CDFs for other polder flood hazards, such as tropical storm rainfall-only and non-tropical rainfall. Low-lying sub-basins might be expected to have higher inundation levels in all cases.

The sub-basin (or node) CDFs are used to construct maps illustrating the polder-wide surge inundation hazards—e.g., 100- and 500-yr return period etc.—such as those shown in Figure 16.2 Flood hazard overlays are then compared against more accurate maps and aerial images. Adjustments can then be made to sub-basin flood level boundary alignments, and to smooth boundary differences.

The fourth step addresses residual uncertainty in the interior CDFs. Sources of potential bias in the various inputs, parameters, and assumptions for all of the model components in $\boldsymbol{\psi_P}$ are first identified and evaluated. If there is reasonable evidence of bias or error—e.g., from a CDF comparison—then the source of the bias is corrected and the CDFs are redeveloped.

The influence of the linear, normally fistributed uncertainties can be readily evaluated by using $\sigma_{\boldsymbol{P}}$ to construct corresponding LCL/UCLs for the local CDF (e.g., 90%). These LCL/UCLs are subject to the limitation regarding the estimate of $\sigma_{\boldsymbol{P}}$.

Two important non-linear uncertainties include:

- The exterior SWL (computed with $\boldsymbol{\psi}$) as it affects overtopping and breaching rates; (exterior SWL uncertainty is discussed in Sections 13. 5 and 13.6); and
- Breach fragility response to exterior SWL.

As discussed above, the influence of these two uncertainties on the polder inundation hazard can be assessed with sensitivity tests. The sensitivity tests can provide a basis for a professional judgment to modify the LCL/UCLs. If significant expansions in the number of scenarios for $\boldsymbol{\psi_{SOBR}}$ and $\boldsymbol{\psi_P}$ modeling can be accommodated, it may be practical to add these uncertainties into the JPA—i.e., expanding $\boldsymbol{p^*}$. (The additional scenarios would be selected using the Monte Carlo technique). The resulting effect of these uncertainties can then be computed and used to adjust the LCL/UCLs.

If a standard PDF curve (e.g., Gumbel, Weibull, etc.) has been fitted to the inundation modeling results, the LCL/UCLs regarding this fit (apart from the uncertainties above) can also be provided.

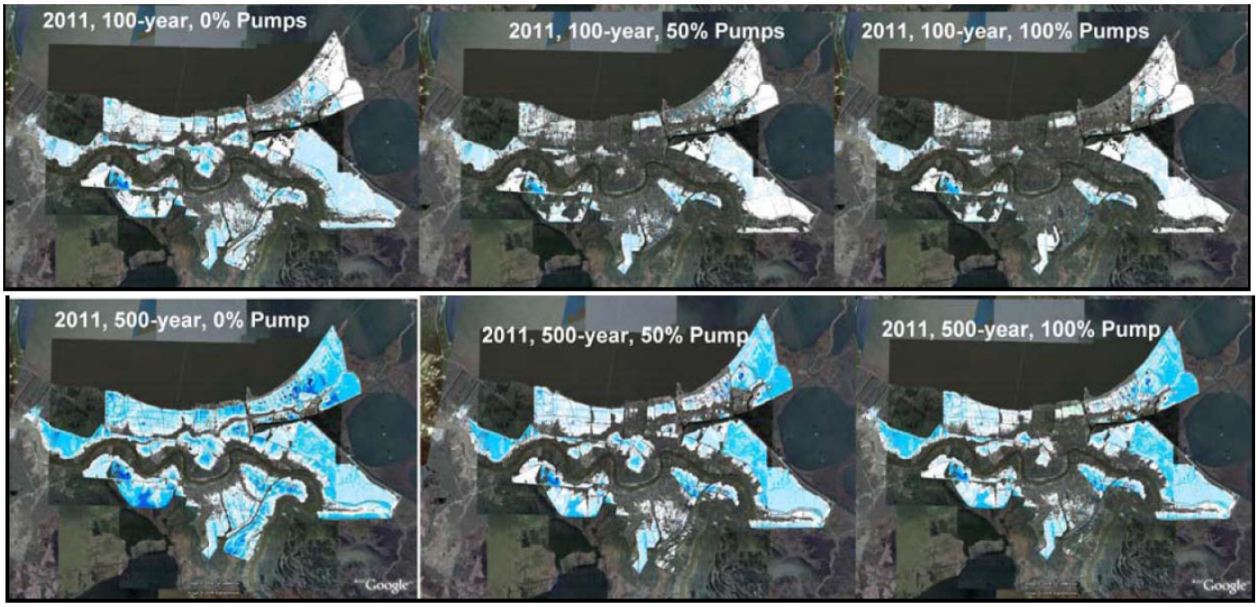

Figure 16.2. Example of Polder Inundation Hazard Maps

IPET 2009b

16.6 Interior Wave Hazard

As with exterior surge wave hazards (see Section 13.7) interest in polder wave hazards is limited primarily to wave conditions that occur at the reference SWL hazard level. These wave conditions can be analyzed using techniques reviewed in Section 15.8, including the breaker parameter. For longer, deeper interior fetches—e.g., wide channels—wave heights at a referenced SWL hazard can be computed for several appropriate hurricane scenarios (storm intensity, size, wind-field, forward speed, track, etc.) and their associated local wind speed, direction, and duration. The wave heights are computed using the simple 1D equations, or models for more elaborate conditions. The maximum wave height—derived from the breaker parameter, equation, or model—can be used for the wave hazard at the referenced SWL hazard. It follows that the wave hazard at a particular SWL hazard can differ widely across a polder due to differences in topography, proximity to wind sheltering features located in the predominant upwind wind direction, and/or the presence of heavy canopy.

Section 17. Recent Applications of Polder Hazard Analysis

The additional hydraulic methods and JPA for polder inundation hazard discussed in Sections 15 and 16 have recently been applied to planning and engineering for the New Orleans regional HSDRRS illustrated in Figure 17.1. The applications include four major efforts:

1. The IPET Performance Evaluation of the New Orleans and Southeast Louisiana Hurricane Protection System (Volume VIII, Risk and Reliability IPET 2009a and 2009b);
2. The USACE LaCPR Study, (Final Technical Report USACE 2009);
3. The USACE HSDRRS Design—(Interim Guidelines and Draft Elevation Report, USACE 2008b and 2010); and
4. The USACE Armoring Alternative Evaluation Process, (Summary Report, USACE 2011).

The following sections discusses these efforts and important limitations. The LaCPR Study and HSDRRS Design, as well as the Louisiana CPRA's 2012 Master Plan, also employed polder inundation hazard analysis to evaluate future conditions—which are covered in Part V.

Figure 17.1. New Orleans HSDRRS

Swenson, D. (Times-Picayune) 2012

17.1 IPET Risk and Reliability Study

In 2009, nearly four years after devastating flooding caused by Hurricane Katrina's surge, IPET published results from a JPA for surge-driven inundation hazard for the New Orleans regional east- and west-bank polders shown in Figure 16.1. IPET employed inundation JPA to compare pre-Katrina HSDRRS risk and reliability versus the 2007 post-Katrina reconstructed HSDRRS and planned 2010 HSDRRS (also referred to as 2011 in IPET 2009b). The IPET 2010 HSDRRS alternative did not include the IHNC/GIWW or Seabrook Barriers or the higher replacement West Return Wall. (Note: a final summary report, IPET 2009b, acknowledges these barriers as having been added to the 2011 HSDRRS design.) The following paragraphs summarize key aspects of the IPET approach together with the results.

As noted in Section 16.1, a Surge Response-OS cannot be used for polder inundation hazard analysis as it does not provide a set of *whole-perimeter* surge events representative of the regional hurricane climatology. The IPET study, as discussed in Section 14.2, therefore improvised a JPM-OS set of perimeter events, utilizing 76 of the 152-storm FIS Surge Response-OS and assigned a value for ***p*** to each storm (see Part III, Attachment 1). However, the 76-storm Surge Response-OS does not include storm intensity above the 200-yr return period, such as a landfalling Category 5 storm. As also described in Section 14.2, IPET 100- and 500-yr exterior surge hazards were notably different from those found in the FIS—24% lower for the 500-yr hazard at an east-bank St. Charles Parish location.

The IPET study utilized the FIS validated ADCIRC-STWAVE model for the pre-Katrina alternative, which was validated in southeast Louisiana (see Section 11.2). For the 2007 alternative IPET employed the FIS 2007 mesh to assess exterior SWL return frequencies. IPET did not address the bias in the validation of the ADCIRC-STWAVE model with respect to the south shore of Lake Pontchartrain and did not provide a bias correction.

IPET (2009a Appendix 8) indicated that a 2010 mesh version was employed for the improved HSDRRS alternative. As the IPET 2010 HSDRRS alternative did not include the IHNC or Seabrook Barriers (as indicated by overtopping and breaching scenarios along the IHNC/GIWW) it is assumed that the 2010 mesh version likewise did not include these structures.

The ADCIRC-STWAVE model provided SWL time series at selected regional locations. Additional hydrographs at about 260 locations were generated around the perimeter for each of the 76 events, for each of the three barrier alternatives (equating to abut 20,000 perimeter SWL hydrographs per alternative). For these additional hydrographs the model result for the peak SWL was taken from the nearest node and the hydrograph shape was then derived from the closest time-series.[1]

IPET applied a breaker parameter of 0.43 to each local SWL hydrograph to estimate the time-varying Zone D H_s condition. As discussed in Section 6.2, there is a critical need for more data on foreshore waves, including the application of breaker parameters. For local wave periods (mean) during each event IPET used the value from the nearest STWAVE grid point.

IPET employed the expanded the JPA discussed in Section 16.2 to address whole-polder SOBRP scenarios for each of the 76 exterior surge/wave events. The whole-polder SOBRP subset for each storm included one potential breach failure I-L case per reach (including transitions and gates):

1. Breach occurrence was conditioned first on the local exterior peak SWL and associated freeboard R_c (crest elevation minus peak SWL). If R_c remained greater than the a defined minimum threshold then no breach occurred at the reach.

[1] The IPET description of this methodology is not fully explained.

2. For R_c less than the threshold, IPET defined a simple one-step location-specific breach I-L case.[2] This case was based on whether:
   - R_c at the peak SWL was positive (peak SWL below the reach crown elevation, i.e., no overtopping) or negative (peak SWL above the crown, i.e., overtopping); and
   - Structure type—levee (hydraulic fill/clay/unknown soil), floodwall, gate, or transition.

   Figure 17.2 presents the IPET breach cases.
3. If R_c was reduced to less than the threshold, then the occurrence of the breach case as defined above was then further conditioned using a fragility expression, as depicted in Figure 17.3, to assign a probability for erosion and collapse breaching:
   - Distinct collapse and erosion fragility relationships were assigned for each structure type. Levee type included hydraulic fill/clay/unknown soil composition subtypes.
   - If the minimum R_c at a reach during a storm resulted in no overtopping (peak SWL remained below the structure crest) collapse fragility was used to estimate the probability of the breach case occurring. The collapse fragility incorporated categories of local subsurface conditions which might lead to soil failures, including seepage mechanisms.
   - If the minimum R_c at a reach during a storm resulted in overtopping, erosion fragility was used to estimate the probability of the breach case occurring. Erosion fragility incorporated the magnitude of negative R_c.
   - In addition to erosion and collapse breaching, IPET considered probabilities for gate closure and transition failures.
4. For peak SWL above the threshold, the no breach probability equals one minus the breach probability.

For each surge event, N reaches (including gates and transitions) implies a maximum of 2N individual breach conditions. Treating each reach breach independently yields 2^N possible combined scenarios. However, the defined threshold R_c for the first condition meant that the vast majority of reaches for the vast majority of storms had the "no breach" condition. Thus, the number of breach scenarios per storm was much less 2^N, but still totaled hundreds per surge event; and many thousands of whole-polder scenarios for the overall 76-storm set. For each storm, with joint probability ***p***, each of the hundreds of whole-polder scenarios was assigned its relative fraction of ***p***—based on the joint probability of the condition at each independent reach.

[2] A breach condition consists of a single combination of breach *depth* (crest minus breach invert) and length. The IPET breach condition therefore does not provide for a dynamic breach with rising SWL.

Reaches						
Levee/Floodwall Breach Model Given Overtopping (erosion breach)						
		0 to 1ft		1ft to 3ft		
Material	**Symbol**	**Depth (ft)**	**Breach Width (w), Reach Length <1000ft**	**Depth (ft)**	**Breach Width (w) (ft), Reach Length <1000ft**	**Depth (ft)**
Hydraulic Fill	H	0	0	9	0.50*L to max 400	18
Clay	C	0	0	3	0.50*L to max 135	13
Unknown (Average)	U	0	0	6	0.50*L to max 290	17
Wall	W	0	0	0	0	17
		Length Modifiers Reach L>1000 ft				
		Overtopping Depth (ft)				
Material	**Symbol**	**0 to 1ft**		**1ft to 3ft**		**>3 ft**
Hydraulic Fill	H	0.0		400 < w < 0.40*L		430 < w < 0.40*L
Clay	C	0.0		135 < w < 0.10*L		135 < w < 0.10*L
Unknown (Average)	U	0.0		290 < w < 0.30*L		315 < w < 0.30*L
Wall	W	0.0		0.0		315 < w < 0.10*L
Levee/Floodwall Breach Model Given No Overtopping						
			Breach Width (w), (ft)			
Material	**Symbol**	**Depth (ft)**	**L ≤ 1000 ft**	**1000 < L≤ 10,000 ft**	**L>10,000 ft**	**Notes**
Hydraulic Fill	H	18	0.50*L to max 500	500 < w ≤ 0.15*L	0.15*L	3 Breaches / 10,000 reach
Clay	C	13	0.50*L to max 500	500 < w ≤ 0.10*L	0.10*L	2 Breaches / 10,000 reach
Unknown (Average)	U	17	0.50*L to max 500	500 < w ≤ 0.125*L	0.125*L	2.5 Breaches / 10,000 reach
Wall	W	17	0.50*L to max 500	500 < w ≤ 0.075*L	0.075*L	1.5 Breaches / 10,000 reach
Transitions						
Transitions Breach Model Given Overtopping						
		Breach size (ft)				
Transition Type	**Symbol**	**width**	**Depth**			
Ramps	R	25	3			
Floodwall-Levee	T	50	3			
Drainage Structures	D	65	5.5			
Pump Stations	P	100	5			
Gates	G	25	5			
Unprotected sections	U	N/A	N/A			
Transitions Breach Model Given No Overtopping						
		Breach size (ft)				
Transition Type	**Symbol**	**width**	**Depth**			
Ramps	R	-	-	Treated as opened or closed (sand bagged)		
Floodwall-Levee	T	-	-	No breaching until OT		
Drainage Structures	D	-	-	No breaching until OT		
Pump Stations	P	-	-	No breaching until OT		
Gates	G	-	-	Treat as opened or closed		
Unprotected sections	U	N/A	N/A			

Figure 17.2. IPET Breach Failure Conditions

IPET 2009a, Volume VIII Appendix 9

IPET computed and routed inflow volumes for each whole-polder scenario using an integrated series of EXCEL spreadsheets. IPET named the spreadsheet program FoRTE for Flood Risk Analysis for Tropical Storm Environments. IPET's FoRTE program included the following steps:

1. Seepage contribution to the polder inundation was ignored.
2. For scenarios with one or more continuously submerged inverts (i.e., remaining below the final local exterior SWL) the entire polder was assumed to equalize with the highest local final exterior SWL from among those submerged inverts. In this case inundation volume additions from overtopping and rainfall, and removal by pumping were ignored.
3. For scenarios with all breach inverts above the final exterior SWL, each cumulative breach inflow to the adjacent sub-basin was calculated using the SWL hydrograph, presumably using the broad crested weir equation. (IPET did not provide breach weir coefficients.)
4. Overtopping for non-breaching perimeter reaches addressed all five phases and used the local exterior SWL hydrograph and wave information. Wave-only contributions were reportedly analyzed using standard runup and overtopping methods (see Section 15.3) but were performed outside of FoRTE spreadsheets and added afterwards. For Phase 5 overtopping the FoRTE spreadsheets employed the standard broad-crested weir equation with C values ($ft^{½}/s$) of 3.0 for floodwalls, 2.6 for levees, and 2.0 for gates.

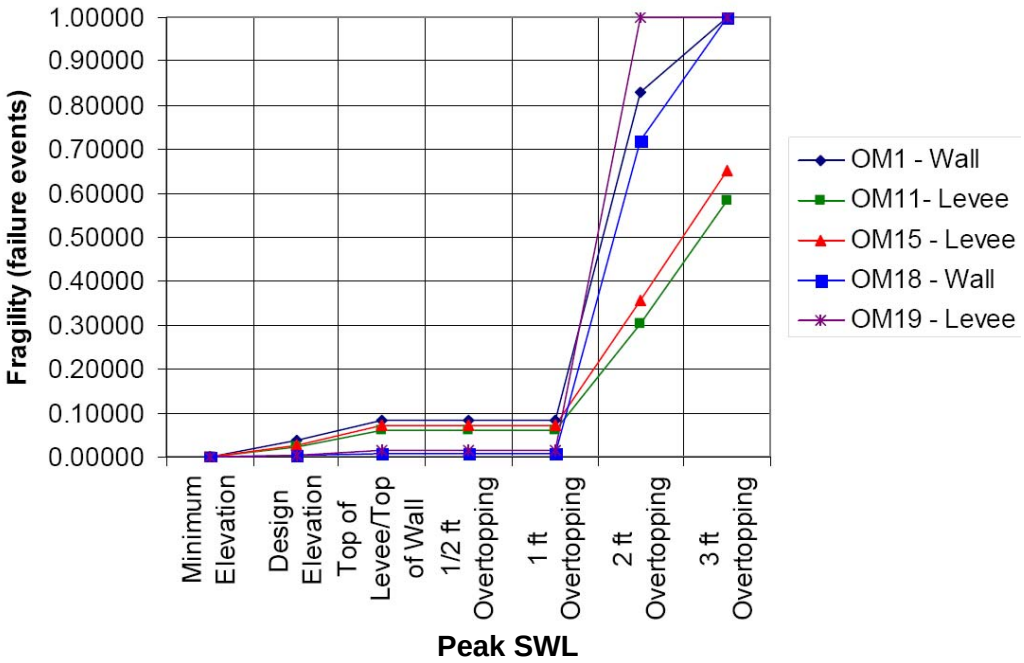

Figure 17.3. Example of IPET Breach Fragility
Selected Metro New Orleans Reaches
IPET 2009b[3]

[3] Other IPET documentation (Link et al Undated) suggests that levee and floodwall overtopping fragility was simplified into a few generalized incremental probabilities.

5. A generalized storm cumulative rainfall by sub-basin was estimated based on storm intensity and distance to the storm center according to Lonfat et al 2004, and a multiplier of 1.5 was applied for rainfall to the right of the hurricane heading.
6. The rainfall cumulative volumes were further adjusted according to three pumping cases:
   - No reduction of volume for a no pumping case;
   - Reduction of volume in accordance with cumulative pumping at 50% capacity; and
   - Reduction of volume in accordance with cumulative pumping at 100% capacity.
7. For scenarios without submerged breaches (without Step 1) level-pool routing with exchanges between sub-basins was used to determine final interior peak SWL for each sub-basin, for each fractional ***p*** scenario, broken down into the three pumping cases.
8. The IPET polder routing did not include interior wind setup and the polder hazard analysis did not consider interior waves.
9. The routing results in each sub-basin for each whole-polder scenario for each storm were assigned the fraction of ***p***.
10. Sub-basin peak SWL CDFs were calculated using the results for the thousands of scenarios. The CDFS were calculated separately for the three different pumping cases.

IPET used the sub-basin inundation SWL CDFs to determine inundation at the 50-, 100- and 500-yr hazard level for the three pumping-cases. Table 17.1 presents the results for the 2010 (2011) HSDRRS. Table 17.1 shows that with the 100% pumping case SWL increased in 13 of 27 sub-basins for the 100-yr versus the 50-yr hazard. Of these, three east-bank sub-basins and one west-bank sub-basin SWLs increased by more than 2 ft: OM1 (6 ft); OM4 (3 ft); Jefferson, JE3 (5 ft); and JW4 (8 ft).

For the 500-yr versus the 50-yr hazard, with the 100% pumping case, SWLs increased in 25 of 27 sub-basins—17 by 3 ft or more, and 10 by 5 ft or more. The IPET report did not discuss the source of these increases, such as the contribution from rainfall. As the IPET 2010 HSDRRS did not include the IHNC and Seabrook Barriers, increased SWLs may also reflect inflow along the IHNC. Figure 17.4. depicts the 50-, 100-, and 500-yr flood depths for 2010 (2011) HSDRRS for the 100% pumping case.

Table 17.2 presents the volumes for 2010 (2011) HSDRRS for the 100% pumping case that correspond to the 100- and 500-yr inundation hazard elevations in each sub-basin. Totals are also included for five combined master drainage areas and the overall polders. Total volumes are provided for reference but as with rainfall-only hazard (Table 16.1), these summed volumes are **not** the associated hazard for these larger areas. IPET did not provide hazard volumes for the master drainage areas or whole-polders.

For comparison Table 17.2 shows the 6-hr/100-yr rainfall (from Table 17.1) minus 6-hr pumping for five combined master drainage areas. *Notably the Orleans master drainage area has a **lower** volume for the 500-yr surge inundation hazard than for the 6-hr/100-yr net rainfall*. However, within the Metro Polder the 500-yr surge inundation volume is a factor of 2.5 times higher than the 6-hr/100-yr net rainfall volume for both East Jefferson and St. Charles. For the Lower 9th Ward/St. Bernard master drainage area the difference is the most, at a factor of 4.3 higher. For New Orleans East the difference is much lower, at 40% higher. Again, these reflect the IPET analysis without the IHNC/GIWW and Seabrook Surge Barriers, and higher West Return Wall.

Table 17.1. IPET Inundation Hazard for the 2010 (2011) HSDRRS

Elevation ft NAVD88-2004.65

Sub-Basin	50-Yr Inundation Hazard			100-Yr Inundation Hazard			500-Yr Inundation Hazard		
	Pumping			Pumping			Pumping		
	0%	50%	100%	0%	50%	100%	0%	50%	100%
OW1	-1	-1	-1	0	-1	-1	1	1	1
OW2	-3	-3	-3	-2	-2	-2	0	0	0
NOE1	0	0	0	0	0	0	3	3	3
NOE2	-4	-5	-5	-3	-4	-4	0	-2	-2
NOE3	-4	-5	-5	-3	-4	-4	-2	-3	-3
NOE4	-1	-2	-3	0	-1	-1	2	0	0
NOE5	-8	-9	-11	-7	-8	-9	-4	-6	-6
OM1	-5	-7	-12	-4	-5	-6	-2	-4	-5
OM2	-5	-12	-12	-4	-12	-12	-2	-7	-12
OM3	-1	-6	-12	-1	-6	-12	1	-2	-12
OM4	-1	-5	-5	-1	-2	-2	1	1	1
OM5	-1	-4	-12	0	-4	-12	1	0	-2
SB1	-1	-5	-12	0	-2	-12	2	1	0
SB2	1	1	1	2	2	2	3	3	3
SB3	0	-1	-3	1	-1	-3	2	0	-1
SB4	2	1	1	3	1	1	5	4	4
SB5	3	3	3	4	3	3	5	5	5
JE1	3	2	2	4	2	2	5	4	4
JE2	-4	-12	-12	-3	-12	-12	-2	-3	-4
JE3	-5	-6	-10	-4	-5	-5	-2	-3	-3
JW1	0	0	0	2	1	1	3	2	2
JW2	-4	-5	-5	-3	-5	-5	0	-2	-2
JW3	-2	-5	-12	0	-1	-2	0	0	0
JW4	-5	-12	-12	-3	-4	-6	-1	-3	-4
PL11	-2	-12	-12	-2	-12	-12	1	-4	-5
SC1	2	2	2	3	3	3	5	5	5
SC2	4	4	3	4	4	3	6	5	5

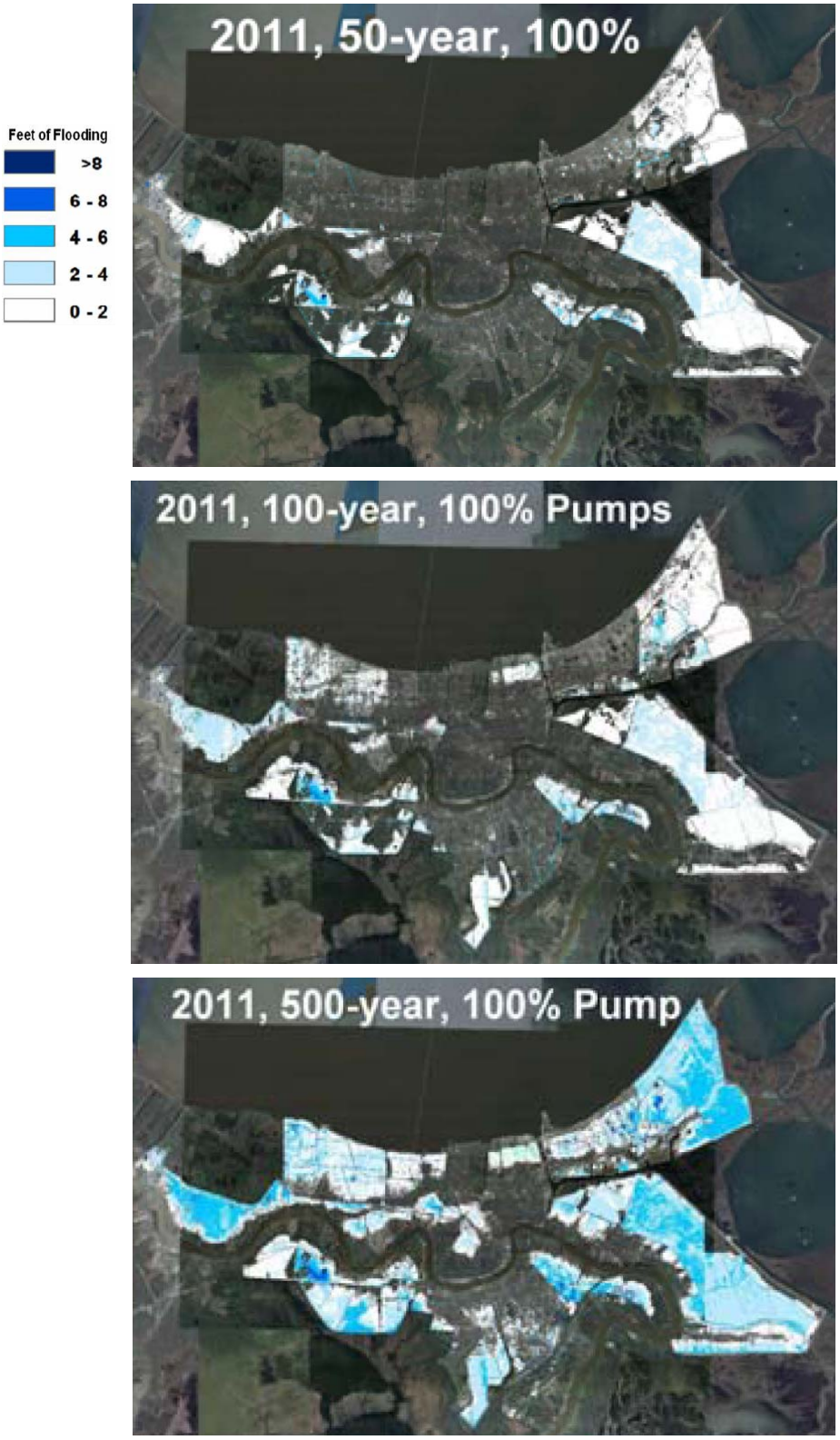

Figure 17.4. IPET Inundation Hazard for the 2010 (2011) HSDRRS
100% Pumping
IPET 2009b

Table 17.2. IPET Inundation Hazard Volume for the 2010 (2011) HSDRRS[4]

100% Pumping

Polder	Sub-Basin	Acres	100-Yr Inundation Hazard		500-Yr Inundation Hazard		6-hr/100-yr Rainfall Minus 6-hr Pumping Acre-ft
			Elev	Vol Acre-ft	Elev	Vol Acre-ft	
New Orleans East	NOE1 Maxent Lagoon	14,233	0	7,975	3	47,635	
	NOE2 Maxent Wetland	5,683	-4	6,206	-2	14,718	
	NOE3	2,866	-4	1,244	-3	2,104	
	NOE4	2,338	-1	1,058	0	1,756	
	NOE5	9,588	-9	2,625	-6	10,598	
	NOE3, 4, 5* (within Maxent Levee)	***14,792***		***4,927***		***14,458***	***12,327 - 1,930 = 10,397***
Lower 9th Ward/ St. Bernard	SB2 Central Wetland	5,066	2	2,475	3	5,462	
	SB5 Central Wetland	24,340	3	21,764	5	62,814	
	SB1	5,115	-12	0	0	35,397	
	SB3	5,485	-3	593	-1	1,706	
	SB4	9,415	1	1,480	4	14,639	
	SB1, 3, 4* within 40 Arpent Levee	***20,015***		***2,073***		***51,742***	***16,679 – 4,518 = 12,161***
Metro New Orleans	SC1 (mostly swamp)	5,906	3	8,057	5	18,654	
	SC2	7,364	3	2,175	5	6,041	
	SC1 & 2*	***13,270***		***10,232***		***24,695***	***11,058 - 1,017) = 10,041***
	JE1	7,784	2	1,995	4	6,366	
	JE2	5,510	-12	45	-4	3,185	
	JE3	15,395	-5	6,721	-3	25,322	
	JE1, 2, 3*	***28,689***		***8,761***		***34,873***	***23,908 – 10,289 = 13,619***
	OM1	5,041	-6	964	-5	2,276	
	OM2	4,176	-12	14	-12	14	
	OM3	4,720	-12	1	-12	1	
	OM4	2,063	-2	468	1	2,361	
	OM5	11,268	-12	16	-2	2,638	
	OM 1, 2, 3, 4, 5*	***27,268***		***1,463***		***7,290***	***22,723 – 12,724 = 9,999***

* Sub-Totals and Totals do NOT represent multi-sub-basin hazard volumes.

[4] IPET's own stage-storage data for the sub-basins were not available and therefore volumes were independently computed using the regional LIDAR DEM.

As discussed in Section 14.2 IPET addressed both epistemic and aleatory uncertainties (see Section 14.5) in exterior surge hazards based on their 76-storm JPM-OS. In the case of one location an asymmetric epistemic uncertainty in the 100-yr SWL (9.7 ft) was illustrated with 90% LCL/UCLs bands at -2.1 and +2.8 ft. This uncertainty included σ_ψ at 10% of SWL (, 0.97 ft, or 90% LCL/UCL bands of about ±1.6 ft) and an asymmetric ε_P, which added more than 1 ft to the ε_ψ 90% UCL band. Components of the aleatory uncertainty were thought to contribute σ_A of 2.1 ft to the 100-yr hazard at the location, indicating an overall σ of 2.3 ft, or a 90% LCL/UCL for normally distributed uncertainty alone of ±3.8 ft. Inclusion of ε_P means the overall magnitude of uncertainty is even higher. However, IPET did NOT address these significant exterior SWLs uncertainties in the analysis of polder inundation hazard. The influence of non-linear contributions was not assessed and confidence limits in the inundation hazard were not identified

17.2 USACE LaCPR Study

The 2009 USACE LaCPR Study examined both exterior surge SWL hazard and surge-related polder inundation under several large-scale planning alternatives. The Study included a current condition alternative reflecting the authorized HSDRRS design—referred to as the 2010 Base Alternative—as well as several future condition alternatives with enhanced surge protection and coastal restoration projects. The USACE's analysis of future alternatives is discussed in Part V, Section 20.1.

The LaCPR Study 2010 Base Alternative version of the authorized HSDRRS used an ADCIRC mesh incorporating the IHNC Surge Barrier (but not the Seabrook Barrier). The Study assessed exterior surge hazards at the 100-, 400-, 1000-, and 2000-yr return periods. The 400-yr hazard was stipulated in the study objectives for evaluating a Katrina-level event. The 400-yr hazard was based on the Resio et al work which estimated Hurricane Katrina's landfall return period for southeast Louisiana at 398 years (see Section 4.2).

The LaCPR Study for the 2010 Base Alternative employed the Surge Response-OS approach used in the FIS JPA of exterior SWL hazards (see Section 14.1). However only 48 of the 152 storms were simulated with the revised mesh (presumably due to limited computational resources). For the 104 storms not rerun, 2010 peak SWLs were instead estimated by applying an adjustment to the 2007 SWLs derived with an algorithm. The algorithm was a quadratic equation specifying the adjustment equal to $A*SWL_{2007} + B*SWL_{2007}^2$. Values for A and B were derived for each output location by fitting this equation to 2007 and 2010 results for the 48 storms that were run. Figure 17.5 illustrates the fitting of the algorithm for two locations. The LaCPR Study report (Hydrology and Hydraulics Appendix) acknowledged that at some locations the quality of fit could be poor.

For the Study, 2010 surge CDFs were computed at each of several hundred locations throughout coastal Louisiana using the 152 local 2010 SWL values (the 48 simulation results plus the 104 estimated values), presumably post-processing similar to the FIS (see Section 14.1). The Study report did not discuss the SWL bias previously noted in the FIS analysis (Section 11.2). The Study report indicated that uncertainty bands were computed for the 2010 SWL hazard levels. However details on how they were developed (including increased uncertainty due to not rerunning all 152 storms), as well as the bands themselves, were not provided.

Zone B Wave H_S and T_P for the 2010 Base Alternative were also developed using a combination of the 48-storm results and the application of fitting algorithms.

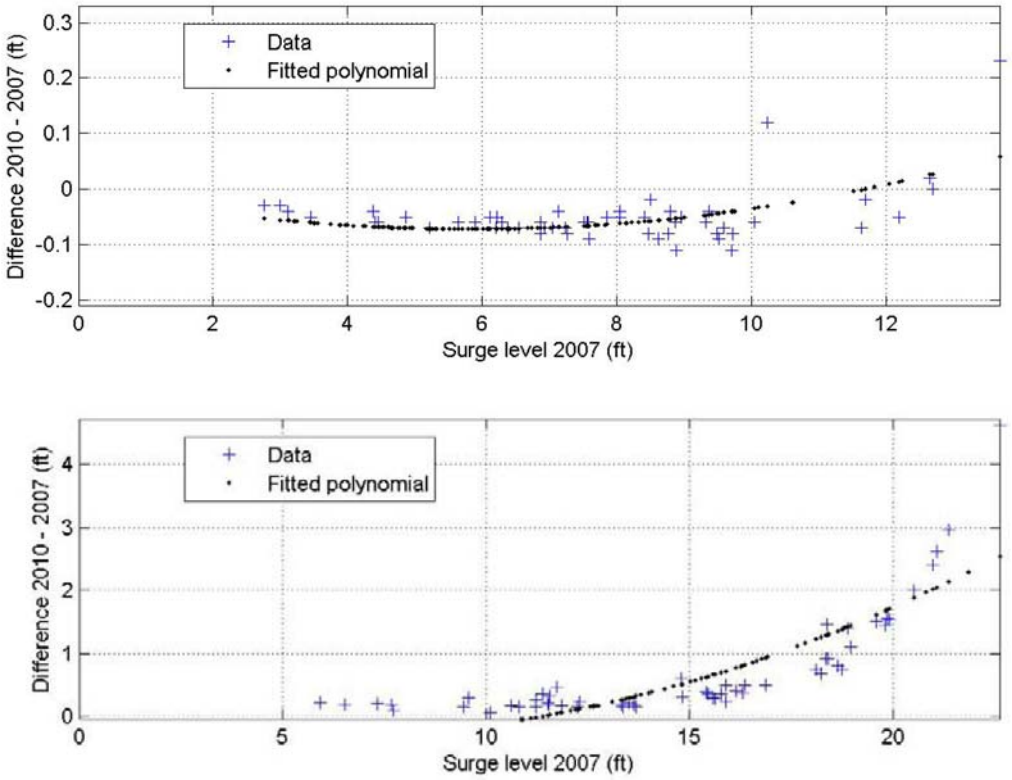

Figure 17.5. Example of 2007-2010 Adjustment Algorithm at Two Locations
USACE 2009

The LaCPR Study did not perform a return frequency for polder inundation or evaluate the cumulative probability of interior SWLs. Unlike the IPET Risk and Reliability Study described above, the LaCPR Study did not assess the joint probability of various inflows associated with probabilistic whole-perimeter surge events. Instead, for this study the USACE simply chose to use the entire set of SWLs around a polder perimeter at the various hazard levels as a "pseudo" surge event. As previously noted, a single storm exceeding the 100-yr (for example) exterior SWL along an entire polder perimeter can have a much greater return period than 100 years. While the study's approach expedited relative comparisons of many alternatives (e.g., future conditions), it cannot be relied upon for estimates of polder inundation hazards. The polder inundation associated with using these "pseudo" surge events are thus better termed *cases*, as in Perimeter Surge Case 100, 400, 1000, and 2000, leaving off any reference to return period to eliminate confusion.

The interior SWLs for the four cases were computed as follows:

- SWL hydrographs were developed at each polder perimeter reach for the three cases using normal distribution curves and values for σ_R and σ_F, obtained by assessing peak SWL versus σ_R and σ_F for the output hydrographs.
- Zone D a wave breaker parameter of 0.4 was applied to the surge depth at the forward embankment toe. and wave T_P was obtained from the STWAVE output. Standard deviations of 10% and 20% were assumed for the Zone D H_S and T_P. Wave θ was assumed to be perpendicular (worst case for overtopping).

- Overtopping hydrographs were computed for each reach (using the structure design elevation) with a combination of the Van der Meer and broad crested weir equations. The Study used C_W and C values of 0.13 and 3.1 $ft^{½}/s$.
- The overtopping estimate included both a 50% (median) and 10% Probability of Exceedance Levels (the same as a 90% Probability of Non-Exceedance and equivalent to the UCL for an 80% Confidence Interval). The overtopping rates at these confidence levels were obtained using the Monte Carlo technique (see GTN-1 Part J) that incorporated uncertainty in the SWL, wave height, wave period, and overtopping coefficients. Figure 17.6 shows an example of a 10%, 50%, and 90% Confidence Level hydrograph at one location, for Perimeter Surge Cases 100, 400, 1000, and 2000
- The LaCPR Study did **NOT** include breaching scenarios.
- Rainfall accumulation was set at 6.5 inches, using the 10-yr 6-hr duration event, with an assumed sinusoidal temporal distribution.
- Pumping volumes were used for each sub-basin based on assumed pump station capacities (not provided in the report).
- Sub-basin peak SWLs were then calculated for the four cases using level-pool routing. Confidence intervals for SWL were based on the overtopping confidence intervals.

Figure 17.7 illustrates the polder inundation results for the 2010 Perimeter Surge Case 1000. (The figure presumably is for the 50% Confidence Level but this information was not clearly stated.)

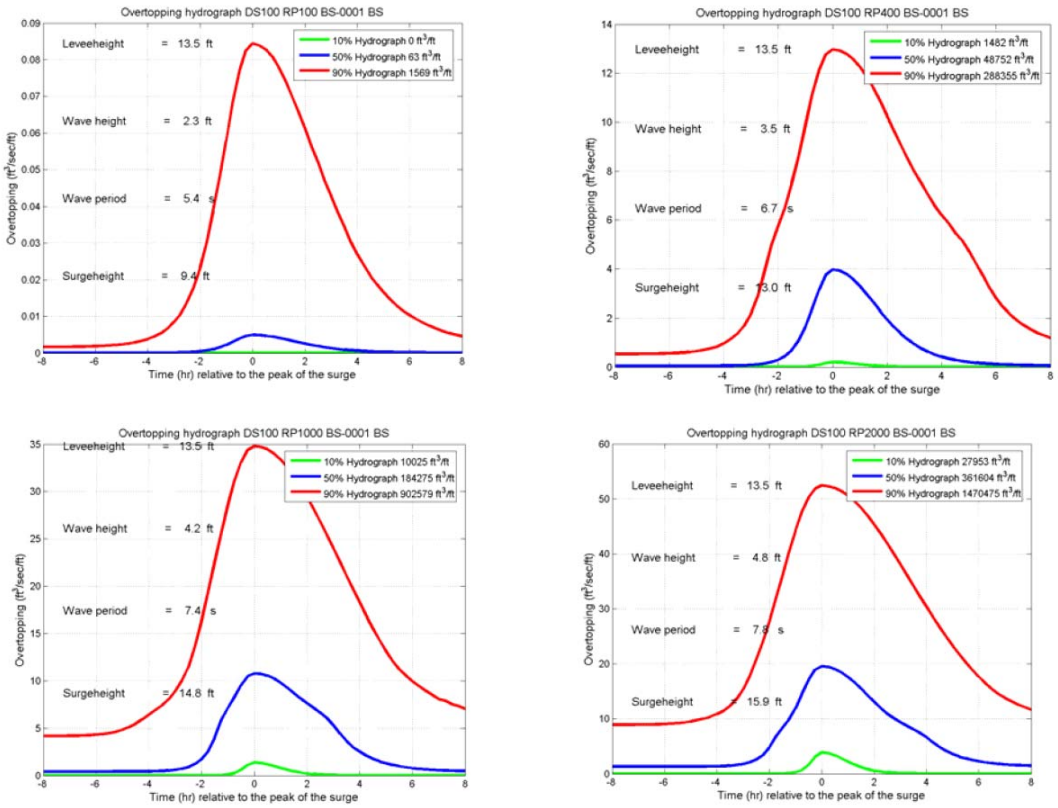

Figure 17.6. Example of Overtopping Hydrographs for Four Cases

USACE 2009

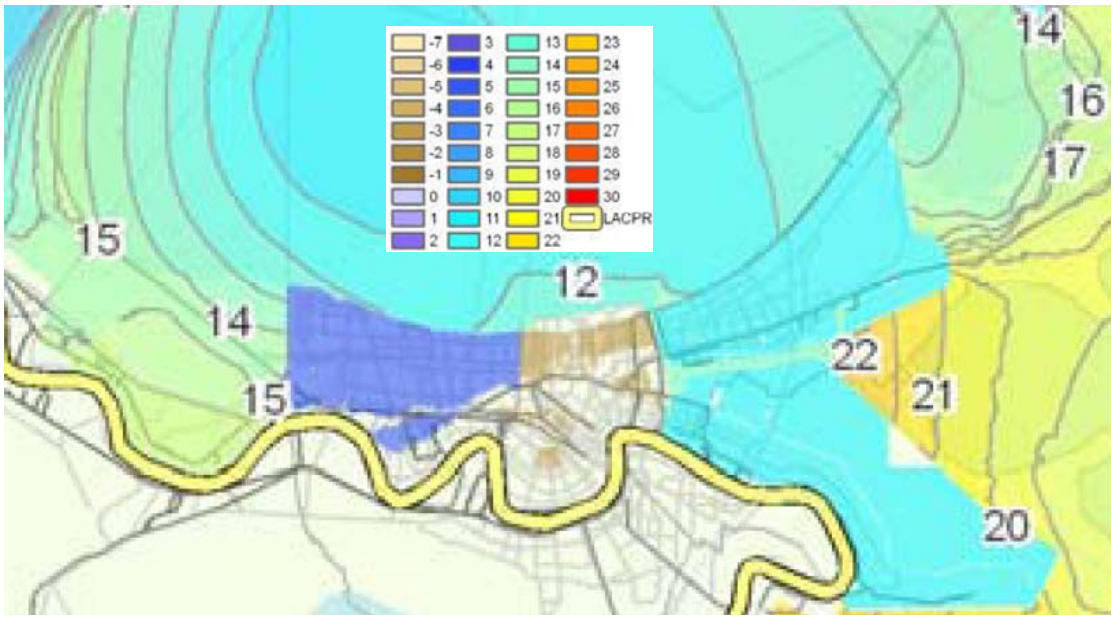

Figure 17.7. Polder Inundation SWLs Associated with Perimeter SWL Case 1000

USACE 2009

(Note the LaCPR Study terrain data mistakenly included a continuous barrier along the St. Charles-Jefferson Parish Line that prevented the 15 ft. high SWL in St. Charles Parish from inundating Jefferson Parish.)

17.3 USACE HSDRRS 100-yr Design

In the wake of Hurricane Katrina Congress authorized the USACE to reconstruct and enhance the New Orleans regional HSDRRS to protect polders from the 100-yr surge hazard.[5] Given that the polders are exposed to substantial 100-yr rainfall flood hazards—even with elaborate drainage systems—the HSDRRS does not eliminate the interior 100-yr flood hazard.[6] The HSDRRS actual design objective therefore is to reduce surge overtopping contributions to the interior 100-yr hazard to a negligible amount (but not zero). T

In accordance with this objective the USACE HSDRRS design provided positive SWL freeboard at the 100-yr SWL—meeting or exceeding NFIP coastal SWL freeboard requirement. (Per 44 CFR 65.10 at least 2 ft of freeboard is required above the 100-yr SWL.) The NFIP also requires 1 ft of clearance above the maximum wave runup for the 100-yr SWL condition unless a lower elevation is supported by appropriate wave overtopping analysis. Given the interior rainfall flood hazard, the USACE proposed HSDRRS design elevations that allowed some *minor* wave-only overtopping at the 100-yr surge hazard. To enhance the design for *minor* wave-only overtopping the USACE addressed some uncertainty in the

[5] As discussed in the Introduction, the 100-yr hazard derives from the NFIP—for which it is a statutorily required (and convenient but somewhat arbitrary) nation-wide benchmark for managing property flood damage risks. However, the 100-yr hazard is widely regarded as an inadequate criteria for comprehensive management of flood risks for a major metropolitan area (see ASCE Louisiana Section 2012).

[6] FEMA and the USACE are currently finalizing FISs for the New Orleans regional polders based on rainfall flood hazards. Some technical documentation is found in FEMA 2012.

overtopping rate estimate. Notably, the NFIP does not require establishing flood hazard elevations with any uncertainty allowance.

The USACE described their approach to specifying 100-yr elevations for each HSDRRS reach in two critical guidance documents (USACE 2008b and 2010). The approach consisted of five steps to account for current (2010) conditions, each with important limitations: (An additional step was also included to address future, 2057, conditions, see Section 20.2).

1. Current 100-yr exterior surge SWL hazards. The USACE 2010 Elevation Report stated that exterior SWL hazards were developed using the 2007 FIS and 2010 ADCIRC meshes (presumably the same one used in the LaCPR Study without the Seabrook Barrier) and the 152-storm Surge Response-OS approach. The design used a combination of 106 storm simulations from the 2007 FIS mesh with 56 storms run on the 2010 mesh (6 more than the 48 used for the LaCPR Study). The 106 2007 SWLs were then adjusted to 2010 conditions, presumably in a manner similar to that described above for the LaCPR Study. The design therefore reflects important limitations in:

   - The treatment of regional hurricane climatology—i.e., joint probability (see Section 4.2);
   - The ADCIRC mesh—as validated for Hurricane Katrina (see Section 11.2), including bias on the south shore of Lake Pontchartrain—lacking the Seabrook Barrier;
   - The Surge Response-OS approach in general (see Section 13.3);
   - The particular Surge Response-OS set used for the southeast Louisiana (see Sections 14.1 and 14.2);
   - The approach to updating the 2010 CDFs (as discussed above in Section 17.2).

   As discussed in Section 15.1, the CDF integration method included smoothing with σ_e , which results in a modest increase in the estimated 100-yr surge hazard.

   Figure 17.8 depicts the 100-yr SWLs used in the east-bank HSDRRS design. Comparing Figure 17.8 HSDRRS 100-yr SWLs with the Figure 14.7 100-yr 2007 SWLs shows little to no difference along Lake Pontchartrain but significant increases along the IHNC, GIWW, and MRGO, due to the inclusion of the IHNC/GIWW Barrier.

2. Current 100-yr exterior surge H_S and T_P hazards. As in the LaCPR Study the USACE established Zone B 100-yr wave conditions based on the 2010 CDFs and adjusted local Zone D wave H_S as necessary with 0.4 breaker parameter. As discussed in Section 6.2, more data are needed on appropriate local breaker parameters. Wave T_P was obtained from the STWAVE output. Wave θ was assumed to be perpendicular (worst case for overtopping).

3. Wave H_S, and T_P within the IHNC/GIWW sub-basin. The USACE estimated wave conditions in the channel confined by the closed IHNC and Seabrook barriers using the Bretschneider Equation (see Section 15.8) and a 1% wind speed of 77 mph. For most reaches a fetch of 0.5 mi was used, providing H_S, and T_P of 3 ft and 3.5 s, respectively. For northern and southern reaches along the IHNC a 0.25 mi fetch was utilized, yielding H_S, and T_P of 2.3 ft and 3.1 s, respectively. Wind setup, as well as more extreme wave conditions, produced along the 6+ mi GIWW fetch—similar to what was observed with Hurricane Gustav, but with the barriers closed—was not considered.

Figure 17.8. 100-yr SWLs for HSDRRS Design

USACE 2010

4. 100-yr SWL and waves in the Mississippi River. The USACE estimated these conditions using a supplementary JPM Surge Response-OS analysis, which has not been finalized:

   - Revised the JPA expression, $\boldsymbol{p}$, to incorporate a probability for the river discharge by month, together with the hurricane landfall frequency by month.
   - Modified the Surge-Response function, $\boldsymbol{\psi}$, to also be a function of Mississippi River discharge. A total of 17 out of the 152-storm set were remodeled using two different Mississippi River discharges (167,000 and 400,000 cfs)
   - Used an improved ADCIRC-STWAVE mesh with greater river details.[7]
   - Recomputed CDFs for points along the river using the revised $\boldsymbol{p}$ and $\boldsymbol{\psi}$.
   - Reran the analysis for sea-level rise of 1 ft (as well as 2, and 3 ft).
   - Estimated the 100-yr $\boldsymbol{H_{1\%}}$, and $\boldsymbol{T_P}$ along the river levees by applying the Bretschneider Equation, along with the location-specific wind speed/direction/fetch conditions at peak SWL for each storm in a subset of the 152 storm set. The subset was similar to the IPET JPM-OS subset and each storm had an assigned probability. For each location, the set of results for $\boldsymbol{H_{1\%}}$, and $\boldsymbol{T_P}$, with their corresponding probabilities, were used to fit a Weibull distribution, which then provided the 100-yr $\boldsymbol{H_{1\%}}$, and $\boldsymbol{T_P}$. The breaking parameter was used to reduce $\boldsymbol{H_{1\%}}$ as appropriate, depending on the local surge depth over the foreshore (batture) at peak SWL.

   The small set size of the southeast Louisiana Surge Response-OS approach may not sufficiently capture critical wind setup variations in the Mississippi River associated with changes in storm V_f and θ. Furthermore, as noted in Sections 14.2 and 17.1 a subset of the southeast Louisiana Surge Response-OS is not likely to provide a JPM-OS representative of more extreme hazards.

5. 100-yr design elevation for 2010 conditions at each reach. The USACE then determined design elevations using the estimates of 100-yr SWL, H_S, and T_P, together with assigned normally distributed uncertainty factors, σ, for each value. Crown design elevations were required to be at least 2 ft above the median (50% Exceedance Level) estimated 100-yr SWL.

   Median estimates of average overtopping rates were then computed with the Van der Meer and Franco equations and crown elevations were raised as necessary to limit the local 100-yr overtopping rate for levees and floodwalls at 0.01 and 0.03 cfs/ft, respectively.

   Next the uncertainty factors were employed with a Monte Carlo technique—using the same overtopping equations—to determine local average overtopping rates at the 10% Exceedance Level. Reach crown elevations were raised as necessary to limit the local 100-yr 10% Exceedance average overtopping rate for levees and floodwalls at 0.1 cfs/ft. Figure 17.9 illustrates the average overtopping rate versus exceedance level for one reach design.

   The USACE guidance (USACE 2010 Appendix E) stated that the technical basis for the average overtopping limits was preventing interior-side scour of embankments and erosion

[7] The USACE stated that the improved ADCIRC mesh was validated for both steady stage-discharge curves at several river locations. However, details of the mesh changes and these validations were not provided in the guidance. The guidance did provide a validation of the ADCIRC model river stages for Hurricanes Katrina, Betsy, and Camille.

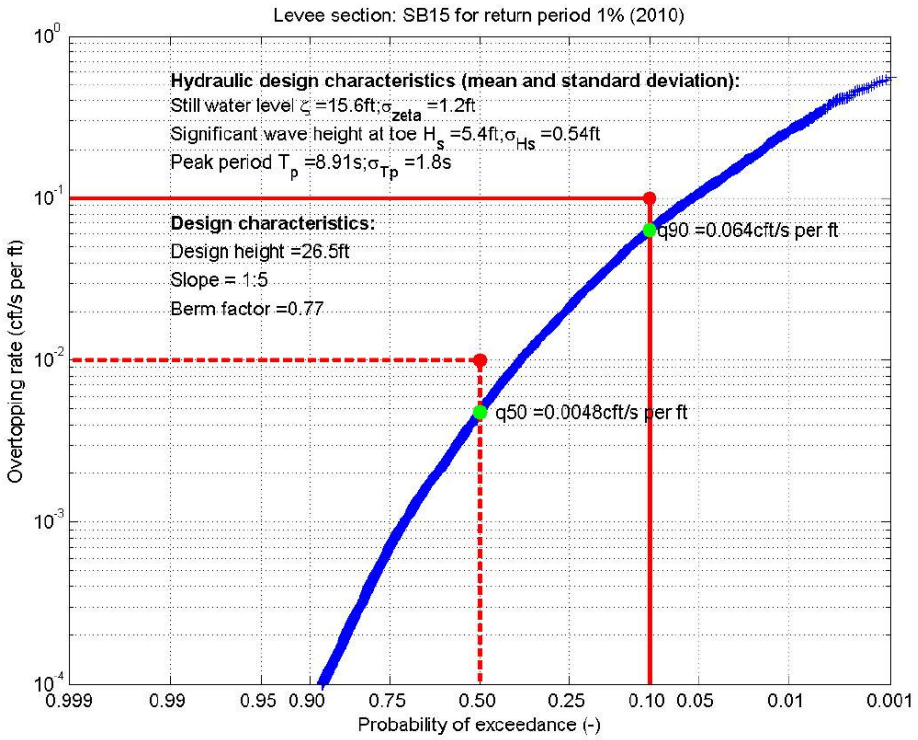

Figure 17.9. Example of Overtopping Rate vs Exceedance Level
USACE 2010

breaching caused by overtopping of extreme waves during brief hurricane surge peaks. On the one hand, concerns regarding overtopping limits may be mitigated to the extent that average overtopping equations can over-predict extreme wave recurrence over short durations, and thus overtopping rates (see Sections 15.1 and 15.3). On the other, however, little experimental data, as well as observations for actual levee and floodwall overtopping under surge type conditions, are available to support development of average overtopping limits. As discussed in Section 15.3, at an average overtopping rate of 0.1 cfs/ft, individual extreme wave overtopping may produce instantaneous velocities of 17 ft/s down the interior-facing slope, as well as cavitation effects on surface soils. A complete discussion of the subject of erosion-based wave overtopping criteria is beyond the scope of this Report.

The USACE an overtopping uncertainty analysis in order to provide some conservativism in the design.[8] Importantly though, the USACE did not utilize the full SWL hazard uncertainty previously determined for the FIS or IPET. Using the information in the FIS documentation, (see Section 14.1) the 100-yr epistemic σ is about $[(2.1)^2 + (0.15*SWL)^2]^{0.5}$—or 18% and 26% at SWLs of 20 and 10 ft, respectively. The HSDRRS design did not employ this σ value in the Monte Carlo analysis, but instead employed values which were below 10%.[9]

[8] The USACE design guidance made frequent use of the word "conservative" but did not explain the use of the 10% Exceedance Level—i.e., 80% Confidence Interval. Goldman 2003 cited the use of a 90% Confidence Interval—i.e., a 5% Exceedance Level—for the design of levees along the Upper Mississippi River.

[9] The Monte Carlo analysis also did not adjust the base value for H_s for draws of higher SWL and depth.

Figures 17.10.a and b illustrate the sensitivity of the wave overtopping rate and levee design elevation to the choice of SWL σ using the Monte Carlo technique. For a SWL of 12 ft an increase of σ from 10% to 20% (1.2 to 2.4) quadruples the 10% Exceedance overtopping and raises the design height by about one foot. An increase to 30% (3.6 ft) raises the 10% Exceedance overtopping by a factor of 10 and raises the design height by two feet.

The design did not discuss the issue of SWL bias associated with the ADCIRC Hurricane Katrina validation (see Section 11.2) and did not introduce bias correction. Figure 17.10.c and d depict the influence of SWL bias on the median (50% Exceedance) overtopping rate and design elevation (ignoring any influence on wave height). A 1.5 ft under-prediction of SWL (13.5 ft versus 12 ft) increases the median overtopping by a factor of three, and requires raising the design by close to 1.5 ft.

Figures 17.11.a, b, c, and d illustrate sensitivities for H_S uncertainty and bias. Overtopping and design elevation are relatively insensitive to H_S uncertainty. However, H_S bias—e.g., if the 0.4 breaking parameter is too low—has a notable influence on overtopping and levee crest height. In the case depicted, a 1 ft H_S under-prediction (3.2 versus 4.2 ft) increases the median overtopping by a factor of five, and requires raising the design by over two feet.

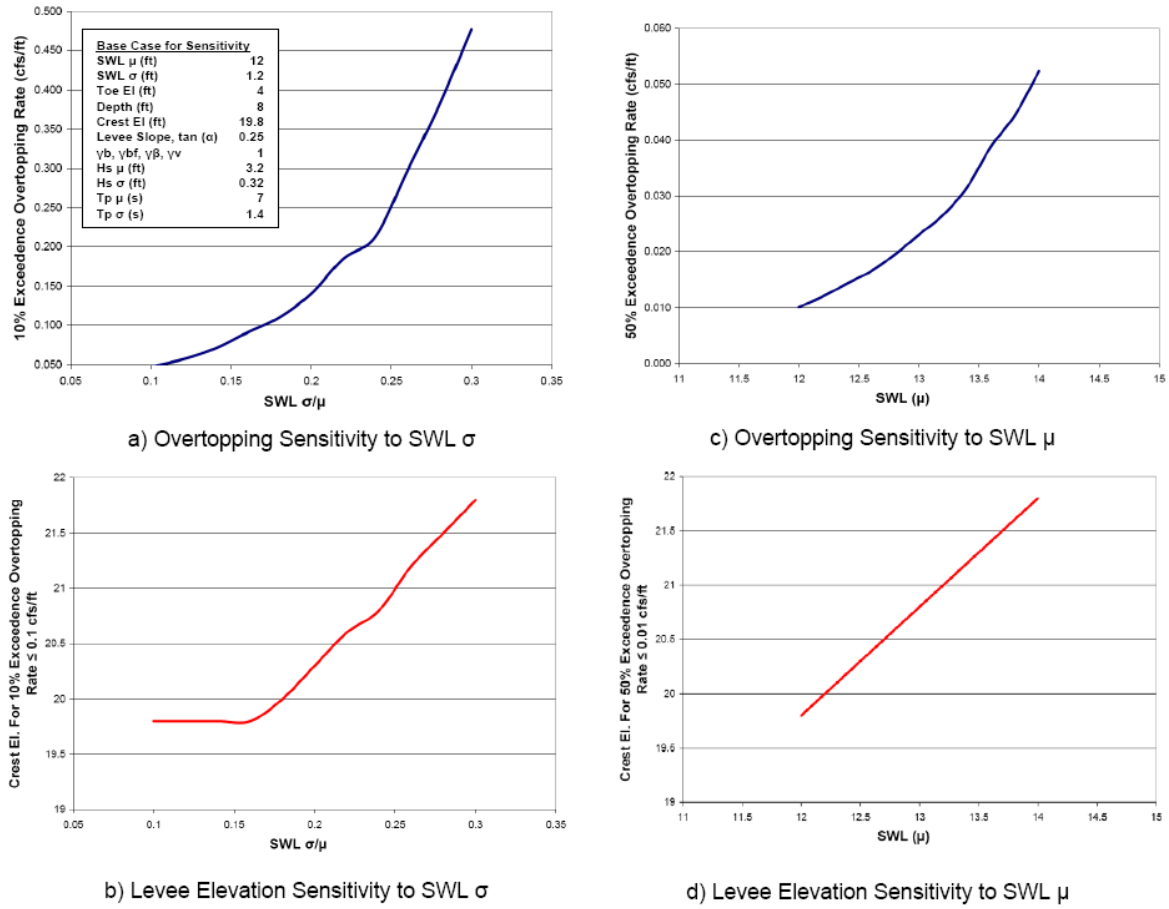

a) Overtopping Sensitivity to SWL σ

c) Overtopping Sensitivity to SWL μ

b) Levee Elevation Sensitivity to SWL σ

d) Levee Elevation Sensitivity to SWL μ

Figure 17.10. Sensitivity of Overtopping Rate and Design Elevation to SWL σ and μ

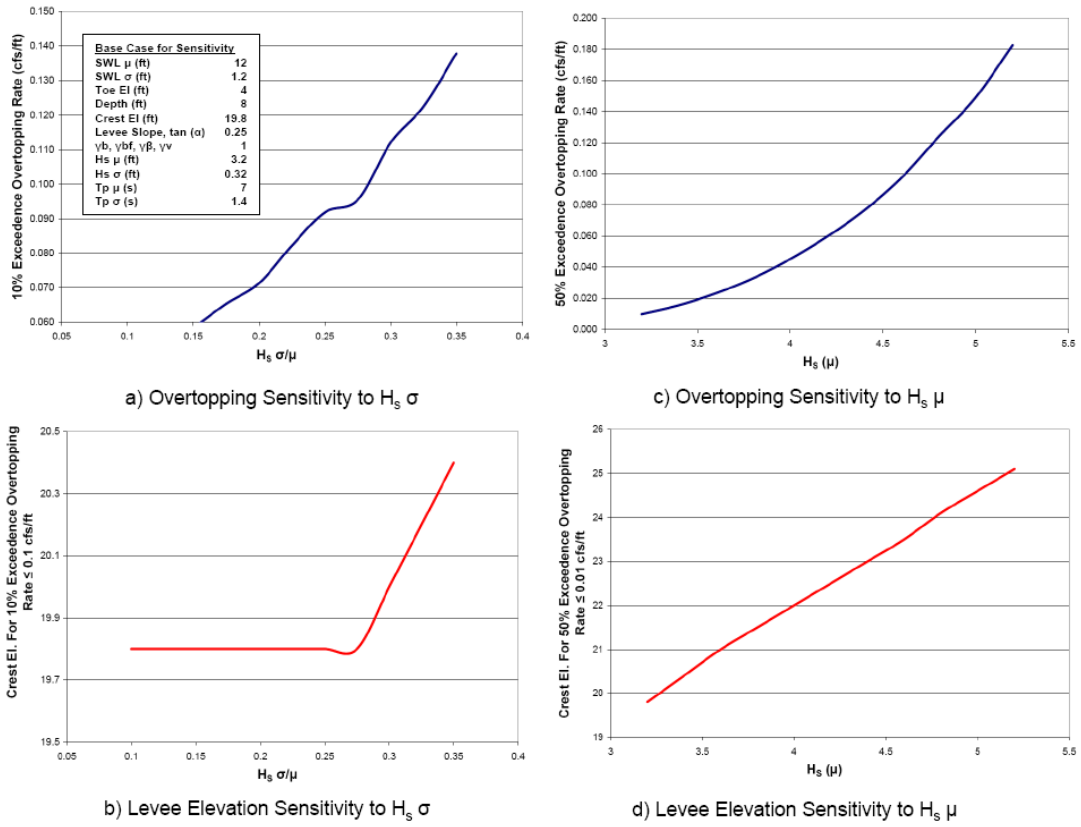

Figure 17.11. Sensitivity of Overtopping Rate and Design Elevation to H_s σ and μ

Attachment 1 provides the current, 2010, 100-yr SWL, H_S, and T_P for each reach, with the respective σ values, together with the 2010 design elevations and overtopping rates derived in Step 5. Final hydraulic design elevations for floodwalls, but not levees, were modified in accordance with future conditions (see Section 20.2). It should be noted that while USACE 2008b required final hydraulic design elevations in accordance with the 10% Exceedance for overtopping in Step 5, it did not specify that all structural components address all hydraulic loads associated with the 10% Exceedance condition. Final plan elevations were adjusted upward in some cases due to geometric design considerations and allowances for post-construction settlement.

The USACE 100-yr elevation design criteria provided for an equal 100-yr overtopping hazard at all reaches (based on levee or floodwall type). However, a consequence of the equivalent 100-yr overtopping criteria was that they necessarily translated into *widely varying 100-yr freeboards.* Figure 17.12 illustrates the range in median 100-yr freeboard for selected HSDRRS levee reaches. Reaches fronted by vast foreshore wetlands generally required less freeboard to minimize wave overtopping. On the other hand, reaches immediately fronted by a large water body necessitated more freeboard to minimize wave overtopping.

The 10% Exceedance average overtopping rate of 0.1 cfs/ft—for a simple case of 3 miles over 6 hours—corresponds to 785 acre-ft. Increasing the length to 10 miles equates to 2,617 acre-ft. At the median overtopping rate of 0.01 cfs/ft the volume for 10 miles of overtopping over 6 hours is 262 acre-ft. Wave-only overtopping volume is not trivial, but is markedly less than the 100-yr 24-hr rainfall for most of the urban sub-basins shown in Table 17.2.

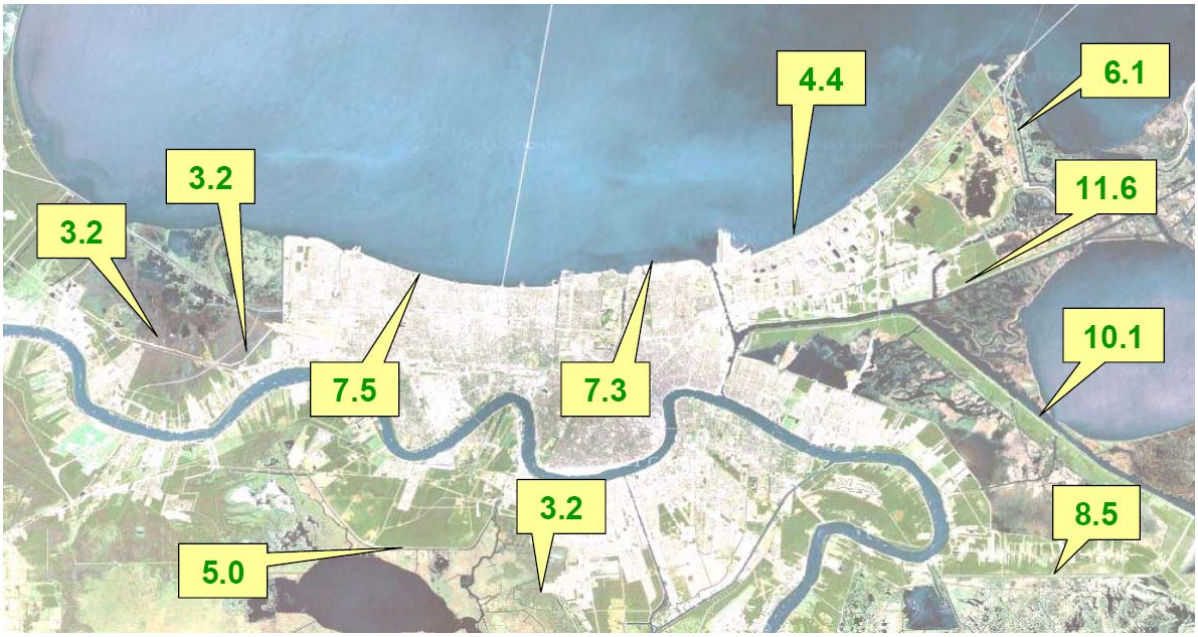

Figure 17.12. Median 100-yr Freeboard at Selected HSDRRS Levee Reaches

A critical design limitation is that—as previously discussed in Section 16.2—local 100-yr overtopping rates, and thus volumes, can correspond to a more frequent equivalent whole-polder inundation volume—due to possible multiple independent reach exposures. For a polder with two independent exposures the 100-yr overtopping hazard associated with either exposure equates to nearly a 50-yr polder volume; and a 100-yr whole-polder- inundation volume is equivalent to nearly a 200-yr overtopping volume at one exposure.

To date, the USACE has not updated the JPA for the 100-yr surge polder inundation hazard associated with the final HSDRRS design. (The IPET analysis described above does not include the IHNC/GIWW and Seabrook Barriers or the upgraded West Return Wall.) The polder FISs do not include an updated JPA of surge inundation hazard (FEMA 2012).

17.4 USACE HSDRRS Resiliency Design

In addition to protecting against the 100-yr surge hazard, Congress authorized HSDRRS resiliency. The USACE has equated resiliency with the secondary objective of reducing the threat of erosion breaching caused by overtopping.[10] To meet this objective the USACE is currently evaluating structural enhancements to reduce embankment interior-side scour. In accordance with guidance the USACE is following two steps (USACE 2008b). Step 1 has been competed while Step 2 is still in progress.

[10] To date, the USACE has determined that other measures are not a subject of their resiliency authorization, including raising reach elevations to provide greater freeboard; protection of the exterior-side from erosion due to waves and long-shore currents associated with non-overtopping surges; and reducing other sources of fragility that could lead to breaching without overtopping. The USACE considers itself prohibited from using resiliency appropriations for such measures even where they achieve greater effective overall risk-reduction.

1. 500-yr SWL overtopping rate for 2010 conditions at each reach. The USACE determined current 500-yr SWL, H_S, and T_P for each reach from the 2010 CDFs, with modifications of H_S in accordance with the breaking parameter of 0.4. Uncertainty factors were also assigned for SWL, H_S, and T_P. The median (50% Probability of Exceedance) and 10% Probability of Exceedance overtopping rates for the current 500-yr conditions were then estimated using the same methods applied to the 100-yr overtopping rate. Attachment 1 includes the current median estimate for the 500-yr SWL and overtopping results for each reach.

   Three important concerns with this first resiliency step are:

   - The USACE JPA is likely to underestimate the 500-yr exterior surge SWL hazard, as noted above in Section 17.2. The USACE design guidance did not address this limitation, nor did it discuss factoring in SWL uncertainty and using a UCL instead of the median estimate for the current 500-yr SWL.
   - The USACE did not provide a minimum freeboard criteria for the 500-yr condition. The general design guidance (USACE 2008b p. I-25) stated that the design elevation is to prevent free flow for the 500-yr condition; the exceedance level is not specified.[11] However, the guidance on HSDRRS elevation (USACE 2010) did not provide for raising reach elevations based on the evaluation of the 500-yr condition. As a result, the current median 500-yr freeboards for eight levee reaches were less than 1 ft, with three being negative:

East-bank St. Charles Parish levee reach east of I-310	0.5 ft
Mississippi River to US 90	0.1 ft
Orleans Village to Ames Pump Station	0.1 ft
Highway 3134 to Old Estelle Pump Station	0.1 ft
Transition Point to Hero Canal	0.1 ft
Robinson Point to Harvey Canal	-0.4 ft
Hero Pump Station to Algiers Canal	-0.4 ft
Hero Canal Area behind Landfill Berm	-1.4 ft

   - At the 500-yr condition, unlike the 100-yr condition, reaches will experience significantly different overtopping rates. Reaches with minimal 500-yr freeboard face the most significant exposure. Figure 17.13 shows that the 2010 10% Exceedance 500-yr overtopping rate can vary by a factor of five.

2. Appropriate interior-side armoring measures to reduce the threat of overtopping induced erosion breaching. Varying overtopping rates above the 100-yr hazard around the HSDRRS—as depicted by Figure 17.13 for the 500-yr hazard—imply that different reaches have significantly different erosion breach probabilities at hazards above the 100-yr level. The USACE is presently evaluating alternative armoring technologies (enhanced turf, turf reinforcement mats, concrete mats, armor stone, etc.) for different overtopping conditions. As part of the evaluation the USACE has conducted initial wave erosion testing at Colorado State University (Thornton et al 2012).

[11] USACE 2008b did not require that structural components address anticipated loads under the 500-yr conditions.

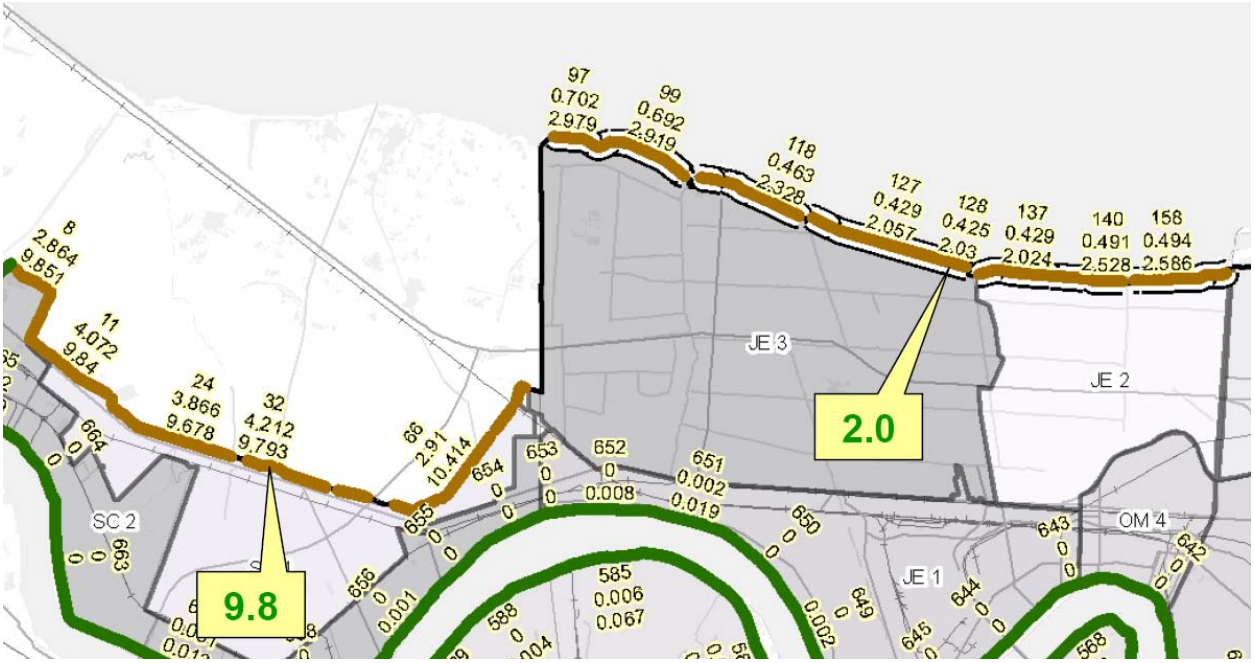

Figure 17.13. 10% Exceedance 500-yr Overtopping at Selected HSDRRS Levee Reaches (cfs/ft)

USACE 2011

To support the selection of cost-effective, reach-specific measures the USACE has indicated it will employ the IPET JPA approach described in Section 17.1. The approach incorporates erosion breach probability (fragility) analysis and uses the FoRTE spreadsheet program to compare polder inundation CDFs under different armoring scenarios. At this time this analysis has not been finalized and documentation for the treatment of breach failure conditions and fragility, as well as uncertainties, has not been released. Figure 17.14 illustrates how hazard comparisons can be compared under different armoring/failure scenarios.

The USACE has indicated that the selection of reach-specific armoring measures are likely to be based primarily on the estimate of the *median* 500-yr overtopping rate, together with information on the degree of hazard reduction, constructability, maintenance issues, and cost (USACE 2011)

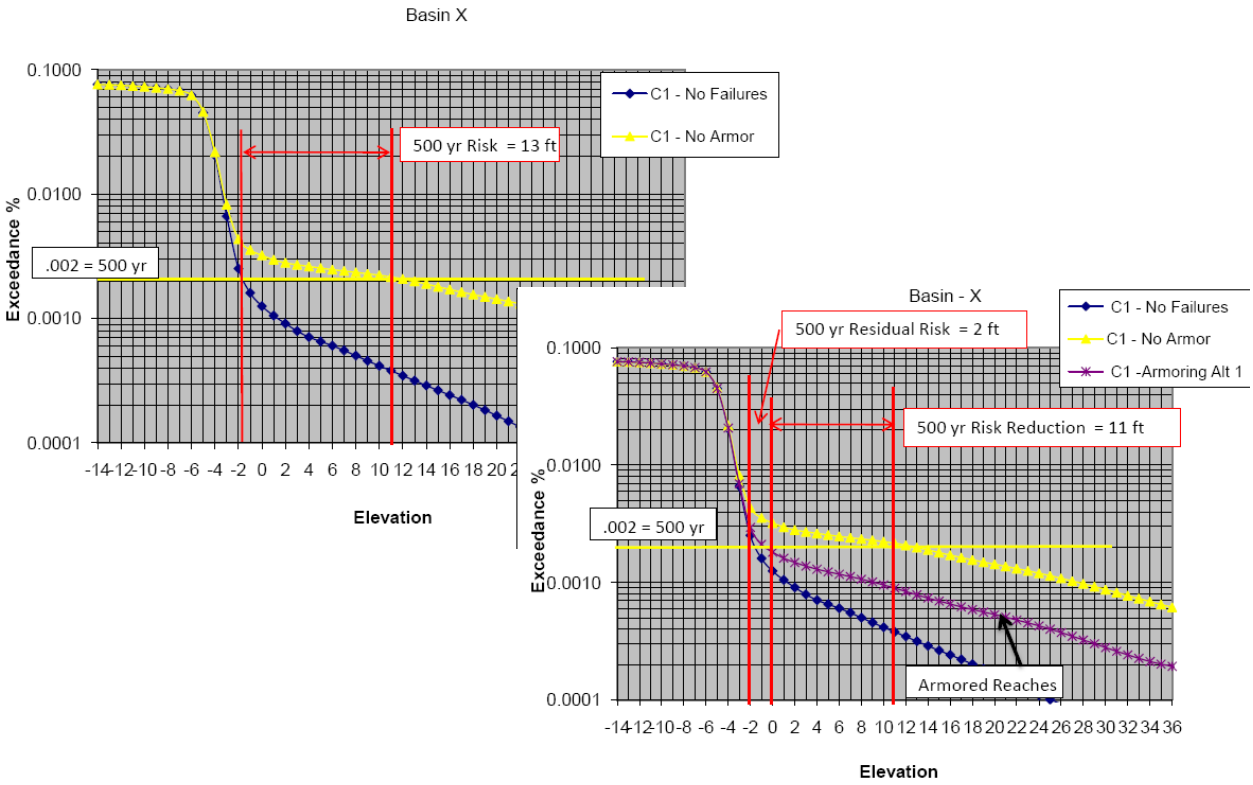

Figure 17.14. Example of Polder Inundation Hazard Comparisons for Armoring Alternatives

USACE 2011

Part IV. Conclusions and Recommendations

Conclusions

Part IV has reviewed methodologies for analyzing polder inundation hazards associated with hurricane surge and recent applications to the New Orleans regional polders. This information supports the following important findings:

1. Eight hydrologic/hydraulic processes control surge inundation of polders. Methodologies are available to quantify these processes but many lack extensive empirical grounding:

    a. The storm surge dynamics. Parts I, II, and III described the approach to estimating exterior surge SWL and wave conditions, with associated limitations and uncertainties. Evaluating polder inundation hazard requires additional attention to local conditions producing SWL variations and wave nearshore and foreshore transformations.

    b. Seepage perimeter inflows. Estimates are limited by data on shallow geology, preferential flow paths, and representative surge-driven seepage rates.

    c. Overtopping perimeter inflows. Analysis usually relies on simple assumptions about wave transformations in the foreshore region—e.g., employing breaker parameters to estimate H_s as a function of depth. However, there are few observations of storm surge foreshore waves. Rayleigh Distribution, which is used to relate the relative frequency of H_s to more extreme waves, may overestimate extreme wave recurrence for surge events. Empirical equations for average wave overtopping—as well as supercritical and submerged weir flow—are subject to limited field observations for defining coefficients. In addition, such overflow estimates have nonlinear sensitivities to estimates of H_s and SWL.

    d. Breach perimeter inflows. Estimates use supercritical and submerged broad-crested weir formulations—but again with limited field observations to define coefficients—and specific breach invert and length (I-L) scenarios for exterior SWL and structure type. Breach occurrence can be conditional, with probability (fragility) also a function of both exterior SWL and structure type. Breach I-L and fragility relationships to exterior SWL and structure type are often restricted to just a few "steps." At this time, the relationships and the steps are highly subjective.

    e. Rainfall accumulation. Estimates typically apply a standard rainfall return event (e.g., 6-hr/10-yr) to the whole-polder. Alternatively, a relationship has been suggested between rainfall accumulation and hurricane intensity, size, forward speed, and track (distance and direction) with respect to polder location. However, such a relationship has not been documented to date.

    f. Drainage pumping outflows. Estimates are based on some percentage of pump station rated capacity. No research has been published to suggest a method for estimating the percentage, or the probability of such performance.

    g. Internal routing of the time-varying and location-specific perimeter inflows, rainfall, and pumping outflows. Evaluating near uniform inundation for whole-polders or sub-basins can be accomplished with a simple level-pool (stage-storage) approach. 2D routing models can describe inundation variability controlled by localized perimeter inflows, interior topographic features, and drainage. Modeling near-field breach dynamics requires special capabilities to examine supercritical flow and shock waves.

h. Local wind-induced interior setup and waves. 2D routing models can include local wind setup. For level-pool routing results can be adjusted using simple 1D wind setup equations accounting for sustained wind speed, fetch, and water depth. For inundated areas with long fetch interior the peak down-wind wave heights can be estimated with breaker parameters. If inundation depths warrant, the Bretschneider, CEM, or other basic equations, or even 1D WHAFIS and 2D STWAVE/SWAN models, can be used to estimate wave conditions(see Part III). These equations are again limited by suitable observations.

2. Evaluation of polder inundation requires a deterministic model of seepage, overtopping, breaching, rainfall, and pumping (SOBRP), that addresses the standard methodologies for quantifying the respective processes. Basic SOBRP modeling, together with level-pool interior routing, can be accomplished with spreadsheets (or programmed with MATLAB or FORTRAN) and coupled (one-way) with the exterior surge and wave model output. Analysis of submerged weir flow and pumping also requires input from the interior routing. Tight coupling of all four models—the high resolution 2D exterior surge and wave model (e.g., ADCIRC-STWAVE or SWAN+ADCIRC), the local wave model, the SOBRP model, and polder routing (with internal wind setup as needed)—has not yet been developed. Furthermore, the limited observations of SOBRP and interior HWMs—such as for Hurricane Katrina—have not enabled detailed validation of four-part polder inundation modeling.

3. Sensitivity tests using the SOBRP model alone, or in combination with the other models, can be used to assess the influence of variability and/or uncertainty in input conditions and process parameters.

4. Polders face other inundation risks apart from surge-driven inundation. The New Orleans regional "bowls" are exposed to notable rainfall-only flood hazards—with some low-lying locations at significant risk from 10-yr rainfall events. Large portions of the Metro New Orleans Polder face a higher SWL for a levee breach during a Mississippi River flood than for an equivalent hurricane surge hazard level.

5. In general, seepage and wave-only overtopping pose a minor inundation hazard, with quantities much less than 6-hr/10-yr rainfall hazards. Wave-only and shallow free-flow overtopping (e.g., SWL less than 1 ft above the crown), over perimeter distances of several miles, produces volumes that are less than the 6-hr/100-yr rainfall hazard. Deeper overtopping and breaching inflows pose the major hazard, exceeding 24-hr/100-yr rainfall quantities.

6. Defining polder inundation hazards from surge requires extending hurricane surge JPA to incorporate those notable SOBRP uncertainties/variabilities with nonlinear influence on inundation volume—such as breach fragility, SWL, H_s/breaker parameter, and crown elevation. JPA is crucial to account for independent reach exposures and to assess the influence of independent SOBRP conditional variables. The inundation JPA requires a JPM set of probability-weighted "whole-polder" surge events to represent the exterior hazard. The exterior surges for each storm in a JPM-OS (or a Full-or Monte Carlo-JPM set) can be used, but not those for a Surge Response-OS as this type of set is not designed to represent the exterior hurricane hazard.

7. A subset of whole-polder scenarios is then employed to represent the range of SOBRP joint probabilities for each JPM-OS storm; a separate subset is required for each JPM-OS storm. The range of scenarios within each subset must reflect the various probabilistic combinations for each independent SOBRP variables at each reach. Computational restrictions can limit the JPA to considering only breach fragility (which may be reasonable as breach volumes can overwhelm the other SOBRP flows) and just a small number of breach I-L steps and/or fragility steps.

8. SWL CDFs throughout the polder interior are computed with the results of the inundation JPA using techniques similar to those described for exterior SWLs (see Part III). Uncertainties/variabilities with a linear influence on inundation volume (e.g., interior terrain data) can be treated as normally distributed and lumped into an overall σ, which can then be used to construct uncertainty bands for the inundation CDF.

9. Interior wind wave hazards at a referenced SWL hazard can be assessed as they are for exterior locations—using breaker parameters. Wave equations and models (e.g., WHAFIS) can be employed to characterize the wave hazards for deeper, longer fetches.

10. IPET employed surge inundation JPA for the New Orleans area polders as part of comparing pre- and post-Katrina HSDRRS risk and reliability.

    - As discussed in Part III, IPET improvised 76 whole-polder exterior events by assigning probabilities to 76 storms from the 152-storm FIS Surge Response-OS. However, the Surge Response-OS was not intended as a JPM-OS and does not adequately represent extreme, >200-yr return, hurricane hazards.
    - The inundation JPA did not address ADCIRC bias on the south shore of Lake Pontchartrain.
    - The improvised 76-storm JPM-OS resulted in notably different estimates of exterior surge hazard than those derived for the FIS.
    - Exterior local wave H_S were set primarily using a breaker parameter of 0.43.
    - The SOBRP scenario subset only addressed breach fragility. The scenarios included independent breach probabilities for each reach. Two breach I-L conditions were identified for each reach—one for overtopping erosion breach and one for non-overtopping breach—each conditioned first on a threshold local SWL. The two breach cases were further conditioned using a few increments of fragility—specified according to structure type and the degree to which peak SWL exceeded the local threshold.
    - The inundation volumes for each of the hundreds of scenarios per storm included the breaching inflow plus any local reach overtopping, rainfall, and pumping at three alternatives (0, 50, and 100% of capacity). IPET performed level-pool routing for each scenario, subdividing each polder into several sub-basins, and computed 50-, 100-, and 500-yr interior hazards using the results.
    - The 500-yr interior surge volume for a 2010 HSDRRS case (without the IHNC/GIWW and Seabrook Surge Barriers and higher West Return Wall) was 25% less than the volume for a 6-hr/100-yr rainfall (less 6-hr pumping) for the Orleans Parish area within the Metro Polder. For the Jefferson and St. Charles Parish areas within the Metro Polder the 500-yr interior surge volume was more than 2.5 times the 6-hr/100-yr rainfall-only volume (less 6-hr pumping). For New Orleans East the 500-yr surge volume was 40% higher.

    While IPET's polder inundation JPA facilitated a comparison of risks for the different HSDRRS cases, the limited empirical basis for breach fragility and breach scenarios meant that the estimates of actual inundation hazard were highly speculative.

11. The USACE's 2009 Louisiana CPR Study used some polder inundation analysis methods, but not an inundation JPA, in order to support planning-level comparisons of potential regional coastal protection and restoration programs. (Additional approaches used to examine future conditions are discussed in Part IV).

- The Study re-evaluated exterior surge hazards for the base (2010) case by modifying the FIS ADCIRC mesh for selected Surge-Response simulations, combined with algorithm-based adjustments for other simulations, and then recomputing the exterior CDFs. As discussed in Part III, the Surge Response-OS does not adequately represent extreme hurricane hazards.
- Exterior local wave H_S were set primarily using a breaker parameter of 0.4.
- Instead of an inundation JPA the study simply used the estimated 100-, 400-, 1000-, and 2000-yr surge hazards around the perimeter as four "pseudo" surge events. Due to the independence of reach exposures around each polder, using the perimeter hazard SWLs as a "pseudo" event equates to a much more extreme whole-polder hazard level—i.e., an event with all reaches attaining the 400-yr SWL is much rarer than a 400-yr event.
- The Study then routed overtopping associated with these "pseudo" events, together with rainfall, but with no breaching, and using a more simplified internal topography than IPET.
- Uncertainties in exterior SWL hazard levels were used to compute UCL/LCLs for overtopping.

While suitable for "what if"-planning-level assessments, the CPR Study approach to inundation analysis is more speculative than that of IPET and cannot be used for estimates of actual inundation hazard.

12. The USACE utilized a simple analysis of local 100-yr overtopping hazard—but not a complete inundation JPA—to design the New Orleans regional HSDRRS for current, 2007, LMSL. (Designs based on future, 2057, LMSL are discussed in Part IV. For some reaches final design elevations were increased to account for construction issues and post-construction settlement.)
    - Exterior 100-yr surge and wave conditions were established in a manner similar to the Louisiana CPR Study. Additional analysis was conducted for 100-yr surge and wave conditions in the IHNC/GIWW sub-basin and Mississippi River.
    - The USACE set crown elevation with at least 2 ft of freeboard for the median estimate of the 100-yr SWL and minimizing local 100-yr wave overtopping to a level intended to prevent interior-side erosion breaching. Minimizing 100-yr wave overtopping produced much higher 100-yr freeboards for reaches with direct open water exposure—e.g., greater than 10 ft for some reaches facing Lake Borgne. A minimal, non-zero local overtopping was apparently adopted given significant residual interior 100-yr flood hazards and as consistent with NFIP requirements.
    - To provide some conservativeness in the overtopping estimate, the design incorporated a sensitivity analysis of the 100-yr overtopping rate as a function of uncertainties in exterior 100-yr SWL, H_S, and T_P (using a Monte Carlo technique). The USACE then specified crown elevations at all levee and floodwall reaches to prevent *average* overtopping from exceeding median criteria (i.e., 50% Exceedance Level) of 0.01 and 0.03 cfs/ft, respectively, and an 80% UCL criteria (i.e., 10% Exceedance Levels) of 0.1 cfs/ft.
    - The elevation design approach would have been more conservative had it employed the more typical 90% UCL/LCLs instead of the 80% UCL/LCLs.
    - Five critical elements of the design were counter to a conservative approach:
        - The ADCIRC model has a noted under-prediction bias along the south shore of Lake Pontchartrain, which was not addressed.

- The assumed breaker parameter value is on the low end of the generally accepted range.
- The design uses a much lower SWL σ in the sensitivity analysis than indicated by the FIS and IPET. At a 100-yr SWL of 12 ft, a more appropriate σ raises the crown design by 1.7 ft. Furthermore, the indicated 10% Exceedance Level is not an actual statistical value.
- The wave height, which is assumed to vary with surge depth, is not a function of surge depth in the sensitivity analysis.
- Criteria for average overtopping rates need to more clearly allow for the dramatically higher instantaneous scour velocities associated with extreme waves, as well as uncertainties in interior-side erosion breach initiation and development.

- One additional factor is likely to contribute additional conservatism in the design. Extreme wave recurrence during short-term wave events, and hence overtopping, is probably over-estimated by empirical equations derived from long duration wave events.

13. The USACE is in the process of additional HSDRRS resiliency design, intended to reduce the threat of interior-side erosion breaching from more extreme surge events. (Structural enhancements to reduce exterior-side wave erosion, improve strength against collapse breaching, or increase freeboard are not addressed in the resiliency design.)
    - The resiliency design has used the Louisiana CPR exterior CDFs—which as noted above do not adequately represent extreme, >200-yr, hurricane hazards. The resiliency design has also assumed a wave breaker parameter of 0.4 to establish exterior 500-yr H_S.
    - The 100-yr overtopping design produced widely varying 500-yr freeboard and overtopping conditions around the polders. Using the median 500-yr SWL, the designs for eight regional New Orleans reaches have 500-yr freeboard of less than 1 ft, with three reaches at negative 500-yr freeboard.
    - Reaches with minimal 500-yr freeboard face the most significant overtopping exposure. At the 10% Exceedance Level, the 500-yr *average* overtopping rate can vary by a factor of five, with some reaches nearing 10 cfs/ft.
    - The USACE is presently evaluating alternative armoring technologies (enhanced turf, turf reinforcement mats, concrete mats, armor stone, etc.) for different overtopping conditions. As part of the evaluation the USACE has conducted initial wave erosion testing.
14. The USACE has initiated but not completed an inundation JPA for the 100-yr design and the resiliency options to facilitate a comparison of alternatives. The JPA follows the IPET approach. Thus, for the reasons noted above, the JPA may not provide a realistic estimate of actual extreme inundation hazard.

Recommendations

The above conclusions indicate that the recent USACE analysis of polder inundation hazard is outdated. They also provide the basis for seven recommendations to improve the New Orleans metropolitan polder inundation hazard analysis:

1. Provide a JPA of the polder inundation hazard, expanding on the IPET approach, and estimate the residual 100-, 500-, and 1000-yr inundation hazards.
2. Base the polder inundation JPA on the larger JPM-OS set of storms as identified in the Part III recommendations.
3. Include a realistic quantification of the range of breach I-L cases and associated fragility conditions for each storm.
4. Estimate local wave conditions and HSDRRS wave overtopping with the state-of-the-practice methods that better account for local peak wave conditions during hurricane peak surge.
5. Further expand the inundation JPA to encompass the nonlinear influence of additional key probabilistics—such as exterior SWL and H_S—on inundation volume.
6. Examine the full influence of uncertainties—associated with the hurricane climatology, the exterior hurricane surge and local wave model, seepage, overtopping, breaching, rainfall, pumping, internal routing, and particular JPMs—on the inundation hazard estimate. Such treatment should be developed to allow estimating a range of confidence intervals—e.g., 80, 90, 95%.
7. Update estimates of the wave overtopping hazard for the HSDRRS design at each reach in accordance with No. 4, and update confidence intervals using full uncertainties for surge and wave conditions.

The Louisiana CPRA, together with federal partners, should fund critical research to improve polder inundation hazard analysis, including:

1. Further research on local wave, SOBRP, and interior routing processes, including laboratory and field studies to evaluate empirical formulations and coefficients. High priority issues are:
    - Appropriate wave height distributions for short duration surge peaks.
    - Appropriate breaker parameters or wave transformation models that can be applied to HSDRRS foreshore regions.
    - The role of preferential seepage pathways in initiating collapse breaching and field investigations to locate and characterize such pathways.
    - The wave and direct (weir) overflow expressions and coefficients for all phases of hurricane surge overtopping and breaching, for a variety of structures and conditions, including both average and instantaneous rates.
    - Exterior- and interior-side wave-induced, and free-flow induced, scour and breach initiation and development.
    - Wind setup and wave equations/models applicable to sheltered southeast Louisiana water bodies (e.g., Lake Borgne and Pontchartrain, Breton Sound, Barataria Bay, Mississippi River, etc.) and inundated polders and sub-basins (e.g., IHNC/GIWW and outfall canals).

2. More efficient coupling of exterior surge, local wave, SOBRP, and internal routing models.
3. Further expansion and enhancement of the inundation JPA to make it less speculative.
4. Better analyses of non-surge polder flood hazards—such as rainfall-only events and overtopping/breaching during a Mississippi River flood—which are critical to evaluating the risk implications of surge inundation hazards.

The above recommendations can mitigate systemic and localized bias in estimates of inundation hazard. Notably, localized bias is typically of less import to the NFIP than to the community, which must deal with the consequences of over- or under-estimating flood hazards.

However, it is important to recognize the large uncertainty that remains in estimating inundation hazards based on JPA. This uncertainty in the inundation hazard for polders is greater than that for exterior surge hazards, which as noted in the Part III is quite considerable. In the near-term, methodological improvements and research are not likely to yield major reductions in uncertainty.

Part IV. References

Aalberts, M. L., The Cost Effectiveness of Compartmentation of the Orleans Metro Bowl, Master Thesis, June 2008.

ADCIRC Development Group, http://www.adcirc.org

ASCE Louisiana Section, 2012 Report Card for Louisiana's Infrastructure, 2012.

Bretschneider, C. L., Wave Forecasting Relations for Wave Generation, Look Lab, Hawaii, 1970.

Donelan, M. A., Similarity Theory Applied to the Forecasting of Wave Heights, Periods, and Directions, Proceedings of the Canadian Coastal Conference, National Research Council of Canada, pp. 47 – 61, 1980.

Etemad-Shahidi, A., M.H. Kazeminezhad, and S.J. Mousavi, On The Prediction of Wave Parameters Using Simplified Methods, Journal of Coastal Research, SI 56, pp 505-509, 2009.

Faiers, G. E., B. D. Keim, R. A. Muller, Rainfall Frequency/Magnitude Atlas for the SouthCentral United States, Southern Regional Climate Center, Louisiana State University, 1997.

FEMA, High Water Mark Collection for Hurricane Katrina in Louisiana, FEMA-1603-DR-LA, Task Orders 412 and 419, March 30, 2006.

FEMA, Guidance for Coastal Flood Hazard Analyses and Mapping in Sheltered Waters, February 2008 http://www.mmrs.fema.gov/library/viewRecord.do?id=3252

FEMA, Hydrologic Analysis Technical Support Data Notebook and Hydraulic Analysis Technical Support for the Hurricane Storm Damage Risk Reduction System (HSDRRS), Louisiana. July 16, 2012

Hasselmann, K., T. P. Barnett, E. Bouws, H. Carlson, D. E. Cartwright, K. Enke, J. A. Weing, H. Gienapp, D. E. Hasselmann, P. Kruseman, A. Meerburg, P. Muller, K. J. Olbers, K. Richter, W. Sell, and W. H. Walden, Measurment of Wind-Wave Growth and Swell Decay During the Joint North Sea Wave Project (JONSWAP), Deutsche Hydrograph, Zeit., 1973.

Hughes,S.A., Estimation of Overtopping Flow Velocities on Earthen Levees Due to Irregular Waves, USACE, Coastal and Hydraulics Laboratory, January 2008.

Hughes,S.A. , N.C. Nadal, "Laboratory study of combined wave overtopping and storm surge overflow of a levee", Coastal Engineering, Volume 56, Issue 3, pp. 244-259, March 2009.

Hughes,S.A., Flood-Side Wave Erosion of Earthen Levees: Present State of Knowledge and Assessment of Armoring Necessity, USACE, Coastal and Hydraulics Laboratory, August 2010.

Independent Levee Investigation Team (ILIT), Investigation of the Performance of the New Orleans Flood Protection Systems in Hurricane Katrina on August 29, 2005, Final Report, July 31, 2006

IPET, Performance Evaluation of the New Orleans and Southeast Louisiana Hurricane Protection System Draft Final Report, Volume V– The Performance—Levees and Floodwalls, June 2006

IPET, Performance Evaluation of the New Orleans and Southeast Louisiana Hurricane Protection System Final Report, Volume VIII– Engineering and Operational Risk and Reliability Analysis, June 2009a

IPET, A General Description of Vulnerability to Flooding and Risk for New Orleans and Vicinity: Past, Present, and Future, June 2009b.

Jonkman, S. N. B Maaskant, E. Boyd, and M. L. Levitan, Loss of Life Caused by the Flooding of New Orleans After Hurricane Katrina: Analysis of the Relationship Between Flood Characteristics and Mortality, Risk Analysis, Vol. 29, No. 5, 2009

Link, E., R. Patev, G. Baecher, M. McCann, T. McAllister, J. Foster, IPET, Engineering and Operational Risk and Reliability Analysis, Presentation, Undated.
http://www.samehuntington.com/shared/content/Presentations/TA_S3_Link.pdf

Lonfat, M., F. D. Marks, Jr., S. S. Chen, Precipitation Distribution in Tropical Cyclones Using the Tropical Rainfall Measuring Mission (TRMM) Microwave Imager: A Global Perspective, Monthly Weather Review, Vol. 132, 1645 – 1660, July 2004.

Lonfat, M., R. Rogers, T. Marchok, F. D. Marks, Jr., A Parametric Model for Predicting Hurricane Rainfall, Monthly Weather Review, Vol. 135, 3086 – 3097, September 2007.

Langousis, A., and D. Veneziano Theoretical Model of Rainfall in Tropical Cyclones for the Assessment of Long-Term Risk, Journal of Geophysical Research, Vol. 114, January 2009.

Louisiana CPRA, Louisiana's Comprehensive Master Plan for a Sustainable Coast, 2012

Lynett, P. J., J. A. Melby, D-H Kim, An Application of Boussinesq Modeling to Hurricane Wave Overtopping and Inundation, Ocean Engineering, Vol. 37, No. 1, p. 135-153, January, 2010.

Néelz S, and G, Pender, Desktop Review of 2D Hydraulic Modelling Packages, Science Report: SC080035, Environment Agency, July 2009.

NOAA, National Weather Service, Service Assessment: Tropical Storm Allison, Heavy Rains and Floods, Texas and Louisiana, June 2001, September 2001

NOAA, National Weather Service, The Historical Flood of May 8 – 10, 1995 Ten Years Later, 2005.

Rand Corporation, Coastal Louisiana Risk Assessment (CLARA) Model, Appendix D-25, Risk Assessment (CLARA) Model Technical Support, Louisiana's Comprehensive Master Plan for a Sustainable Coast, Louisiana CPRA, 2012.

Reeve, D.E., A. Soliman and P.Z. Lin, Numerical study of combined overflow and wave overtopping over a smooth impermeable seawall, Coastal Engineer- ing vol. 55, Elsevier (2008), pp. 155166.

Resio, D. T., J. L. Irish, J. J. Westerink, N. J. Powell, The Effect of Uncertainty on Estimates of Hurricane Surge Hazards, Natural Hazards, October 2012.

Schüttrumpf, H., and H. Oumeraci. 2005. Layer thicknesses and velocities of wave overtopping flow at seadikes. Coastal Engineering 52:473–95.

Schüttrumpf, H., and M. R. van Gent. 2003. Wave overtopping at seadikes. In Proceedings, Coastal Structures, '03, 431–443. Washington, DC: American Society of Civil Engineers.

Schüttrumpf, H., J. Möller, and H. Oumeraci. 2002. Overtopping flow parameters on the inner slope of seadikes. In Proceedings, 28th International Coastal Engineering Conference, 2: 2,116–2,127. World Scientific.

Royal Haskoning, Polder Modeling Orleans Metro Effects of Compartments on Flooding Extent, prepared for the Flood Protection Alliance, March 2009.

Swenson, D. (Times-Picayune) 2012.
http://www.nola.com/hurricane/index.ssf/2012/08/graphic_shows_new_orleans_area.html

Team Louisiana, The Failure of the New Orleans Levee System During Hurricane Katrina, A Report Prepared for Louisiana Department of Transportation and Development, Baton Rouge, Louisiana, December 18, 2006.

Thornton, C., B. Scholl, S. Hughes, and S. Abt, Full-Scale Testing of Levee Resiliency During Wave Overtopping, US Society on Dams Annual Conference Proceedings, 2012.
http://ussdams.com/proceedings/2012Proc/721.pdf

USACE, Coastal Engineering Manual, Part VI, EM1110-2-1100, February 2005.

USACE, Unsteady Flood Model for Forecasting the Mississippi and Missouri Rivers, February 1997, http://www.hec.usace.army.mil/publications/TechnicalPapers/TP-157.pdfUSACE, Coastal Engineering Manual (CEM) Volume II, Chapter 2: Meteorology and Wave Climate, 2006.

USACE, Flood Insurance Study, Southeast Parishes of Louisiana, Intermediate Submission 2: Offshore Water Levels and Waves, for FEMA, July 2008a.

USACE (New Orleans District), Hurricane and Storm Damage Reduction System Design Guidelines INTERIM, October 2007, Revised June 12, 2008b.

USACE, Louisiana Coastal Protection and Restoration, Final Technical Report, June 2009.

USACE (New Orleans District), Hurricane and Storm Damage Risk Reduction System, Design Elevation Report, Draft Report Version 4.0, August 18, 2010.

USACE, Summary Report for the Armoring Alternative Evaluation Process (Draft, and related communications from Reuben Mabry), June 2011

Van der Meer, J., Wave Run-up and Overtopping, in Dikes and Revetments: Design, Maintenance and Safety Assessment, K. W. Pilarczyk, Editor, 1998.

Van Gent, M. R,. Wave overtopping events at dikes. In Proceedings, 28th International Coastal Engineering Conference, 2:2203–2215, World Scientific, 2002.

Powell, N. and M and van Ledden, Hydraulic Assessment at the New Orleans District, Presentation, September 10, 2009.

Wilson, B. W., Numerical Prediction of Ocean Waves in the North Atlantic for December 1959, Deutsche Hydrograph Zeit., Vol. 18, No. 3, 1965.

Attachment 1

HSDRRS 100-yr Surge Conditions and Design Elevations and 500-yr Surge Conditions

Source:

USACE (New Orleans District), Hurricane and Storm Damage Risk Reduction System, Design Elevation Report, Draft Report Version 4.0, August 18, 2010.

St. Charles Parish East Bank Reaches

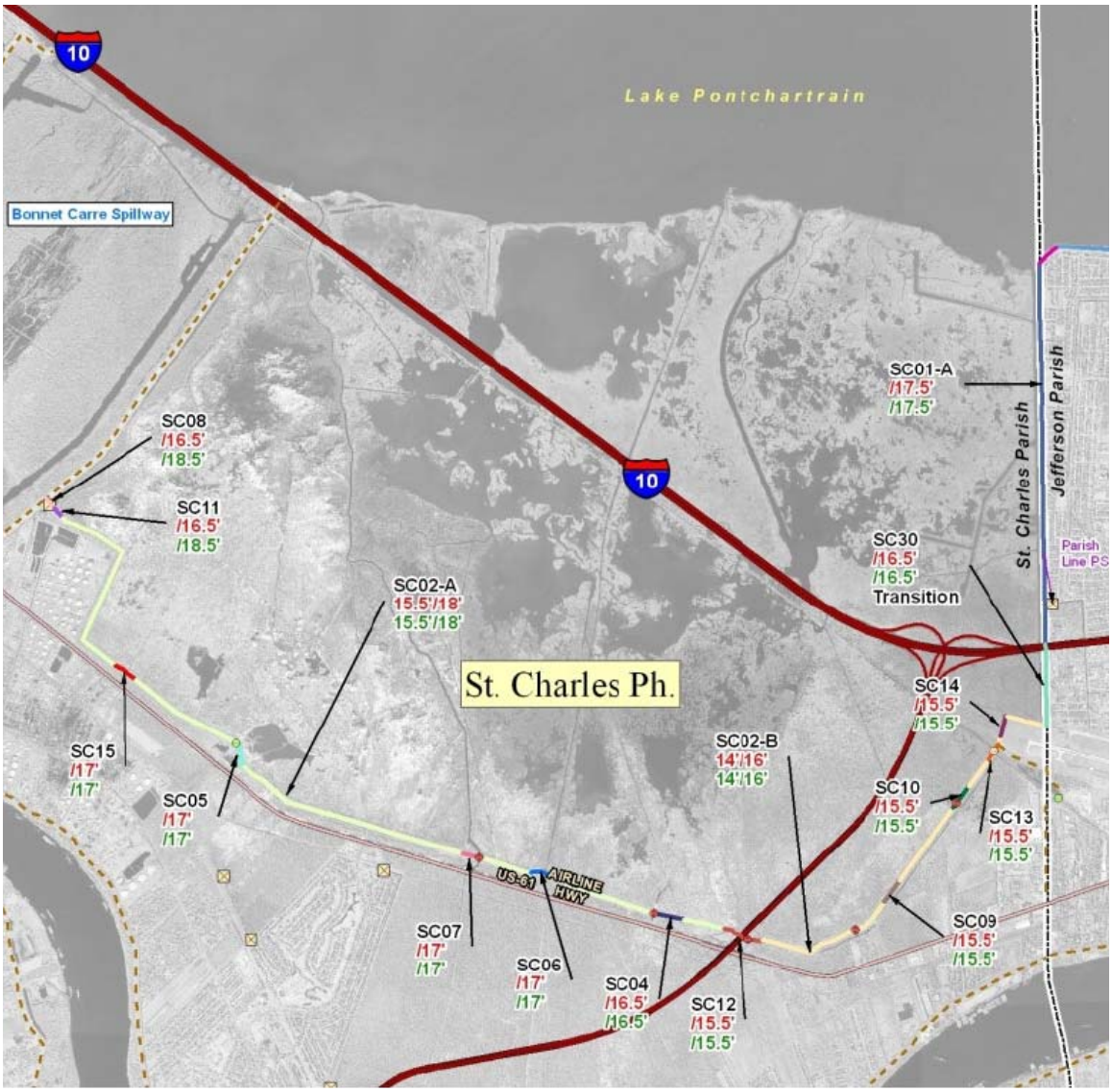

St Charles Parish Sections 1% Hydraulic boundary conditions									
				Surge level (ft)		Significant wave height (ft)		Peak period (s)	
Segment	Name	Type	Condition	Mean	Std	Mean	Std	Mean	Std
SC08	Bayou Trepagnier Pump Station	Structure/Wall	Future	12.8	0.7	2.7	0.2	4.0	0.7
SC11	Bonnet Carre Tie-in Floodwall	Structure/Wall	Future	12.8	0.7	2.7	0.2	4.0	0.7
SC05	Good Hope Floodwall	Structure/Wall	Future	12.9	0.8	3.1	0.2	4.7	0.8
SC02-A	St.Charles Parish Levee west of I-310	Levee	Existing	11.3	0.8	2.3	0.2	4.2	0.8
SC02-A	St.Charles Parish Levee west of I-310	Levee	Future	12.8	0.8	3.1	0.2	4.8	0.8
SC07	Cross Bayou Canal T-Wall	Structure/Wall	Future	12.9	0.8	3.1	0.2	4.7	0.8
SC06	Gulf South Pipeline T-Wall	Structure/Wall	Future	12.9	0.8	3.1	0.2	4.8	0.8
SC04	St. Rose Canal Drainage Structure T-Wall	Structure/Wall	Future	12.6	1.0	2.7	0.2	4.5	0.8
SC12	I-310 Floodwall	Structure/Wall	Future	12.3	0.8	2.3	0.2	3.9	0.6
SC02-B	St.Charles Parish Levee east of I-310	Levee	Existing	10.8	0.8	1.6	0.2	3.2	0.6
SC02-B	St.Charles Parish Levee east of I-310	Levee	Future	12.3	0.8	2.4	0.2	3.9	0.6
SC09	Almedia Drainage Structure	Structure/Wall	Future	12.3	0.8	2.4	0.2	3.9	0.6
SC10	Walker Drainage Structure	Structure/Wall	Future	12.2	0.8	2.5	0.2	3.8	0.6
SC13	Armstrong Airport Floodwall	Structure/Wall	Future	12.1	0.8	2.4	0.2	4.0	0.7
SC14	ICRR Floodgate	Structure/Wall	Future	12.1	0.8	2.4	0.2	4.1	0.7
SC30	Transition	Structure/Wall	Future	11.9	0.8	2.9	0.2	5.0	0.9
SC01-A	St. Charles Return Levee/Wall	Structure/Wall	Future	11.1	0.7	4.1	0.3	6.1	1.1
SC15	Shell Pipeline Floodwall	Structure/Wall	Future	12.9	0.8	3.1	0.2	4.7	0.8

St Charles Parish Sections 1% Design heights							
						Overtopping rate	
Segment	Name	Type	Condition	Depth at toe (ft)	Height (ft)	q50 (cft/s per ft)	q90 (cft/s per ft)
SC08	Bayou Trepagnier Pump Station	Structure/Wall	Future	12.8	18.5	0.001	0.004
SC11	Bonnet Carre Tie-in Floodwall	Structure/Wall	Future	12.8	18.5	0.001	0.004
SC05	Good Hope Floodwall	Structure/Wall	Future	12.9	17.0	0.020	0.078
SC02-A	St.Charles Parish Levee west of I-310	Levee	Existing	11.3	15.5	0.009	0.079
SC02-A	St.Charles Parish Levee west of I-310	Levee	Future	12.8	18.0	0.008	0.071
SC07	Cross Bayou Canal T-Wall	Structure/Wall	Future	12.9	17.0	0.019	0.078
SC06	Gulf South Pipeline T-Wall	Structure/Wall	Future	12.9	17.0	0.020	0.077
SC04	St. Rose Canal Drainage Structure T-Wall	Structure/Wall	Future	12.6	16.5	0.011	0.067
SC12	I-310 Floodwall	Structure/Wall	Future	12.3	15.5	0.009	0.054
SC02-B	St.Charles Parish Levee east of I-310	Levee	Existing	10.8	14.0	0.007	0.064
SC02-B	St.Charles Parish Levee east of I-310	Levee	Future	12.3	16.0	0.008	0.072
SC09	Almedia Drainage Structure	Structure/Wall	Future	12.3	15.5	0.012	0.066
SC10	Walker Drainage Structure	Structure/Wall	Future	12.2	15.5	0.015	0.071
SC13	Armstrong Airport Floodwall	Structure/Wall	Future	12.1	15.5	0.009	0.050
SC14	ICRR Floodgate	Structure/Wall	Future	12.1	15.5	0.009	0.049
SC30	Transition	Structure/Wall	Future	11.9	16.5	0.007	0.031
SC01-A	St. Charles Return Levee/Wall	Structure/Wall	Future	11.1	17.5	0.012	0.041
SC15	Shell Pipeline Floodwall	Structure/Wall	Future	12.9	17.0	0.020	0.075

St Charles Parish Sections Resiliency analysis (0.2% event)						
					Best estimates during 0.2% event	
Segment	Name	Type	Condition	Height (ft)	Surge level (ft)	Overtopping rate (cft/s per ft)
SC08	Bayou Trepagnier Pump Station	Structure/Wall	Future	18.5	15.4	0.156
SC11	Bonnet Carre Tie-in Floodwall	Structure/Wall	Future	18.5	15.4	0.155
SC05	Good Hope Floodwall	Structure/Wall	Future	17.0	15.6	1.242
SC02-A	St.Charles Parish Levee west of I-310	Levee	Existing	15.5	14.0	1.672
SC02-A	St.Charles Parish Levee west of I-310	Levee	Future	18.0	15.5	1.167
SC07	Cross Bayou Canal T-Wall	Structure/Wall	Future	17.0	15.6	1.256
SC06	Gulf South Pipeline T-Wall	Structure/Wall	Future	17.0	15.7	1.277
SC04	St. Rose Canal Drainage Structure T-Wall	Structure/Wall	Future	16.5	16.0	1.531
SC12	I-310 Floodwall	Structure/Wall	Future	15.5	15.1	1.408
SC02-B	St.Charles Parish Levee east of I-310	Levee	Existing	14.0	13.5	1.889
SC02-B	St.Charles Parish Levee east of I-310	Levee	Future	16.0	15.0	1.498
SC09	Almedia Drainage Structure	Structure/Wall	Future	15.5	15.0	1.375
SC10	Walker Drainage Structure	Structure/Wall	Future	15.5	14.9	1.348
SC13	Armstrong Airport Floodwall	Structure/Wall	Future	15.5	14.8	1.204
SC14	ICRR Floodgate	Structure/Wall	Future	15.5	14.8	1.188
SC30	Transition	Structure/Wall	Future	16.5	14.7	0.847
SC01-A	St. Charles Return Levee/Wall	Structure/Wall	Future	17.5	13.7	0.413
SC15	Shell Pipeline Floodwall	Structure/Wall	Future	17.0	15.6	1.248

Jefferson Parish East Bank Reaches

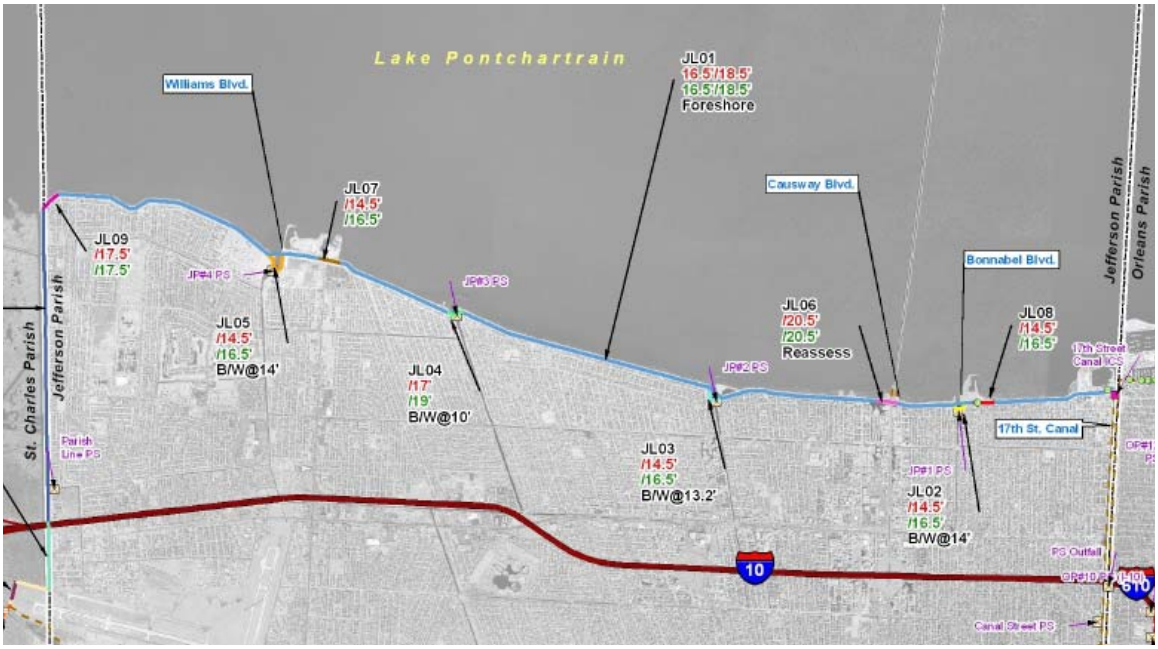

Jefferson Parish Sections 1% Hydraulic boundary conditions									
				Surge level (ft)		Significant wave height (ft)		Peak period (s)	
Segment	Name	Type	Condition	Mean	Std	Mean	Std	Mean	Std
JL01	Lakefront levee	Levee	Existing	9.0	0.6	3.6	0.4	7.7	1.5
JL01	Lakefront levee	Levee	Future	10.5	0.6	4.2	0.4	8.3	1.5
JL02	Pump station 1 with breakwater at 14ft	Structure/Wall	Future	10.3	0.7	2.5	0.3	8.1	1.6
JL03	Pump station 2 with breakwater at 13.2ft	Structure/Wall	Future	10.4	0.7	2.8	0.3	8.1	1.6
JL04	Pump station 3 with breakwater at 10ft	Structure/Wall	Future	10.5	0.6	4.2	0.4	8.1	1.6
JL05	Pump station 4 with breakwater at 14ft	Structure/Wall	Future	10.5	0.7	2.5	0.3	8.1	1.6
JL06	Causeway Crib wall	Structure/Wall	Future	10.3	0.7	6.5	0.6	7.8	1.5
JL07	Williams Blvd Floodgate	Structure/Wall	Future	10.4	0.6	2.8	0.2	8.5	1.5
JL08	Bonnabel Boat Launch Floodgate	Structure/Wall	Future	10.3	0.7	2.7	0.2	8.3	1.5
JL09	Return wall	Structure/Wall	Future	10.8	0.7	4.9	0.4	8.3	1.6

Jefferson Parish Sections 1% Design heights							
						Overtopping rate	
Segment	Name	Type	Condition	Depth at toe (ft)	Height (ft)	q50 (cft/s per ft)	q90 (cft/s per ft)
JL01	Lakefront levee	Levee	Existing	9.0	16.5	0.001	0.015
JL01	Lakefront levee	Levee	Future	10.5	18.5	0.002	0.024
JL02	Pump station 1 with breakwater at 14ft	Structure/Wall	Future	15.3	16.5	0.000	0.002
JL03	Pump station 2 with breakwater at 13.2ft	Structure/Wall	Future	15.4	16.5	0.001	0.005
JL04	Pump station 3 with breakwater at 10ft	Structure/Wall	Future	15.5	19.0	0.003	0.011
JL05	Pump station 4 with breakwater at 14ft	Structure/Wall	Future	15.5	16.5	0.000	0.002
JL06	Causeway Crib wall	Structure/Wall	Future	16.3	20.5	0.021	0.058
JL07	Williams Blvd Floodgate	Structure/Wall	Future	6.9	16.5	0.000	0.003
JL08	Bonnabel Boat Launch Floodgate	Structure/Wall	Future	6.8	16.5	0.000	0.003
JL09	Return wall	Structure/Wall	Future	12.3	17.5	0.029	0.087

Jefferson Parish Sections Resiliency analysis (0.2% event)						
					Best estimates during 0.2% event	
Segment	Name	Type	Condition	Height (ft)	Surge level (ft)	Overtopping rate (cft/s per ft)
JL01	Lakefront levee	Levee	Existing	16.5	11.2	0.088
JL01	Lakefront levee	Levee	Future	18.5	12.7	0.096
JL02	Pump station 1 with breakwater at 14ft	Structure/Wall	Future	16.5	12.7	0.008
JL03	Pump station 2 with breakwater at 13.2ft	Structure/Wall	Future	16.5	12.7	0.018
JL04	Pump station 3 with breakwater at 10ft	Structure/Wall	Future	19.0	12.7	0.019
JL05	Pump station 4 with breakwater at 14ft	Structure/Wall	Future	16.5	12.8	0.010
JL06	Causeway Crib wall	Structure/Wall	Future	20.5	12.7	0.174
JL07	Williams Blvd Floodgate	Structure/Wall	Future	16.5	12.6	0.056
JL08	Bonnabel Boat Launch Floodgate	Structure/Wall	Future	16.5	12.7	0.064
JL09	Return wall	Structure/Wall	Future	17.5	13.1	0.362

Orleans Parish East Bank Metro Reaches

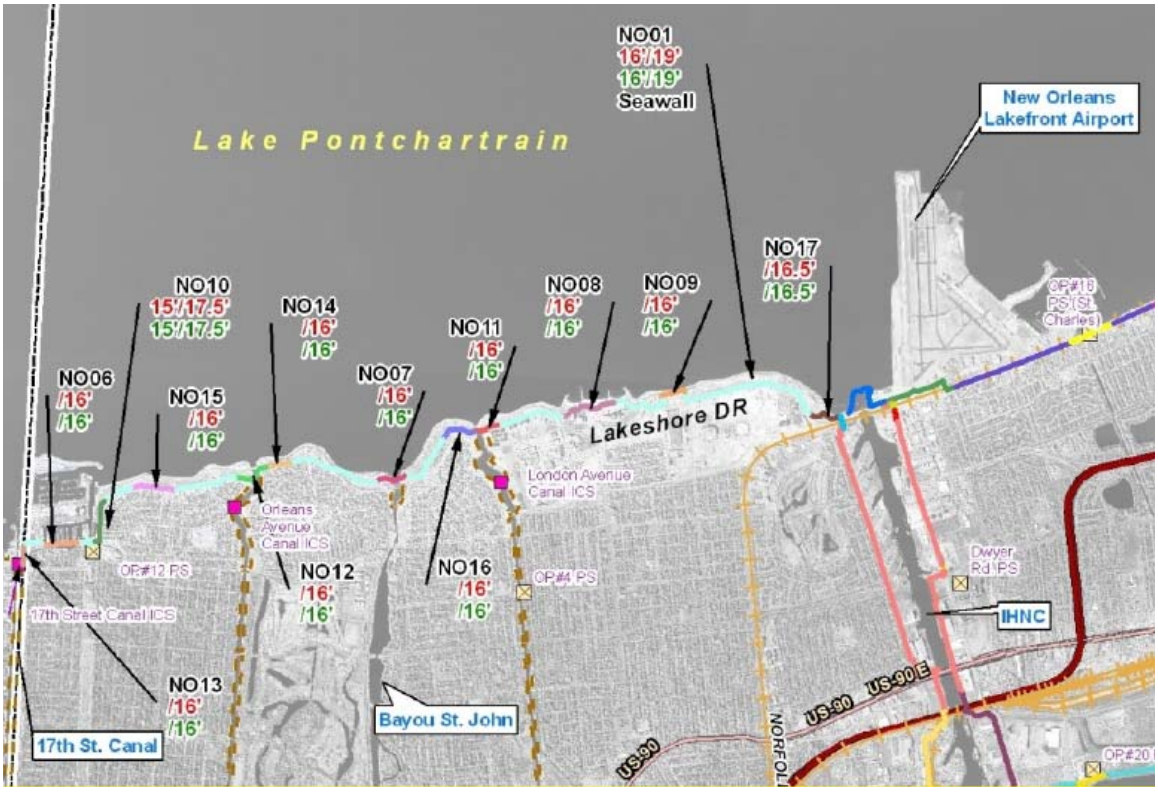

Orleans Parish Metro Lakefront Sections 1% Hydraulic boundary conditions									
				Surge level (ft)		Significant wave height (ft)		Peak period (s)	
Segment	Name	Type	Condition	Mean	Std	Mean	Std	Mean	Std
NO06	NO Marina	Structure/Wall	Future	10.2	0.7	3.3	0.3	8.0	1.4
NO10	Topaz St. Levee	Levee	Existing	8.7	0.7	2.3	0.2	7.2	1.4
NO10	Topaz St. Levee	Levee	Future	10.2	0.7	2.9	0.2	8.1	1.4
NO15	Type II Floodgate similar to Canal Blvd	Structure/Wall	Future	10.2	0.7	2.3	0.2	8.4	1.4
NO13	17th St. Outfall Canal Closure	Structure/Wall	Future	10.2	0.7	4.0	0.4	4.5	0.9
NO12	Orleans Ave Outfall Canal Closure	Structure/Wall	Future	10.2	0.8	3.0	0.3	4.0	0.8
NO14	Type I Floodgate Similar to Marconi Drive	Structure/Wall	Future	10.2	0.8	2.5	0.2	7.9	1.4
NO16	Lakeshore Drive near Rail St FG	Structure/Wall	Future	10.1	0.8	4.4	0.4	7.4	1.4
NO07	Bayou St. John	Structure/Wall	Future	10.1	0.8	3.0	0.3	4.0	0.8
NO11	London Ave Outfall Canal Closures	Structure/Wall	Future	10.1	0.8	3.0	0.3	4.0	0.8
NO08	Pontchartrain	Structure/Wall	Future	10.1	0.8	3.6	0.3	7.3	1.3
NO09	American Std FW	Structure/Wall	Future	10.1	0.8	4.4	0.4	7.1	1.3
NO01	New Orleans Lakefront Levee	Levee	Existing	8.7	0.7	5.1	0.5	7.2	1.4
NO01	New Orleans Lakefront Levee	Levee	Future	10.2	0.7	5.7	0.5	7.6	1.4
NO17	Leroy Johnson	Structure/Wall	Future	10.1	0.8	4.0	0.3	7.0	1.3

Orleans Parish Metro Lakefront Sections 1% Design heights							
						Overtopping rate	
Segment	Name	Type	Condition	Depth at toe (ft)	Height (ft)	q50 (cft/s per ft)	q90 (cft/s per ft)
NO06	NO Marina	Structure/Wall	Future	8.2	16.0	0.003	0.016
NO10	Topaz St. Levee	Levee	Existing	5.7	15.0	0.002	0.015
NO10	Topaz St. Levee	Levee	Future	7.2	17.5	0.005	0.029
NO15	Type II Floodgate similar to Canal Blvd	Structure/Wall	Future	5.7	16.0	0.000	0.001
NO13	17th St. Outfall Canal Closure	Structure/Wall	Future	10.2	16.0	0.015	0.056
NO12	Orleans Ave Outfall Canal Closure	Structure/Wall	Future	10.2	16.0	0.002	0.012
NO14	Type I Floodgate Similar to Marconi Drive	Structure/Wall	Future	6.2	16.0	0.000	0.002
NO16	Lakeshore Drive near Rail St FG	Structure/Wall	Future	11.1	16.0	0.028	0.097
NO07	Bayou St. John	Structure/Wall	Future	10.1	16.0	0.002	0.011
NO11	London Ave Outfall Canal Closures	Structure/Wall	Future	10.1	16.0	0.002	0.011
NO08	Pontchartrain	Structure/Wall	Future	9.1	16.0	0.007	0.033
NO09	American Std FW	Structure/Wall	Future	11.1	16.0	0.028	0.096
NO01	New Orleans Lakefront Levee	Levee	Existing	12.7	16.0	0.006	0.060
NO01	New Orleans Lakefront Levee	Levee	Future	14.2	19.0	0.008	0.066
NO17	Leroy Johnson	Structure/Wall	Future	10.1	16.5	0.009	0.038

Orleans Parish Metro Lakefront Sections Resiliency analysis (0.2% event)						
					Best estimates during 0.2% event	
Segment	Name	Type	Condition	Height (ft)	Surge level (ft)	Overtopping rate (cft/s per ft)
NO06	NO Marina	Structure/Wall	Future	16.0	12.8	0.244
NO10	Topaz St. Levee	Levee	Existing	15.0	11.3	0.314
NO10	Topaz St. Levee	Levee	Future	17.5	12.8	0.323
NO15	Type II Floodgate similar to Canal Blvd	Structure/Wall	Future	16.0	12.8	0.074
NO13	17th St. Outfall Canal Closure	Structure/Wall	Future	16.0	12.8	0.211
NO12	Orleans Ave Outfall Canal Closure	Structure/Wall	Future	16.0	13.1	0.076
NO14	Type I Floodgate Similar to Marconi Drive	Structure/Wall	Future	16.0	13.1	0.156
NO16	Lakeshore Drive near Rail St FG	Structure/Wall	Future	16.0	13.1	0.854
NO07	Bayou St. John	Structure/Wall	Future	16.0	13.1	0.075
NO11	London Ave Outfall Canal Closures	Structure/Wall	Future	16.0	12.9	0.059
NO08	Pontchartrain	Structure/Wall	Future	16.0	12.9	0.396
NO09	American Std FW	Structure/Wall	Future	16.0	12.8	0.648
NO01	New Orleans Lakefront Levee	Levee	Existing	16.0	11.3	0.335
NO01	New Orleans Lakefront Levee	Levee	Future	19.0	12.8	0.276
NO17	Leroy Johnson	Structure/Wall	Future	16.5	12.8	0.336

Orleans Parish East Bank, New Orleans East Lakefront, Reaches

Orleans Parish East Lakefront Sections 1% Hydraulic boundary conditions									
				Surge level (ft)		Significant wave height (ft)		Peak period (s)	
Segment	Name	Type	Condition	Mean	Std	Mean	Std	Mean	Std
NE04	NO Lakefront Airport West	Structure/Wall	Future	10.0	0.7	3.2	0.3	7.5	1.4
NE03	NO Lakefront Airport East	Structure/Wall	Future	9.9	0.7	3.2	0.3	7.4	1.3
NE09	St Charles Pump station	Structure/Wall	Future	9.9	0.7	4.0	0.3	7.3	1.3
NE07	Citrus Pump station	Structure/Wall	Future	10.0	0.7	4.0	0.3	7.2	1.3
NE01	Citrus Lakefront Levee	Levee	Existing	8.6	0.7	2.0	0.2	6.7	1.3
NE01	Citrus Lakefront Levee	Levee	Future	10.1	0.7	2.5	0.3	7.1	1.4
NE08	Jahncke Pump station	Structure/Wall	Future	10.0	0.7	4.0	0.3	7.3	1.3
NE05	Lincoln Beach	Structure/Wall	Future	10.1	0.7	2.4	0.2	7.6	1.3
NE06	Collins Pipeline Crossing	Structure/Wall	Future	10.4	0.7	3.8	0.3	7.1	1.3
NE30	Transition Reach NE01 to NE02	Levee	Existing	8.6	0.7	2.9	0.3	6.7	1.3
NE30	Transition Reach NE01 to NE02	Levee	Future	10.1	0.7	3.4	0.3	7.1	1.4
NE02	New Orleans East Lakefront Levee	Levee	Existing	8.9	0.7	3.7	0.4	6.7	1.3
NE02	New Orleans East Lakefront Levee	Levee	Future	10.4	0.7	4.3	0.4	7.1	1.4
NE31	South Point transition reach	Levee	Existing	9.0	0.8	3.7	0.4	6.7	1.3
NE31	South Point transition reach	Levee	Future	10.5	0.8	4.3	0.4	7.1	1.4

Orleans Parish East Lakefront Sections 1% Design heights							
						Overtopping rate	
Segment	Name	Type	Condition	Depth at toe (ft)	Height (ft)	q50 (cft/s per ft)	q90 (cft/s per ft)
NE04	NO Lakefront Airport West	Structure/Wall	Future	8.0	15.5	0.004	0.019
NE03	NO Lakefront Airport East	Structure/Wall	Future	7.9	15.5	0.003	0.015
NE09	St Charles Pump station	Structure/Wall	Future	9.9	15.5	0.017	0.060
NE07	Citrus Pump station	Structure/Wall	Future	10.0	15.5	0.020	0.069
NE01	Citrus Lakefront Levee	Levee	Existing	8.6	13.0	0.007	0.044
NE01	Citrus Lakefront Levee	Levee	Future	10.1	15.5	0.010	0.057
NE08	Jahncke Pump station	Structure/Wall	Future	10.0	15.5	0.020	0.069
NE05	Lincoln Beach	Structure/Wall	Future	6.1	15.5	0.000	0.003
NE06	Collins Pipeline Crossing	Structure/Wall	Future	9.4	17.5	0.003	0.012
NE30	Transition Reach NE01 to NE02	Levee	Existing	9.6	14.5	0.010	0.064
NE30	Transition Reach NE01 to NE02	Levee	Future	11.1	16.5	0.007	0.066
NE02	New Orleans East Lakefront Levee	Levee	Existing	9.9	15.5	0.003	0.033
NE02	New Orleans East Lakefront Levee	Levee	Future	11.4	17.5	0.006	0.062
NE31	South Point transition reach	Levee	Existing	9.0	16.5	0.002	0.025
NE31	South Point transition reach	Levee	Future	10.5	18.5	0.005	0.052

Orleans Parish East Lakefront Sections Resiliency analysis (0.2% event)						
					Best estimates during 0.2% event	
Segment	Name	Type	Condition	Height (ft)	Surge level (ft)	Overtopping rate (cft/s per ft)
NE04	NO Lakefront Airport West	Structure/Wall	Future	15.5	12.6	0.291
NE03	NO Lakefront Airport East	Structure/Wall	Future	15.5	12.3	0.203
NE09	St Charles Pump station	Structure/Wall	Future	15.5	12.3	0.422
NE07	Citrus Pump station	Structure/Wall	Future	15.5	12.4	0.458
NE01	Citrus Lakefront Levee	Levee	Existing	13.0	11.0	0.216
NE01	Citrus Lakefront Levee	Levee	Future	15.5	12.5	0.158
NE08	Jahncke Pump station	Structure/Wall	Future	15.5	12.4	0.456
NE05	Lincoln Beach	Structure/Wall	Future	15.5	12.5	0.101
NE06	Collins Pipeline Crossing	Structure/Wall	Future	17.5	13.0	0.136
NE30	Transition Reach NE01 to NE02	Levee	Existing	14.5	11.1	0.148
NE30	Transition Reach NE01 to NE02	Levee	Future	16.5	12.6	0.100
NE02	New Orleans East Lakefront Levee	Levee	Existing	15.5	11.5	0.065
NE02	New Orleans East Lakefront Levee	Levee	Future	17.5	13.0	0.093
NE31	South Point transition reach	Levee	Existing	16.5	11.7	0.050
NE31	South Point transition reach	Levee	Future	18.5	13.2	0.081

Orleans Parish East, New Orleans East Back Levee Reaches

GIWW Sections (outside MRGO gate) 1% Hydraulic boundary conditions									
				Surge level (ft)		Significant wave height (ft)		Peak period (s)	
Segment	Name	Type	Condition	Mean	Std	Mean	Std	Mean	Std
NE13	Highway 11 Floodgate	Structure/Wall	Future	11.1	0.9	4.4	0.4	5.8	1.1
NE10	South Point to Highway 90 Levee	Levee	Existing	10.9	0.9	4.4	0.4	5.4	1.1
NE10	South Point to Highway 90 Levee	Levee	Future	12.4	0.9	5.0	0.4	5.8	1.1
NE14	Highway 90 Floodgate	Structure/Wall	Future	12.5	0.9	5.0	0.4	5.6	1.1
NE11A	Highway 90 to CSX RR Levee	Levee	Existing	14.3	0.9	4.0	0.4	8.3	1.7
NE11A	Highway 90 to CSX RR Levee	Levee	Future	15.8	0.9	4.8	0.4	9.0	1.7
NE15	CSX RR Floodgate	Structure/Wall	Future	17.3	1.0	6.7	0.6	7.1	1.3
NE11B	CSX RR to GIWW Levee	Levee	Existing	16.2	1.0	5.9	0.6	7.7	1.5
NE11B	CSX RR to GIWW Levee	Levee	Future	17.7	1.0	6.7	0.6	8.2	1.5
NE32	Transition Levee	Levee	Existing	16.2	1.0	5.4	0.5	7.9	1.6
NE32	Transition Levee	Levee	Future	17.7	1.0	6.2	0.5	8.5	1.6
NE12A	NO East Back Levee from PS15 East along GIWW	Levee	Existing	17.4	1.0	5.4	0.5	8.0	1.6
NE12A	NO East Back Levee from PS15 East along GIWW	Levee	Future	18.9	1.0	6.2	0.5	8.6	1.6
NE16	NO East Pump Station 15	Structure/Wall	Future	18.9	1.0	5.5	0.5	7.8	1.5
NE12B	NO East Back Levee from Gate to PS15	Levee	Existing	18.4	1.0	7.1	0.7	7.9	1.6
NE12B	NO East Back Levee from Gate to PS15	Levee	Future	19.9	1.0	7.9	0.7	8.3	1.6

GIWW Sections (outside MRGO gate) 1% Design heights							
						Overtopping rate	
Segment	Name	Type	Condition	Depth at toe (ft)	Height (ft)	q50 (cft/s per ft)	q90 (cft/s per ft)
NE13	Highway 11 Floodgate	Structure/Wall	Future	11.1	18.5	0.007	0.034
NE10	South Point to Highway 90 Levee	Levee	Existing	10.9	17.0	0.006	0.063
NE10	South Point to Highway 90 Levee	Levee	Future	12.4	19.0	0.008	0.077
NE14	Highway 90 Floodgate	Structure/Wall	Future	12.5	22.0	0.004	0.016
NE11A	Highway 90 to CSX RR Levee	Levee	Existing	14.3	22.0	0.006	0.064
NE11A	Highway 90 to CSX RR Levee	Levee	Future	15.8	25.0	0.008	0.071
NE15	CSX RR Floodgate	Structure/Wall	Future	17.3	30.0	0.007	0.025
NE11B	CSX RR to GIWW Levee	Levee	Existing	16.2	25.0	0.005	0.067
NE11B	CSX RR to GIWW Levee	Levee	Future	17.7	28.0	0.005	0.056
NE32	Transition Levee	Levee	Existing	16.2	28.0	0.001	0.020
NE32	Transition Levee	Levee	Future	17.7	31.0	0.004	0.046
NE12A	NO East Back Levee from PS15 East along GIWW	Levee	Existing	17.4	28.0	0.003	0.046
NE12A	NO East Back Levee from PS15 East along GIWW	Levee	Future	18.9	31.0	0.009	0.087
NE16	NO East Pump Station 15	Structure/Wall	Future	18.9	34.0	0.000	0.002
NE12B	NO East Back Levee from Gate to PS15	Levee	Existing	18.4	29.0	0.007	0.080
NE12B	NO East Back Levee from Gate to PS15	Levee	Future	19.9	31.5	0.009	0.085

GIWW Sections (outside MRGO gate) Resiliency analysis (0.2% event)						
					Best estimates during 0.2% event	
Segment	Name	Type	Condition	Height (ft)	Surge level (ft)	Overtopping rate (cft/s per ft)
NE13	Highway 11 Floodgate	Structure/Wall	Future	18.5	14.4	0.432
NE10	South Point to Highway 90 Levee	Levee	Existing	17.0	14.2	0.933
NE10	South Point to Highway 90 Levee	Levee	Future	19.0	15.7	0.860
NE14	Highway 90 Floodgate	Structure/Wall	Future	22.0	15.7	0.160
NE11A	Highway 90 to CSX RR Levee	Levee	Existing	22.0	17.5	0.831
NE11A	Highway 90 to CSX RR Levee	Levee	Future	25.0	19.0	0.586
NE15	CSX RR Floodgate	Structure/Wall	Future	30.0	20.7	0.145
NE11B	CSX RR to GIWW Levee	Levee	Existing	25.0	19.7	0.451
NE11B	CSX RR to GIWW Levee	Levee	Future	28.0	21.2	0.282
NE32	Transition Levee	Levee	Existing	28.0	19.7	0.100
NE32	Transition Levee	Levee	Future	31.0	21.2	0.153
NE12A	NO East Back Levee from PS15 East along GIWW	Levee	Existing	28.0	20.9	0.228
NE12A	NO East Back Levee from PS15 East along GIWW	Levee	Future	31.0	22.4	0.321
NE16	NO East Pump Station 15	Structure/Wall	Future	34.0	22.4	0.024
NE12B	NO East Back Levee from Gate to PS15	Levee	Existing	29.0	22.1	0.380
NE12B	NO East Back Levee from Gate to PS15	Levee	Future	31.5	23.6	0.322

Orleans and St. Bernard Parishes East Bank, Inside IHNC and Seabrook Barriers

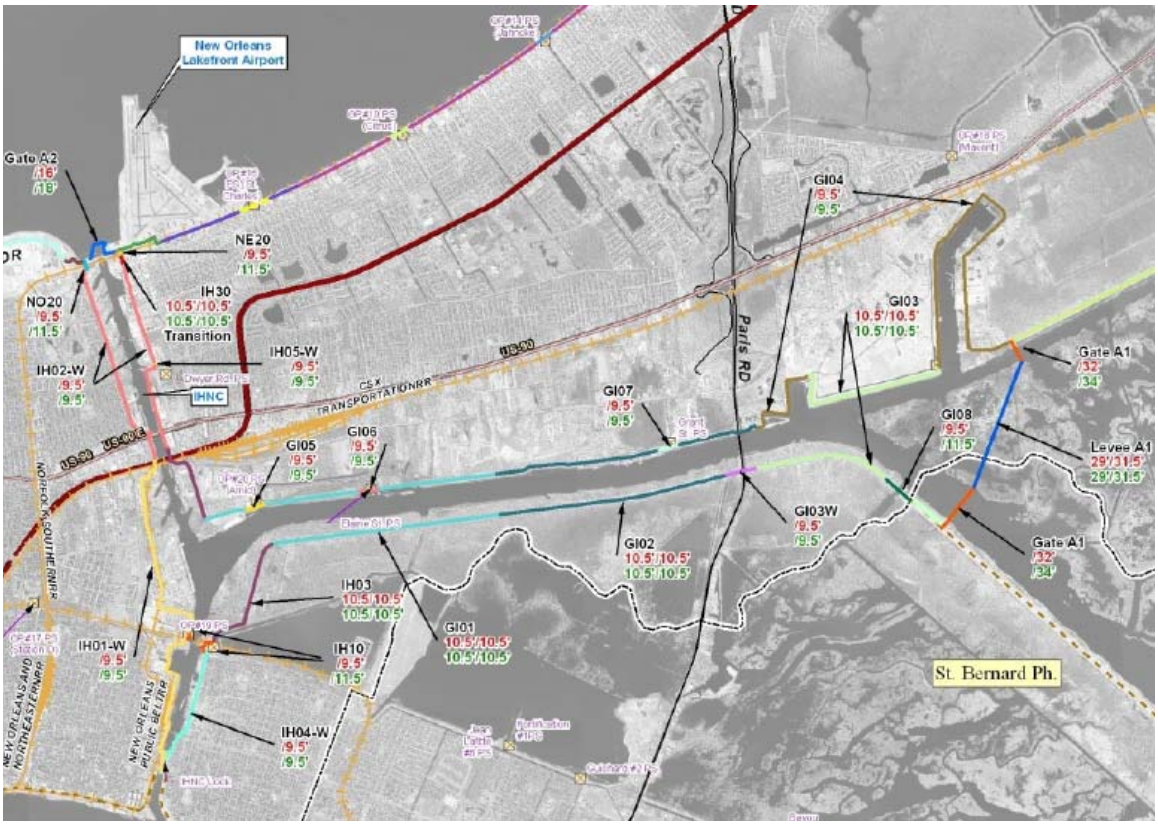

IHNC and GIWW sections (with MRGO/GIWW and Seabrook closures) 1% Hydraulic boundary conditions									
				Surge level (ft)		Significant wave height (ft)		Peak period (s)	
Segment	Name	Type	Condition	Mean	Std	Mean	Std	Mean	Std
GID8	Bienvenue Floodgate	Structure/Wall	Future	6.0	0.5	3.0	0.3	3.5	0.7
GID3	Michoud Canal to Michoud Slip and Paris Rd Bridge to Bienvenue Floodgate	Levee	Existing	6.0	0.5	3.0	0.3	3.5	0.7
GID3	Michoud Canal to Michoud Slip and Paris Rd Bridge to Bienvenue Floodgate	Levee	Future	6.0	0.5	3.0	0.3	3.5	0.7
GID4	Michoud Canal and Slip	Structure/Wall	Future	6.0	0.5	3.0	0.3	3.5	0.7
GID7	Grant Pump Station	Structure/Wall	Future	6.0	0.5	3.0	0.3	3.5	0.7
GID3-W	Floodwall under Paris Rd Bridge	Structure/Wall	Future	6.0	0.5	3.0	0.3	3.5	0.7
GID2	Paris Road to levee section GI01	Levee	Existing	6.0	0.5	3.0	0.3	3.5	0.7
GID2	Paris Road to levee section GI01	Levee	Future	6.0	0.5	3.0	0.3	3.5	0.7
GID1	Levee Section GI02 to IHNC	Levee	Existing	6.0	0.5	3.0	0.3	3.5	0.7
GID1	Levee Section GI02 to IHNC	Levee	Future	6.0	0.5	3.0	0.3	3.5	0.7
GID6	Elaine Pump Station	Structure/Wall	Future	6.0	0.5	3.0	0.3	3.5	0.7
GID5	Amid Pump Station (PS#20)	Structure/Wall	Future	6.0	0.5	3.0	0.3	3.5	0.7
IH30	Transition Reach	Levee	Existing	6.0	0.5	2.3	0.2	3.1	0.6
IH30	Transition Reach	Levee	Future	6.0	0.5	2.3	0.2	3.1	0.6
IH02-W	IHNC North of I-10	Structure/Wall	Future	6.0	0.5	2.3	0.2	3.1	0.6
IH01-W	IHNC South of I-10 to Pump Station #19	Structure/Wall	Future	6.0	0.5	3.0	0.3	3.5	0.7
IH04-W	IHNC Lock to Pump Stations (PS#5 and PS#19)	Structure/Wall	Future	6.0	0.5	2.3	0.2	3.1	0.6
IH10	Orleans Pump Stations #5 and Pump Station #19	Structure/Wall	Future	6.0	0.5	2.3	0.2	3.1	0.6
IH03	IHNC Levee South from I-10	Levee	Existing	6.0	0.5	3.0	0.3	3.5	0.7
IH03	IHNC Levee South from I-10	Levee	Future	6.0	0.5	3.0	0.3	3.5	0.7
IH05-W	Dwyer Pump Station	Structure/Wall	Future	6.0	0.5	2.3	0.2	3.1	0.6
NO20	NS Railroad gates near Seabrook (west)	Structure/Wall	Future	6.0	0.5	2.3	0.2	3.1	0.6
NE20	NS Railroad gates near Seabrook (east)	Structure/Wall	Future	6.0	0.5	2.3	0.2	3.1	0.6

IHNC and GIWW sections (with MRGO/GIWW and Seabrook closures) 1% Design heights							
						Overtopping rate	
Segment	Name	Type	Condition	Depth at toe (ft)	Height (ft)	q50 (cft/s per ft)	q90 (cft/s per ft)
GI08	Bienvenue Floodgate	Structure/Wall	Future	20.0	11.5	0.003	0.013
GI03	Michoud Canal to Michoud Slip and	Levee	Existing	6.0	10.5	0.010	0.058
GI03	Michoud Canal to Michoud Slip and	Levee	Future	6.0	10.5	0.010	0.057
GI04	Michoud Canal and Slip	Structure/Wall	Future	6.0	9.5	0.009	0.043
GI07	Grant Pump Station	Structure/Wall	Future	5.0	9.5	0.002	0.018
GI03-W	Floodwall under Paris Rd Bridge	Structure/Wall	Future	5.0	9.5	0.002	0.018
GI02	Paris Road to levee section GI01	Levee	Existing	6.0	10.5	0.010	0.057
GI02	Paris Road to levee section GI01	Levee	Future	6.0	10.5	0.009	0.055
GI01	Levee Section GI02 to IHNC	Levee	Existing	6.0	10.5	0.009	0.056
GI01	Levee Section GI02 to IHNC	Levee	Future	6.0	10.5	0.010	0.056
GI06	Elaine Pump Station	Structure/Wall	Future	7.0	9.5	0.022	0.076
GI05	Amid Pump Station (PS#20)	Structure/Wall	Future	7.0	9.5	0.021	0.075
IH30	Transition Reach	Levee	Existing	6.0	10.5	0.004	0.029
IH30	Transition Reach	Levee	Future	6.0	10.5	0.003	0.029
IH02-W	IHNC North of I-10	Structure/Wall	Future	5.0	9.5	0.002	0.015
IH01-W	IHNC South of I-10 to Pump Station #19	Structure/Wall	Future	5.0	9.5	0.002	0.017
IH04-W	IHNC Lock to Pump Stations (PS#5 and PS#19)	Structure/Wall	Future	5.0	9.5	0.002	0.015
IH10	Orleans Pump Stations #5 and Pump Station #19	Structure/Wall	Future	5.0	11.5	0.000	0.001
IH03	IHNC Levee South from I-10	Levee	Existing	6.0	10.5	0.009	0.056
IH03	IHNC Levee South from I-10	Levee	Future	6.0	10.5	0.010	0.056
IH05-W	Dwyer Pump Station	Structure/Wall	Future	5.0	9.5	0.002	0.015
NO20	NS Railroad gates near Seabrook (west)	Structure/Wall	Future	5.0	11.5	0.000	0.001
NE20	NS Railroad gates near Seabrook (east)	Structure/Wall	Future	5.0	11.5	0.000	0.001

Note. The Resiliency Analysis (0.2% Event) was not performed for the IHNC and GIWW with MRGO.GIWW and Seabrook closures.

Near IHNC and Seabrook Surge Barriers

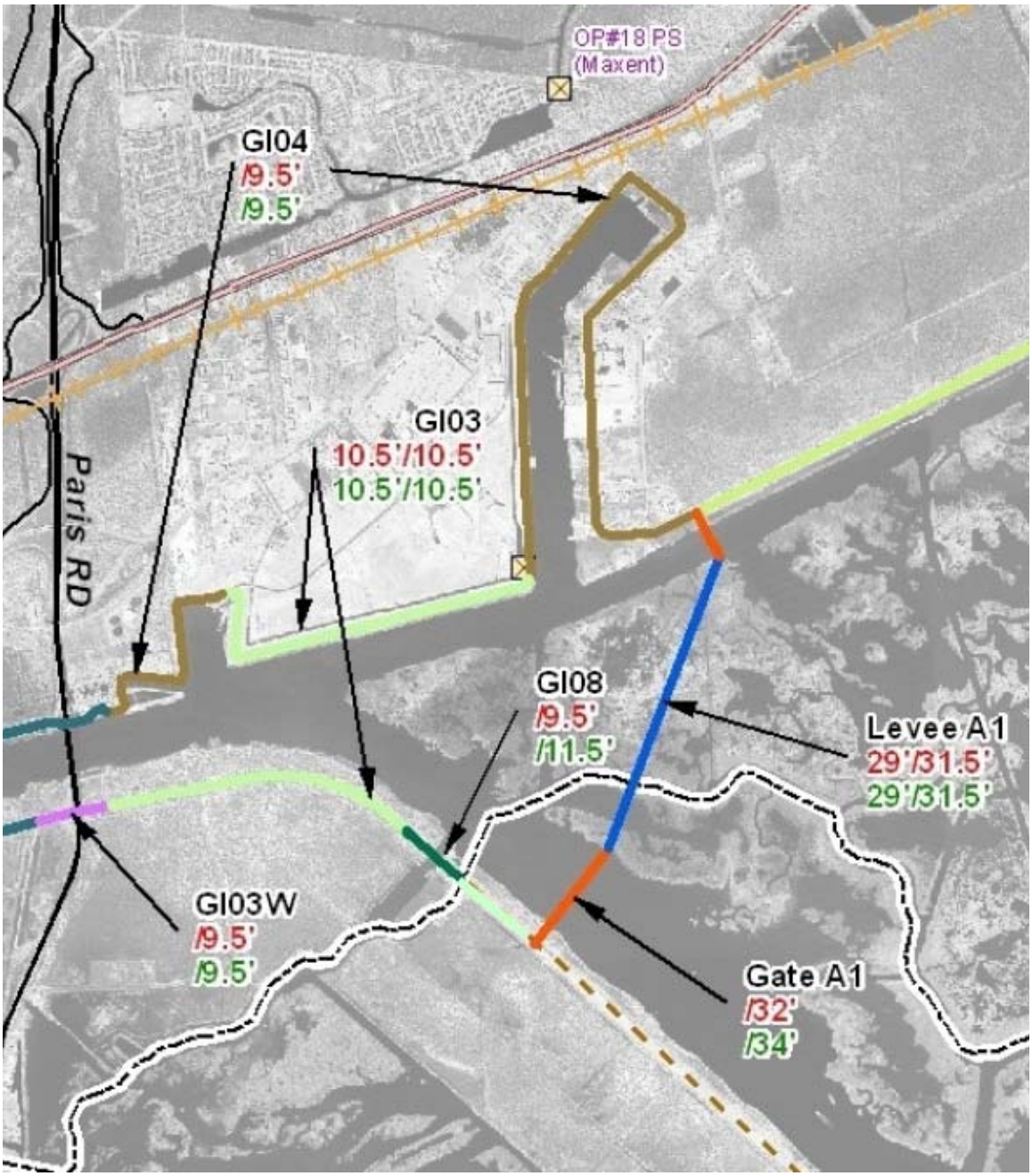


New Orleans
Lakefront Airport
Gate A2
/16'
/18'
OP#16
PS (St.
Charles)
NE20
/9.5'
/11.5'
e DR
NO20
/9.5'
/11.5'
IH30
10.5'/10.5'
10.5'/10.5'
Transition
IH05A1-W
/9.5'
/9.5'
IH02A1-W
/9.5'
/9.5'
IHNC

MRGO-GIWW and Seabrook Closure Sections
1% Hydraulic boundary conditions

				Surge level (ft)		Significant wave height (ft)		Peak period (s)	
Segment	Name	Type	Condition	Mean	Std	Mean	Std	Mean	Std
GATE-A1	Closure gate at MRGO - GIWW intersection	Structure/Wall	Future	19.9	1.0	7.2	0.6	8.4	1.6
LEVEE-A1	Closure levee at MRGO - GIWW intersection	Levee	Existing	18.4	1.0	7.1	0.7	7.9	1.6
LEVEE-A1	Closure levee at MRGO - GIWW intersection	Levee	Future	19.9	1.0	7.9	0.7	8.3	1.6
GATE-A2	Closure gate at Seabrook	Structure/Wall	Future	10.0	0.8	4.0	0.3	6.2	1.1

MRGO-GIWW and Seabrook Closure Sections
1% Design heights

						Overtopping rate	
Segment	Name	Type	Condition	Depth at toe (ft)	Height (ft)	q50 (cft/s per ft)	q90 (cft/s per ft)
GATE-A1	Closure gate at MRGO - GIWW intersection	Structure/Wall	Future	39.9	34.0	0.007	0.027
LEVEE-A1	Closure levee at MRGO - GIWW intersection	Levee	Existing	18.4	29.0	0.008	0.082
LEVEE-A1	Closure levee at MRGO - GIWW intersection	Levee	Future	19.9	31.5	0.009	0.089
GATE-A2	Closure gate at Seabrook	Structure/Wall	Future	10.0	18.0	0.002	0.009

MRGO-GIWW and Seabrook Closure Sections
Resiliency analysis (0.2% event)

					Best estimates during 0.2% event	
Segment	Name	Type	Condition	Height (ft)	Surge level (ft)	Overtopping rate (cft/s per ft)
GATE-A1	Closure gate at MRGO - GIWW intersection	Structure/Wall	Future	34.0	23.6	1.780
LEVEE-A1	Closure levee at MRGO - GIWW intersection	Levee	Existing	29.0	22.1	1.780
LEVEE-A1	Closure levee at MRGO - GIWW intersection	Levee	Future	31.5	23.6	1.780
GATE-A2	Closure gate at Seabrook	Structure/Wall	Future	18.0	12.8	1.390

St. Bernard Parish East Bank Reaches

St Bernard Parish Sections 1% Hydraulic boundary conditions									
				Surge level (ft)		Significant wave height (ft)		Peak period (s)	
Segment	Name	Type	Condition	Mean	Std	Mean	Std	Mean	Std
SB11	MRGO levee	Levee	Existing	18.4	1.0	7.1	0.7	7.9	1.6
SB11	MRGO levee	Levee	Future	19.9	1.0	7.9	0.7	8.3	1.6
SB12	MRGO levee	Levee	Existing	17.3	1.1	6.9	0.7	5.9	1.2
SB12	MRGO levee	Levee	Future	18.8	1.1	7.5	0.7	6.2	1.2
SB13	MRGO levee	Levee	Existing	16.4	1.1	6.6	0.7	6.3	1.3
SB13	MRGO levee	Levee	Future	17.9	1.1	7.2	0.7	6.6	1.3
SB15	MRGO levee	Levee	Existing	15.6	1.2	5.4	0.5	8.9	1.8
SB15	MRGO levee	Levee	Future	17.1	1.2	6.2	0.5	9.5	1.8
SB16	Caernarvon levee	Levee	Existing	17.5	1.1	5.4	0.5	8.4	1.7
SB16	Caernarvon levee	Levee	Future	19.0	1.1	6.2	0.5	8.9	1.7
SB17	Caernarvon levee	Levee	Existing	18.0	1.2	5.1	0.5	8.1	1.6
SB17	Caernarvon levee	Levee	Future	19.5	1.2	5.9	0.5	8.7	1.6
SB19	Bayou Dupre Control structure	Structure/Wall	Future	17.3	1.0	5.6	0.5	6.5	1.2
SB20	St Mary Pump Station (PS#8)	Structure/Wall	Future	18.5	1.0	6.2	0.5	8.6	1.6

St Bernard Parish Sections 1% Design heights							
						Overtopping rate	
Segment	Name	Type	Condition	Depth at toe (ft)	Height (ft)	q50 (cft/s per ft)	q90 (cft/s per ft)
SB11	MRGO levee	Levee	Existing	18.4	29.0	0.008	0.083
SB11	MRGO levee	Levee	Future	19.9	31.5	0.009	0.091
SB12	MRGO levee	Levee	Existing	17.3	27.5	0.001	0.019
SB12	MRGO levee	Levee	Future	18.8	30.0	0.002	0.022
SB13	MRGO levee	Levee	Existing	16.4	26.5	0.002	0.027
SB13	MRGO levee	Levee	Future	17.9	29.0	0.002	0.030
SB15	MRGO levee	Levee	Existing	15.6	26.5	0.005	0.062
SB15	MRGO levee	Levee	Future	17.1	29.0	0.007	0.077
SB16	Caernarvon levee	Levee	Existing	17.5	26.5	0.007	0.087
SB16	Caernarvon levee	Levee	Future	19.0	29.0	0.006	0.072
SB17	Caernarvon levee	Levee	Existing	18.0	26.5	0.002	0.040
SB17	Caernarvon levee	Levee	Future	19.5	29.0	0.009	0.097
SB19	Bayou Dupre Control structure	Structure/Wall	Future	17.3	31.0	0.001	0.004
SB20	St Mary Pump Station (PS#8)	Structure/Wall	Future	18.5	30.5	0.006	0.023

St Bernard Parish Sections Resiliency analysis (0.2% event)						
					Best estimates during 0.2% event	
Segment	Name	Type	Condition	Height (ft)	Surge level (ft)	Overtopping rate (cft/s per ft)
SB11	MRGO levee	Levee	Existing	29.0	22.1	0.374
SB11	MRGO levee	Levee	Future	31.5	23.6	0.322
SB12	MRGO levee	Levee	Existing	27.5	21.1	0.163
SB12	MRGO levee	Levee	Future	30.0	22.6	0.150
SB13	MRGO levee	Levee	Existing	26.5	20.2	2.355
SB13	MRGO levee	Levee	Future	29.0	21.7	2.284
SB15	MRGO levee	Levee	Existing	26.5	19.9	1.842
SB15	MRGO levee	Levee	Future	29.0	21.4	1.689
SB16	Caernarvon levee	Levee	Existing	26.5	21.3	1.319
SB16	Caernarvon levee	Levee	Future	29.0	22.8	0.920
SB17	Caernarvon levee	Levee	Existing	26.5	22.1	0.778
SB17	Caernarvon levee	Levee	Future	29.0	23.6	1.028
SB19	Bayou Dupre Control structure	Structure/Wall	Future	31.0	21.0	0.112
SB20	St Mary Pump Station (PS#8)	Structure/Wall	Future	30.5	21.9	0.253

St. Charles and Jefferson Parishes, Lake Cataouache Reaches

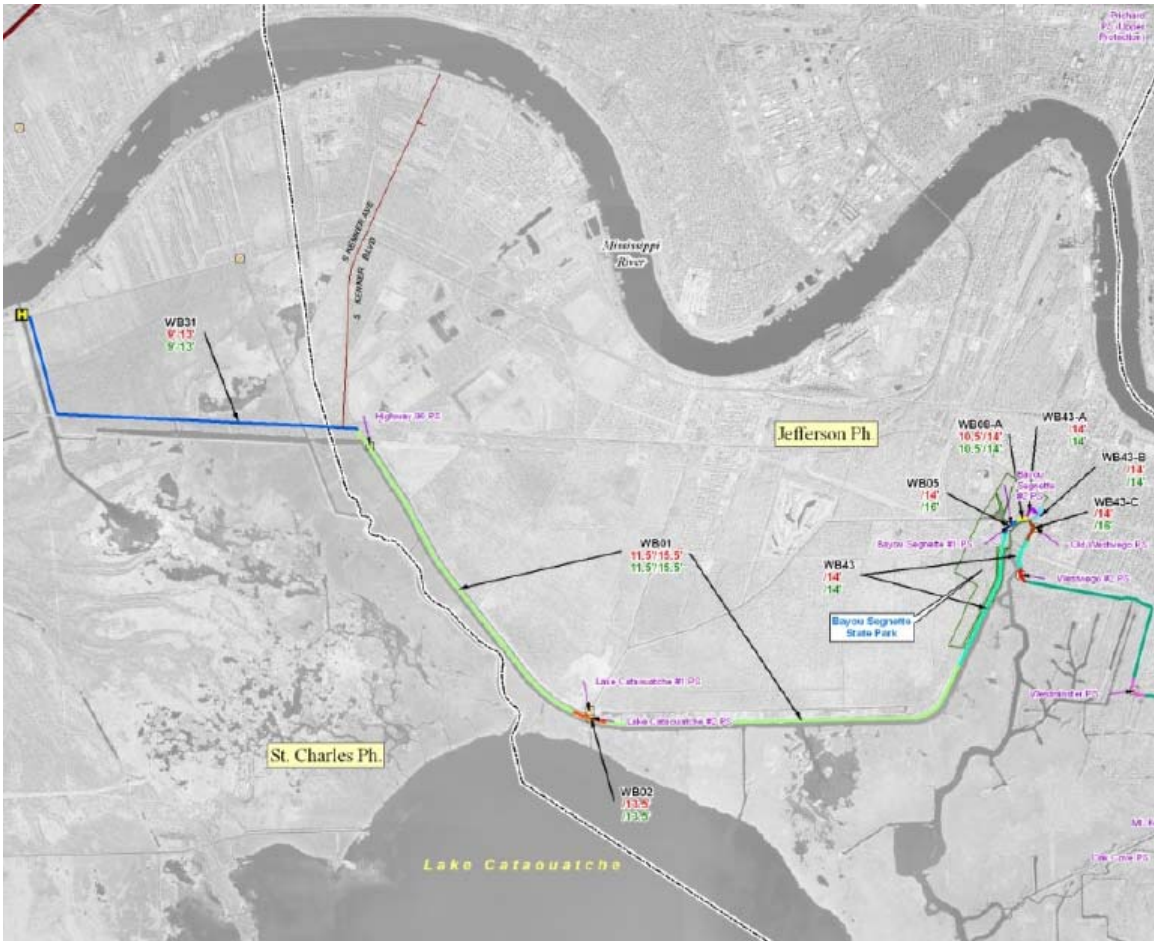

Westbank Sections (Lake Cataouache Reach) 1% Hydraulic boundary conditions									
				Surge level (ft)		Significant wave height (ft)		Peak period (s)	
Segment	Name	Type	Condition	Mean	Std	Mean	Std	Mean	Std
WB31	Mississippi River to US90 Levees	Levee	Existing	6.5	0.7	1.6	0.2	5.4	1.1
WB31	Mississippi River to US90 Levees	Levee	Future	8.5	0.7	2.6	0.2	6.9	1.1
WB01	US Highway 90 to the Bayou Segnette State Park	Levee	Existing	6.5	0.7	2.1	0.2	5.5	1.1
WB01	US Highway 90 to the Bayou Segnette State Park	Levee	Future	8.5	0.7	3.1	0.2	6.7	1.1
WB02	Lake Cataouatche Pump Station 1 and 2	Structure/Wall	Future	8.5	0.7	3.1	0.2	6.7	1.1
WB43	Bayou Segnette State Park Floodwall	Structure/Wall	Future	8.5	0.7	2.4	0.1	5.6	0.9
WB05	Bayou Segnette Pump Station 1 and 2	Structure/Wall	Future	8.5	0.7	2.4	0.1	5.6	0.9

Westbank Sections (Lake Cataouache Reach) 1% Design heights							
						Overtopping rate	
Segment	Name	Type	Condition	Depth at toe (ft)	Height (ft)	q50 (cft/s per ft)	q90 (cft/s per ft)
WB31	Mississippi River to US90 Levees	Levee	Existing	5.5	9.0	0.002	0.044
WB31	Mississippi River to US90 Levees	Levee	Future	7.5	13.0	0.003	0.030
WB01	US Highway 90 to the Bayou Segnette State Park	Levee	Existing	6.5	11.5	0.003	0.024
WB01	US Highway 90 to the Bayou Segnette State Park	Levee	Future	8.5	15.5	0.006	0.034
WB02	Lake Cataouatche Pump Station 1 and 2	Structure/Wall	Future	8.5	15.5	0.001	0.003
WB43	Bayou Segnette State Park Floodwall	Structure/Wall	Future	8.5	14.0	0.000	0.002
WB05	Bayou Segnette Pump Station 1 and 2	Structure/Wall	Future	8.5	16.0	0.000	0.000

Westbank Sections (Lake Cataouache Reach) Resiliency analysis (0.2% event)						
					Best estimates during 0.2% event	
Segment	Name	Type	Condition	Height (ft)	Surge level (ft)	Overtopping rate (cft/s per ft)
WB31	Mississippi River to US90 Levees	Levee	Existing	9.0	8.9	1.803
WB31	Mississippi River to US90 Levees	Levee	Future	13.0	10.9	0.584
WB01	US Highway 90 to the Bayou Segnette State Park	Levee	Existing	11.5	9.0	0.575
WB01	US Highway 90 to the Bayou Segnette State Park	Levee	Future	15.5	11.0	0.343
WB02	Lake Cataouatche Pump Station 1 and 2	Structure/Wall	Future	15.5	11.0	0.072
WB43	Bayou Segnette State Park Floodwall	Structure/Wall	Future	14.0	11.1	0.141
WB05	Bayou Segnette Pump Station 1 and 2	Structure/Wall	Future	16.0	11.1	0.017

Jefferson and Orleans Parishes, Westwego to Harvey Canal Reaches

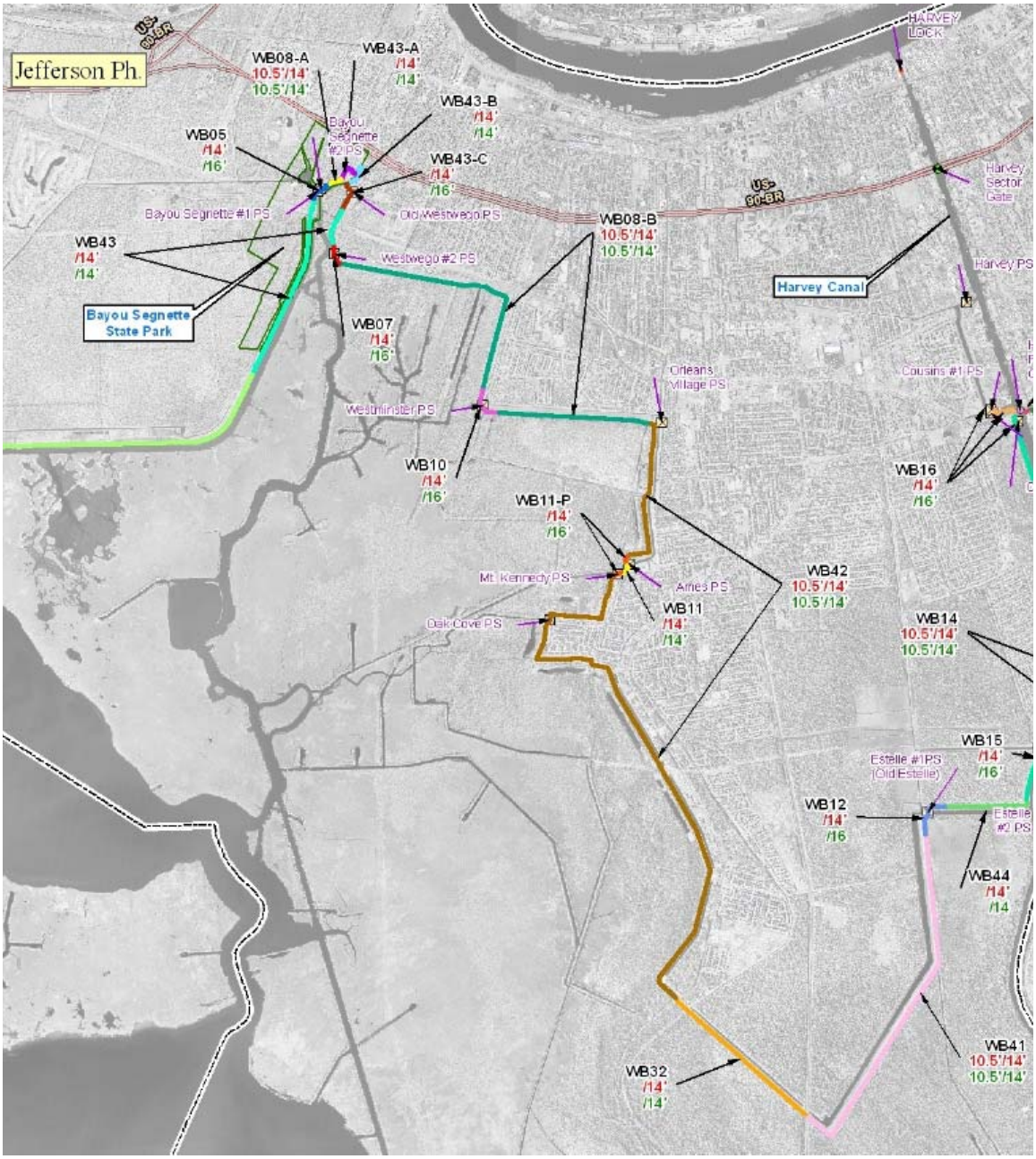

Westbank Sections (Westwego to Harvey Canal Reach) 1% Hydraulic boundary conditions									
				Surge level (ft)		Significant wave height (ft)		Peak period (s)	
Segment	Name	Type	Condition	Mean	Std	Mean	Std	Mean	Std
WB08-a	Segnette Pump Station to Company Canal Floodwall	Levee	Existing	6.5	0.7	1.4	0.1	4.3	0.9
WB08-a	Segnette Pump Station to Company Canal Floodwall	Levee	Future	8.5	0.7	2.4	0.1	5.6	0.9
WB08-b	New Westwego Pump Station to Orleans Village Levee	Levee	Existing	6.5	0.7	1.4	0.1	4.3	0.9
WB08-b	New Westwego Pump Station to Orleans Village Levee	Levee	Future	8.5	0.7	2.4	0.1	5.6	0.9
WB43-a	Segnette Pump Station to Company Canal Floodwall	Structure/Wall	Future	8.5	0.7	2.4	0.1	5.6	0.9
WB43-b	Company Canal & Westwego Floodwall	Structure/Wall	Future	8.5	0.7	2.4	0.1	5.6	0.9
WB43-c	Old Westwego Pump Station	Structure/Wall	Future	8.5	0.7	2.4	0.1	5.6	0.9
WB07	New Westwego Pump Station	Structure/Wall	Future	8.5	0.7	2.4	0.1	5.6	0.9
WB10	Westminster Pump Station	Structure/Wall	Future	8.5	0.7	2.4	0.1	5.6	0.9
WB11	Ames to Kennedy Floodwall	Structure/Wall	Future	9.3	0.9	2.3	0.1	4.9	0.7
WB11-P	Ames & Kennedy Pump Station	Structure/Wall	Future	9.3	0.9	2.3	0.1	4.9	0.7
WB42	Orleans Village to Ames Pump Station Levee	Levee	Existing	7.3	0.9	1.3	0.1	3.7	0.7
WB42	Orleans Village to Ames Pump Station Levee	Levee	Future	9.3	0.9	2.3	0.1	4.9	0.7
WB32	Highway 45 to Highway 3134	Structure/Wall	Future	9.3	0.9	2.3	0.1	4.9	0.7
WB41	Highway 3134 to Old Estelle Pump Station Levee	Levee	Existing	7.3	0.9	1.3	0.1	3.7	0.7
WB41	Highway 3134 to Old Estelle Pump Station Levee	Levee	Future	9.3	0.9	2.3	0.1	4.9	0.7
WB12	Old Estelle Pump Station	Structure/Wall	Future	9.3	0.9	2.3	0.1	4.9	0.7
WB44	Old Estelle to Robinson Point	Structure/Wall	Future	9.3	0.9	2.3	0.1	4.9	0.7

Westbank Sections (Westwego to Harvey Canal Reach) 1% Design heights							
						Overtopping rate	
Segment	Name	Type	Condition	Depth at toe (ft)	Height (ft)	q50 (cft/s per ft)	q90 (cft/s per ft)
WB08-a	Segnette Pump Station to Company Canal Floodwall	Levee	Existing	5.5	10.5	0.001	0.010
WB08-a	Segnette Pump Station to Company Canal Floodwall	Levee	Future	7.5	14.0	0.008	0.037
WB08-b	New Westwego Pump Station to Orleans Village Levee	Levee	Existing	5.5	10.5	0.001	0.010
WB08-b	New Westwego Pump Station to Orleans Village Levee	Levee	Future	7.5	14.0	0.008	0.035
WB43-a	Segnette Pump Station to Company Canal Floodwall	Structure/Wall	Future	8.5	14.0	0.000	0.003
WB43-b	Company Canal & Westwego Floodwall	Structure/Wall	Future	8.5	14.0	0.000	0.002
WB43-c	Old Westwego Pump Station	Structure/Wall	Future	8.5	16.0	0.000	0.000
WB07	New Westwego Pump Station	Structure/Wall	Future	8.5	16.0	0.000	0.000
WB10	Westminster Pump Station	Structure/Wall	Future	8.5	16.0	0.000	0.000
WB11	Ames to Kennedy Floodwall	Structure/Wall	Future	9.3	14.0	0.001	0.008
WB11-P	Ames & Kennedy Pump Station	Structure/Wall	Future	9.3	16.0	0.000	0.000
WB42	Orleans Village to Ames Pump Station Levee	Levee	Existing	7.3	10.5	0.003	0.035
WB42	Orleans Village to Ames Pump Station Levee	Levee	Future	9.3	14.0	0.010	0.063
WB32	Highway 45 to Highway 3134	Structure/Wall	Future	9.3	14.0	0.001	0.008
WB41	Highway 3134 to Old Estelle Pump Station Levee	Levee	Existing	7.3	10.5	0.003	0.034
WB41	Highway 3134 to Old Estelle Pump Station Levee	Levee	Future	9.3	14.0	0.010	0.061
WB12	Old Estelle Pump Station	Structure/Wall	Future	9.3	16.0	0.000	0.000
WB44	Old Estelle to Robinson Point	Structure/Wall	Future	9.3	14.0	0.001	0.008

Westbank Sections (Westwego to Harvey Canal Reach) Resiliency analysis (0.2% event)						
					Best estimates during 0.2% event	
Segment	Name	Type	Condition	Height (ft)	Surge level (ft)	Overtopping rate (cft/s per ft)
WB08-a	Segnette Pump Station to Company Canal Floodwall	Levee	Existing	10.5	9.1	0.945
WB08-a	Segnette Pump Station to Company Canal Floodwall	Levee	Future	14.0	11.1	0.727
WB08-b	New Westwego Pump Station to Orleans Village Levee	Levee	Existing	10.5	9.1	0.955
WB08-b	New Westwego Pump Station to Orleans Village Levee	Levee	Future	14.0	11.1	0.729
WB43-a	Segnette Pump Station to Company Canal Floodwall	Structure/Wall	Future	14.0	11.1	0.138
WB43-b	Company Canal & Westwego Floodwall	Structure/Wall	Future	14.0	11.1	0.140
WB43-c	Old Westwego Pump Station	Structure/Wall	Future	16.0	11.1	0.016
WB07	New Westwego Pump Station	Structure/Wall	Future	16.0	11.1	0.017
WB10	Westminster Pump Station	Structure/Wall	Future	16.0	11.1	0.016
WB11	Ames to Kennedy Floodwall	Structure/Wall	Future	14.0	12.4	0.434
WB11-P	Ames & Kennedy Pump Station	Structure/Wall	Future	16.0	12.4	0.047
WB42	Orleans Village to Ames Pump Station Levee	Levee	Existing	10.5	10.4	2.076
WB42	Orleans Village to Ames Pump Station Levee	Levee	Future	14.0	12.4	1.237
WB32	Highway 45 to Highway 3134	Structure/Wall	Future	14.0	12.4	0.447
WB41	Highway 3134 to Old Estelle Pump Station Levee	Levee	Existing	10.5	10.4	2.075
WB41	Highway 3134 to Old Estelle Pump Station Levee	Levee	Future	14.0	12.4	1.265
WB12	Old Estelle Pump Station	Structure/Wall	Future	16.0	12.4	0.047
WB44	Old Estelle to Robinson Point	Structure/Wall	Future	14.0	12.4	0.429

Jefferson and Orleans Parishes, East of Harvey Canal Reaches

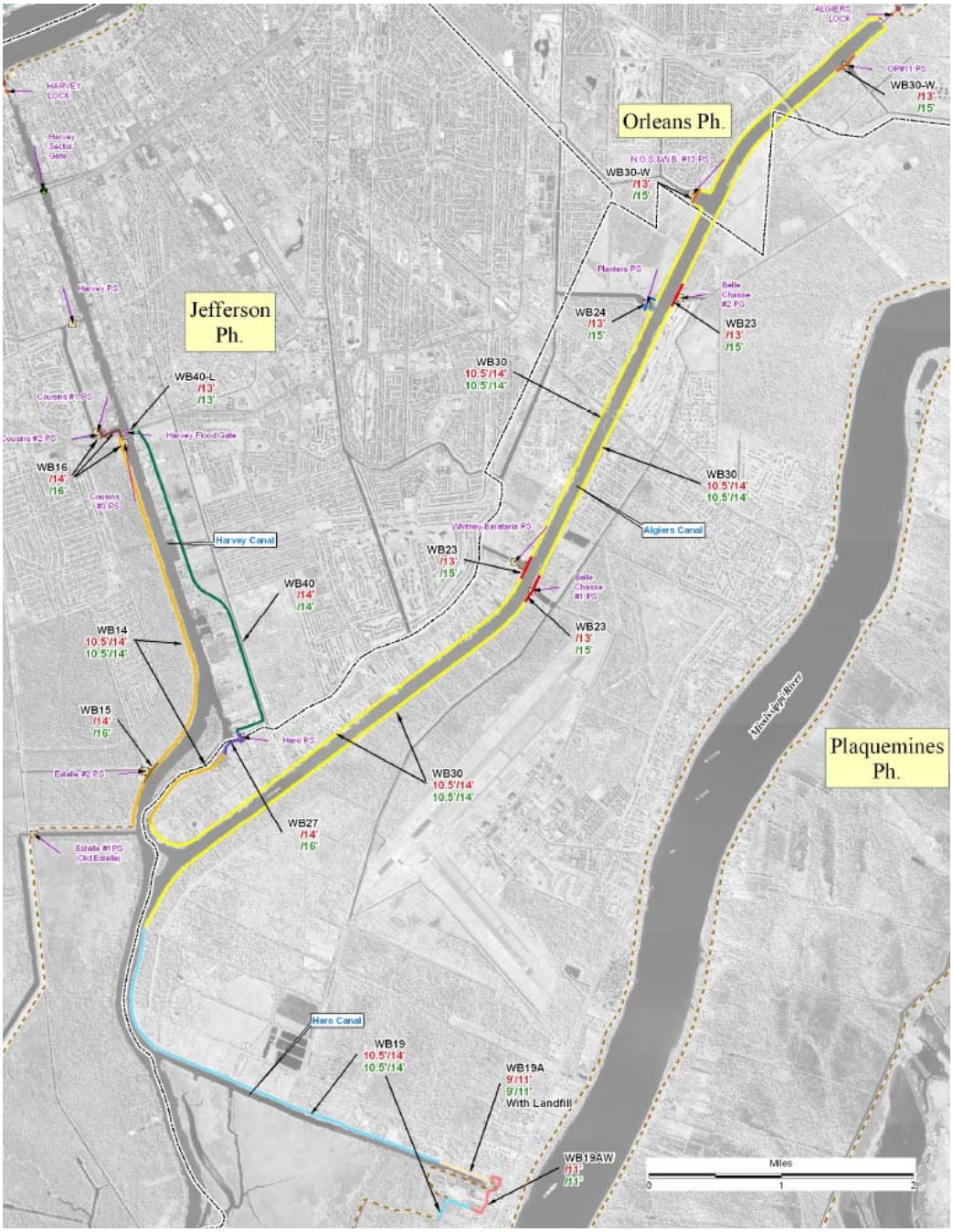

Westbank Sections (East of Harvey Canal Reach) 1% Hydraulic boundary conditions									
				Surge level (ft)		Significant wave height (ft)		Peak period (s)	
Segment	Name	Type	Condition	Mean	Std	Mean	Std	Mean	Std
WB14	Robinson Pt. to Harvey Canal W. Levee	Levee	Existing	7.8	0.9	1.3	0.1	3.7	0.7
WB14	Robinson Pt. to Harvey Canal W. Levee	Levee	Future	9.8	0.9	2.3	0.1	4.9	0.7
WB15	New Estelle Pump Station	Structure/Wall	Future	9.8	0.9	2.3	0.1	4.9	0.7
WB40	Harvey Canal Floodwall	Structure/Wall	Future	9.8	0.9	2.3	0.1	4.9	0.7
WB16	Cousins Pump Station 1, 2 and 3 (on Harvey Canal)	Structure/Wall	Future	9.8	0.9	2.3	0.1	4.9	0.7
WB40-L	Sector Gate at Lapalco Overpass on Harvey Canal	Structure/Wall	Future	9.8	0.9	2.3	0.1	4.9	0.7
WB27	Hero Pump Station (on Harvey Canal)	Structure/Wall	Future	9.8	0.9	2.3	0.1	4.9	0.7
WB30	Algiers Canal - Hero Pump Station to Algiers Lock	Levee	Existing	7.8	0.9	1.3	0.1	3.7	0.7
WB30	Algiers Canal - Hero Pump Station to Algiers Lock	Levee	Future	9.8	0.9	2.3	0.1	4.9	0.7
WB23	Whitney Barataria and Belle Chase 1 and 2 Pump Stations	Structure/Wall	Future	9.8	0.9	2.3	0.1	4.9	0.7
WB24	Planters Pump Station	Structure/Wall	Future	9.8	0.9	2.3	0.1	4.9	0.7
WB30-W	NO SBW Pump Station 11 and 13	Structure/Wall	Future	9.8	0.9	2.3	0.1	4.9	0.7
WB19	Transition Point to Hero Canal to Oakville	Levee	Existing	7.3	0.9	1.3	0.1	3.7	0.7
WB19	Transition Point to Hero Canal to Oakville	Levee	Future	9.3	0.9	2.3	0.1	4.9	0.7
WB19-A	Hero Canal-Area Behind Landfill Berm	Levee	Existing	7.3	0.9	1.0	0.1	2.0	0.4
WB19-A	Hero Canal-Area Behind Landfill Berm	Levee	Future	9.3	0.9	1.0	0.1	2.0	0.4
WB19-AW	Hero Canal Floodwall behind Landfill Berm	Structure/Wall	Future	9.3	0.9	1.0	0.1	2.0	0.4

Westbank Sections (East of Harvey Canal Reach) 1% Design heights							
						Overtopping rate	
Segment	Name	Type	Condition	Depth at toe (ft)	Height (ft)	q50 (cft/s per ft)	q90 (cft/s per ft)
WB14	Robinson Pt. to Harvey Canal W. Wall Levee	Levee	Existing	7.8	10.5	0.004	0.069
WB14	Robinson Pt. to Harvey Canal W. Wall Levee	Levee	Future	9.8	14.0	0.006	0.060
WB15	New Estelle Pump Station	Structure/Wall	Future	9.8	16.0	0.000	0.001
WB40	Harvey Canal Floodwall	Structure/Wall	Future	9.8	14.0	0.002	0.016
WB16	Cousins Pump Station 1, 2 and 3 (on Harvey Canal)	Structure/Wall	Future	9.8	16.0	0.000	0.001
WB40-L	Sector Gate at Lapalco Overpass on Harvey Canal	Structure/Wall	Future	9.8	13.0	0.011	0.073
WB27	Hero Pump Station (on Harvey Canal)	Structure/Wall	Future	9.8	16.0	0.000	0.001
WB30	Hero Pump Station to Algiers Canal Levee	Levee	Existing	7.8	10.5	0.004	0.068
WB30	Hero Pump Station to Algiers Canal Levee	Levee	Future	9.8	14.0	0.006	0.058
WB23	Whitney Barataria Pump Station	Structure/Wall	Future	9.8	15.0	0.000	0.004
WB24	Planters Pump Station	Structure/Wall	Future	9.8	15.0	0.000	0.004
WB30-W	NO SBW Pump Station 11	Structure/Wall	Future	9.8	15.0	0.000	0.004
WB19	Transition Point to Hero Canal to Oakville	Levee	Existing	7.3	10.5	0.001	0.024
WB19	Transition Point to Hero Canal to Oakville	Levee	Future	9.3	14.0	0.003	0.030
WB19-W	Hero Canal Floodwall	Structure/Wall	Future	9.3	13.0	0.005	0.033
WB19-A	Hero Canal-Area Behind Landfill Berm	Levee	Existing	7.3	9.0	0.000	0.078
WB19-A	Hero Canal-Area Behind Landfill Berm	Levee	Future	9.3	11.0	0.000	0.077
WB19-AW	Hero Canal Floodwall behind Landfill Berm	Structure/Wall	Future	9.3	11.0	0.001	0.067

Westbank Sections (East of Harvey Canal Reach) Resiliency analysis (0.2% event)						
					Best estimates during 0.2% event	
Segment	Name	Type	Condition	Height (ft)	Surge level (ft)	Overtopping rate (cft/s per ft)
WB14	Robinson Pt. to Harvey Canal W. Wall Levee	Levee	Existing	10.5	10.9	2.947
WB14	Robinson Pt. to Harvey Canal W. Wall Levee	Levee	Future	14.0	12.9	1.343
WB15	New Estelle Pump Station	Structure/Wall	Future	16.0	12.9	0.084
WB40	Harvey Canal Floodwall	Structure/Wall	Future	14.0	12.9	0.803
WB16	Cousins Pump Station 1, 2 and 3 (on Harvey Canal)	Structure/Wall	Future	16.0	12.9	0.082
WB40-L	Sector Gate at Lapalco Overpass on Harvey Canal	Structure/Wall	Future	13.0	12.9	1.671
WB27	Hero Pump Station (on Harvey Canal)	Structure/Wall	Future	16.0	12.9	0.084
WB30	Hero Pump Station to Algiers Canal Levee	Levee	Existing	10.5	10.9	3.001
WB30	Hero Pump Station to Algiers Canal Levee	Levee	Future	14.0	12.9	1.405
WB23	Whitney Barataria Pump Station	Structure/Wall	Future	15.0	12.9	0.260
WB24	Planters Pump Station	Structure/Wall	Future	15.0	12.9	0.251
WB30-W	NO SBW Pump Station 11	Structure/Wall	Future	15.0	12.9	0.259
WB19	Transition Point to Hero Canal to Oakville	Levee	Existing	10.5	10.4	1.934
WB19	Transition Point to Hero Canal to Oakville	Levee	Future	14.0	12.4	0.901
WB19-W	Hero Canal Floodwall	Structure/Wall	Future	13.0	12.4	1.202
WB19-A	Hero Canal-Area Behind Landfill Berm	Levee	Existing	9.0	10.4	8.151
WB19-A	Hero Canal-Area Behind Landfill Berm	Levee	Future	11.0	12.4	8.218
WB19-AW	Hero Canal Floodwall behind Landfill Berm	Structure/Wall	Future	11.0	12.4	8.114

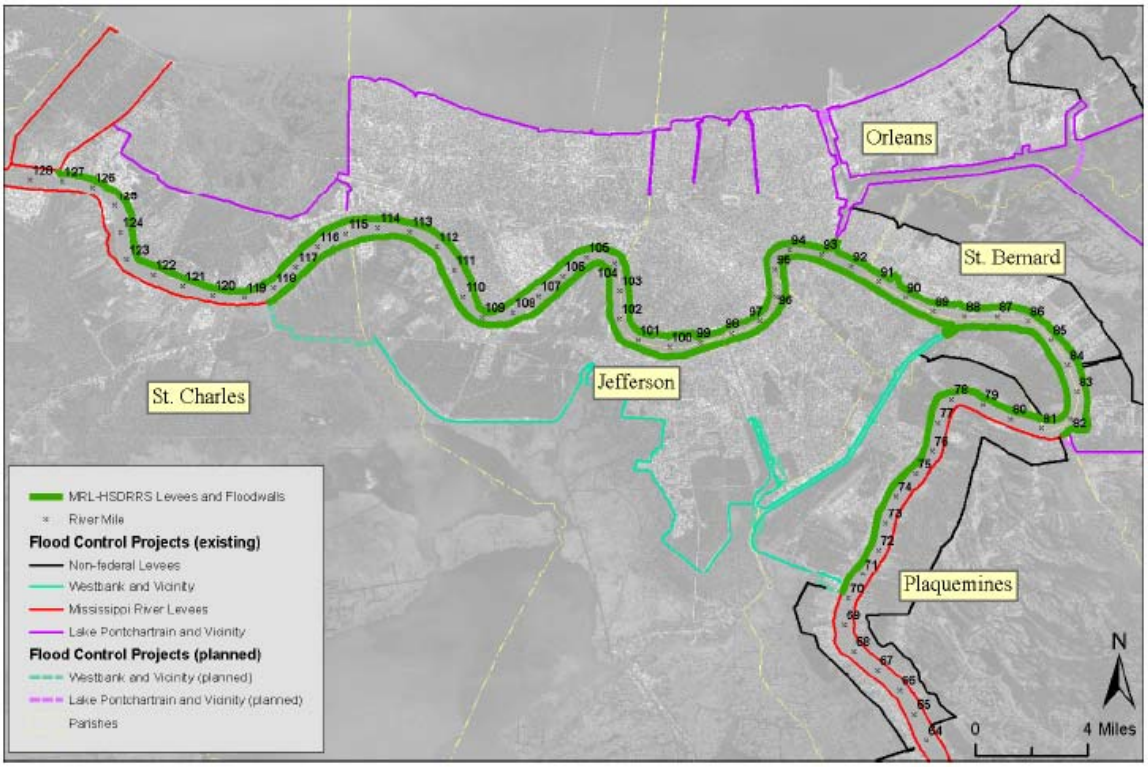

Analysis of 1% Hydraulic Conditions, Design Heights, and Resiliency have not been completed.